Evaluation of the Shear Strength of Ultra-High Performance Concrete

Danielle M. Voytko

A thesis
submitted in partial fulfilment of the
requirements for a degree of

Master of Science in Civil Engineering

University of Washington
2021

Committee:
Paolo M. Calvi
John F. Stanton

Program Authorized to Offer Degree:
Civil and Environmental Engineering

University of Washington

Abstract

Evaluation of the Shear Strength of Ultra-High Performance Concrete

Danielle M. Voytko

Co-Chairs of the Supervisory Committee:
Paolo M. Calvi
Civil and Environmental Engineering
John F. Stanton
Civil and Environmental Engineering

Ultra-High Performance Concrete (UHPC) is a cementitious concrete with reinforcing fibers that has exceptionally high compressive, tensile, flexural, and bond strengths, but not much is known about its shear strength. It is typically composed of cementitious material, fine sand, steel fiber reinforcement, admixtures, and water. The inclusion of steel fiber reinforcement and admixtures lead to higher costs than conventional concrete. Due to its high cost, UHPC applications in the United States have been associated with connections, in which its high strength is advantageous and the quantities are small enough to make it cost-effective.

Proprietary UHPC mixes have been developed by private companies for use on large-scale projects, but these mixes are not always an option due to high cost. In an effort to make UHPC more accessible, proprietary mixes using local materials and varying percentages of fiber content have been developed. An experimental program was undertaken by the University of Washington, in collaboration with the University of Oklahoma (OU) and Florida International University (FIU), to study one such mix. Seven batches of UHPC were mixed and cast at UW, altering the material sourcing and fiber content. In total, five batches used UW materials and 2% fiber content, 1 batch used UW materials and 1% fiber content, and one batch used OU materials and 2% fiber content.

Each batch of UHPC was subject to compression, modulus of elasticity, direct tension, and flexural beam tests. Additionally, they were tested in pure shear using the UW Panel Element Tester. After testing, the experimental data was analyzed to determine the effect of material sourcing and fiber content on UHPC behavior. It was concluded that the effect from material sourcing was negligible, at least partly because critical materials such as fibers and admixtures were obtained nationally and so were unchanged, and the effect from fiber content was little on compression and modulus of elasticity, but large on tension, flexural, and shear. The results were then compared to compression, modulus of elasticity, direct tension, and flexural beam test results from OU that used the same mix design but sourced materials locally and used different mixing equipment and mixing procedures. The conclusions from this comparison were consistent with the initial analysis.

Finally, the UW test results were compared with strengths predicted by available equations. However, no such equations exist for UHPC panels tested in pure shear. Therefore, the shear test results were compared with mix parameters such as fiber content, compressive strength, and tensile strength. It was found that the results were best correlated with fiber content and tensile strength. Equations based on these correlations were proposed to estimate shear strength of UHPC.

Acknowledgements

I would first like to thank my advisors, Professor Paolo Calvi and Professor John Stanton, for their continued guidance and support throughout this research project. I am extremely thankful to have had the opportunity to work with and learn from them. I would also like to thank Professor Travis Thonstad for serving on my committee and providing feedback.

I would like to thank Vince Chaijaroen for his guidance and patience in the experimental lab, without which this project would not have been completed. A special thanks to both Vince and Professor Dawn Lehman for maintaining safe operating procedures in the UW Structural Research Lab during unprecedented times with a global pandemic. Also, thank you to Don Janssen for acting as a consultant on the experimental work. Thank you to all of those who have helped me in the lab in one way or another: Michelle Chang, Ken Sullivan, Stephan Ahn, Chris Pyke, Sam Turner, Alec Yeutter, Ben Terry, Sara Mahoney, Joe Kaldestad, Rueben Madewell, and Clayton Black. It would not have been possible without them.

I want to thank Accelerated Bridge Construction- University Transportation Center (ABC-UTC) at Florida International University for providing project funding and collaboration. Thank you to the collaborators at the University of Oklahoma as well.

Lastly, thank you to my family and friends for supporting me along the way.

Table of Contents

List of Figures

List of Tables

Chapter 1: Introduction

1.1 Research Impetus

Ultra High-Performance Concrete (UHPC) is a cementitious concrete with exceptional mechanical properties. In the hardened state, its compressive, tensile, flexural, and bond strengths are significantly greater than those of conventional concrete. It is also significantly more expensive than conventional concrete. Thus, the applications in which it has been used most, at least in the US, have been associated with connections, in which its high strength is advantageous and the quantities used are small enough to make it cost-effective.

The name UHPC applies to a class of materials rather than a single material. There is no single mix design for it nor a unique definition for the properties required to qualify a material to be UHPC. Guidelines on compressive, tensile, and flexural strengths have been provided by the American Concrete Institute (ACI) [1] , the Federal Highway Administration (FHWA) [2], and the Portland Cement Association (PCA) [3].

UHPC is typically composed of cementitious material, fine sand, fiber reinforcement, admixtures, and water. Course aggregate is seldom used. Therefore, it has a very dense cementitious matrix with a discontinuous pore structure [4]. The cementitious component of UHPC can include materials such as cement, slag, silica fume, quartz, fly ash, and basalt powder. Its properties are usually achieved in a number of ways. The high compressive strength, typically between 120 MPa and 200 MPa, and modulus of elasticity are achieved by the closely packed cementitious particles and low water-to-cement (w/c) ratio. Since the w/c ratio is low, typically in the range of 0.17-0.25, a high range water reducer admixture (HRWRA) is needed to increase the flowability of the material. The tension strength of UHPC is most impressive due to its ductility, which is the result of fiber reinforcement. Its peak tensile strength is greater than that of conventional concrete and UHPC typically retains over half of its peak strength at a strain of 1%. The fibrous component of UHPC also increases its bond capacity. Fiber reinforcement usually makes up 2% of the UHPC mix by volume. The fibers can be made of a variety of materials, shapes, and sizes and they are typically intended to fail via pull out rather than fracture. A common specification of fibers is smooth, straight, steel fibers with dimensions 0.2 mm diameter, 13 mm length, and a strength of

2000 MPa. The fibers are particularly effective in UHPC since there is no coarse aggregate present to disturb the path of the fibers. Less is known about the shear strength of UHPC than of other properties. Correcting that deficit is one of the primary goals of the present work.

Ultra-High Performance Concrete was officially created in 1994, but its development started in the 80's when high-performance concrete and fiber reinforced concrete were combined to reach high strength and durability [5]. Since then, UHPC has been studied to optimize its mix design and learn more about its properties. The earliest UHPC mixes were developed by private companies such as Lafarge Holcim [6] and they continue to supply the majority of the UHPC used in the US today. The proprietary UHPC mixes can cost anywhere from 20 to 80 times more than conventional concrete due to necessary materials and the common need for a manufacturer's representative to be present on site. Non-proprietary mixes have also been developed over the years but they are still victim to high costs, mainly due to the price of steel fibers and admixtures.

Additionally, since UHPC is extremely dense due to its cementitious and fibrous content, it requires special mixing practices. Typically high power pan mixers work best, but even then, the mixer is only able to accommodate about two-thirds its capacity for conventional concrete. Due to the cost and uncertainty associated with mixing, contractors have typically decided that the money saved from using a non-proprietary mix was insufficient to justify the risk of mixing and using a new and unfamiliar material.

With that being said, UHPC is an attractive material for many uses. Since UHPC is strong in both tension and compression, it has a lower dependency on reinforcing bars than does conventional concrete. Additionally, since there is no coarse aggregate in UHPC, it is able to fit better in narrow or irregularly shaped areas. This makes UHPC the perfect material for connections between precast concrete elements, which are particularly relevant to Accelerated Bridge Construction (ABC). By 2016, the United States had built a total of 100 UHPC bridges [7]. Applications of UHPC related to bridges are connections between precast bridge elements (Figure 1.1), rehabilitation of existing structures (Figure 1.2), and, potentially, 100 percent UHPC girders (Figure 1.3). Girders made of 100% UHPC have not yet been built in the U.S. due to cost limitations. Although the UHPC girders can be designed to use less material than conventional concrete, as shown in Figure 1.3, the

reduced area does not make up for the high cost of UHPC. More cost-effective UHPC projects have been undertaken by Yen Lei Voo in Malaysia which prove to maximize the advantages of UHPC [8]. Voo utilizes a non-proprietary mix, local materials, and lightweight designs to accelerate infrastructure development mostly through the construction of UHPC bridges.

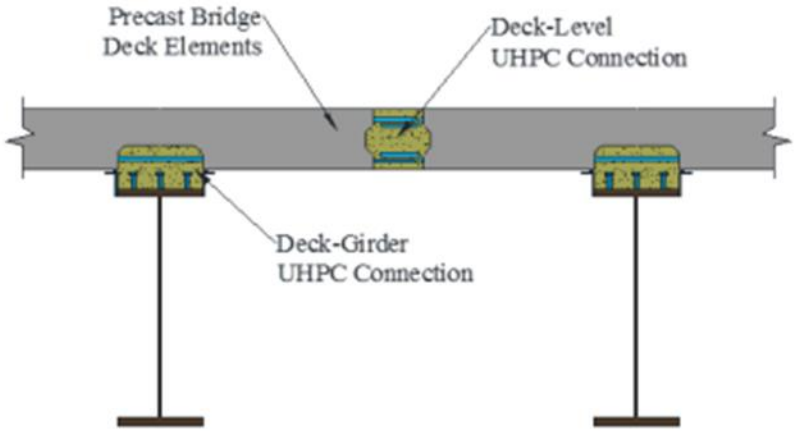

Figure 1.1: UHPC bridge deck connections [9]

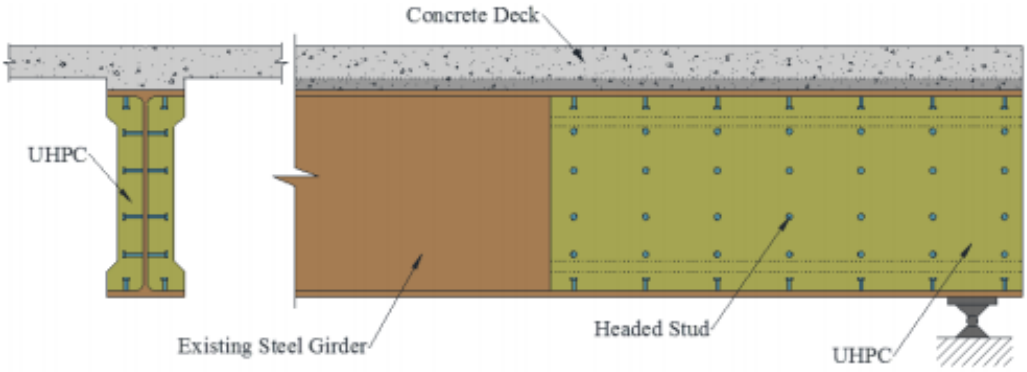

Figure 1.2: UHPC rehabilitation of existing structure [9]

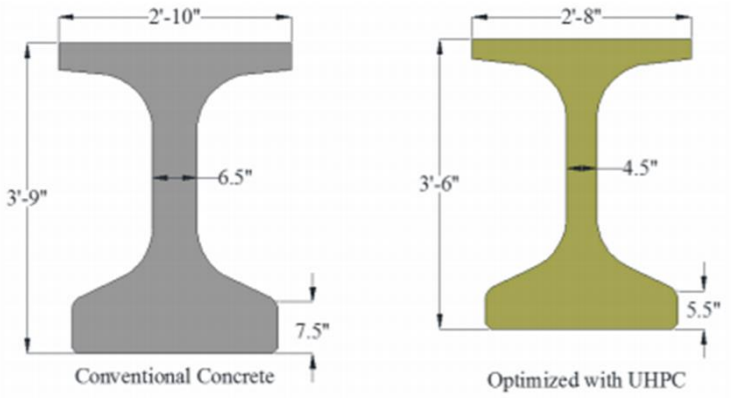

Figure 1.3: UHPC precast girder vs. conventional concrete precast girder [9]

1.2 Research Objectives

The main objective of the project was to study the shear response of UHPC. This objective was met by testing UHPC panels in pure shear using the UW Panel Tester. A secondary objective was to contribute to a multi-university effort to investigate the effects of UHPC properties of variations in local material sourcing and local mixing equipment and procedure. This project was completed in collaboration with the University of Oklahoma (OU) and Florida International University (FIU), where material tests were conducted on UHPC created using the same non-proprietary mix design but locally sourced materials. The material test results were used as a measure of the properties of the UHPC used in shear panel tests and as input to the FIU program guide. To answer questions about the importance of fibers in UHPC and the effectiveness of a non-proprietary mix, the fiber content and material sourcing location were varied throughout the experiments. The steps that were followed to meet the research objectives were as follows:

1. Mix and cast seven batches of UHPC, varying fiber content and material source location, resulting in five 2% fiber UW batches, one 1% fiber UW batch, and one 2% fiber OU batch.
2. Test each batch in compression, modulus of elasticity, direct tension, flexural beam, and pure shear (in the UW Panel Element Tester).
3. Analyze results to determine the effects of fiber content and material source on the performance of UHPC.
4. Compare results against those of other researchers to further evaluate the effect of the input parameters.
5. Compare results against widely used shear models.

The deliverables of this project were the materials data and comparisons of them with those of the other partner institutions, and the performance data on shear.

1.3 Overview of Thesis

The report is organized as follows:

- Chapter 2: UHPC Background and Literature Review
    - A collection of past experiments conducted on UHPC are summarized to provide a clear understanding of the material. There is a focus on relevant equations that will be utilized in later chapters.
- Chapter 3: Experimental Test Program
    - The mix design, mixing and casting procedure, and testing plan for compression, modulus of elasticity, direct tension, flexural beam, and pure shear panels is presented. This includes test setup, instrumentation, and data processing.
- Chapter 4: Experimental Results
    - Test results are reported for each specimen through tables, plots, and photos.
- Chapter 5: Analysis of Results
    - Test results are discussed and analyzed focusing on the influence of fiber content and material source location.
- Chapter 6: Comparison of Results
    - Results are compared with outside sources such as UHPC experiments conducted at different institutions, and with commonly accepted equations to estimate strength. An equation to estimate shear strength of UHPC is proposed.
- Chapter 7: Summary, Conclusions, and Recommendations
    - A summary of the completed work, conclusions drawn based on the results of the study, and recommendations for future work are outlined.

Chapter 2: Literature Review

In the following section, experimental programs relevant to this study are reviewed. The work is separated into three subsections based on the area of focus. The subsections are material properties, shear beam tests, and pure shear panel tests. In some cases, equations to model behavior of UHPC were developed. They are provided in this section and are compared with the results of this study in Chapter 6.

2.1 Material Properties

2.1.1 Graybeal (2018)

Graybeal et al. (2018) [9] tested six types of proprietary UHPC mixes, shown in Table 2-1. The mixes varied in fiber content and were subject to a large number of materials tests. The most relevant to the current study were compression, modulus of elasticity, and direct tension.

Table 2-1: Table 8 from Graybeal [9] Summary of UHPC Mix Proportions and Fiber Properties

ID		U-A		U-B		U-C		U-D		U-E		U-F	
Mix Design		lb/yd³	(kg/m³)	lb/yd³	(kg/m³)	lb/yd³	(kg/m³)	lb/yd³	(kg/m³)	lb/yd³	(kg/m³)	lb/yd³	(kg/m³)
Pre-blended dry powders		3503†	(2078)†	3516	(2086)	3600	(2136)	3700	(2195)	3236	(1920)	3725	(2210)
Water		278	(165)	354	(210)	268	(159)	219	(130)	379	(225)	241	(143)
Chemical admixtures	Liquid	23	(13.7)	48	(28.7)	na		89††	(53)††	73	(44)	65.7	(39)
	Solid	na		na		preblended*		na		na		1.5	(0.89)
Steel fiber content (Percent)		Short / Long Fibers											
	2	277	(126)	**88 / 179**	**(52 / 106)**	272	(123.6)	**263**	**(156)**	**263**	**(156)**	284	(168)
	3	**416**	**(247)**	132 / 269	(78 / 159)	408	(242)	395	(234)	395	(234)	-	-
	3.25	-	-	-	-	-	-	-	-	-	-	**426**	**(253)**
	4	554	(329)	176 / 358	(104 / 212)	544	(323)	526	(312)	526	(312)	568	(337)
	4.50	623	(370)	198 / 403	(117 / 239)	**612**	**(363)**	592	(351)	592	(351)	639	(379)
Steel Fiber		Short / Long Fibers											
Tensile strength, ksi (MPa)		160 (1100)‡		≥305 (2100)		348 (2400)		399 (3750)		399 (3750)		399 (3750)	
Length, in (mm)		1.18 (30)‡		0.5 (13) / 0.79 (20)		0.5 (13)		0.5 (13)		0.5 (13)		0.5 (13)	
Diameter, in (mm)		0.022 (0.55)‡		0.012 (0.3)		0.012 (0.3)		0.008 (0.2)		0.008 (0.2)		0.008 (0.2)	

† = Not pre-blended but come in as separate ingredients, which include fine silica sand, finely ground quartz flour, portland cement, and amorphous micro-silica
* = The chemical admixtures were dry powders and pre-blended with other powder ingredients
†† = It includes three chemicals, a modified phosphonate plasticizer, a modified polycarboxylate high-range water-reducing admixture, and a non-chloride accelerator
‡ = Fibers were straight with hooked ends and did not have a brass coating
na = Not applicable

The mixing process for UHPC was discussed by Graybeal. Mixing UHPC requires more energy than conventional concrete, so the maximum volume of material was reduced significantly from the recommended mixer capacity. Three different types of mixers were used depending on batch size. For weaker mixers, mix time was increased. The mixing procedure varied slightly for each

mix, but the main steps were the same. The main steps were premixing dry constituents, slowly adding the water and a small portion of the admixtures into the dry mix with the mixer turned on, and finally slowly incorporating the fibers and remaining admixtures once the wet and dry materials were completely incorporated.

Compression tests were performed on cylinders up to 250 days after casting. The results for mixes with two percent fiber content are summarized in Figure 2.1.

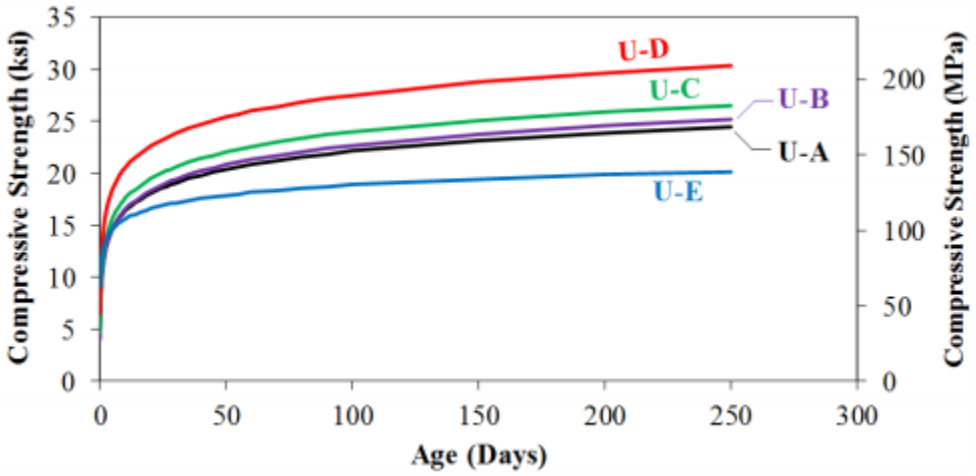

Figure 2.1: Figure 37 from Graybeal [9] Compressive strength gain for UHPC with 2% fiber

Compressive strengths at 28 days for 2% fiber mixes were between 120 MPa and 200 MPa. All of the UHPC batches, except for U-E, meet the guideline from FHWA for UHPC to have a strength of at least 150 MPa in compression. The water-to-cement ratio was unable to be determined for the UHPC mixes since all dry materials were combined into one mix. However, the UHPC mixes with lower water/dry material ratios typically had higher compressive strength. This relationship is shown for the 14-day compressive strengths in Figure 2.2.

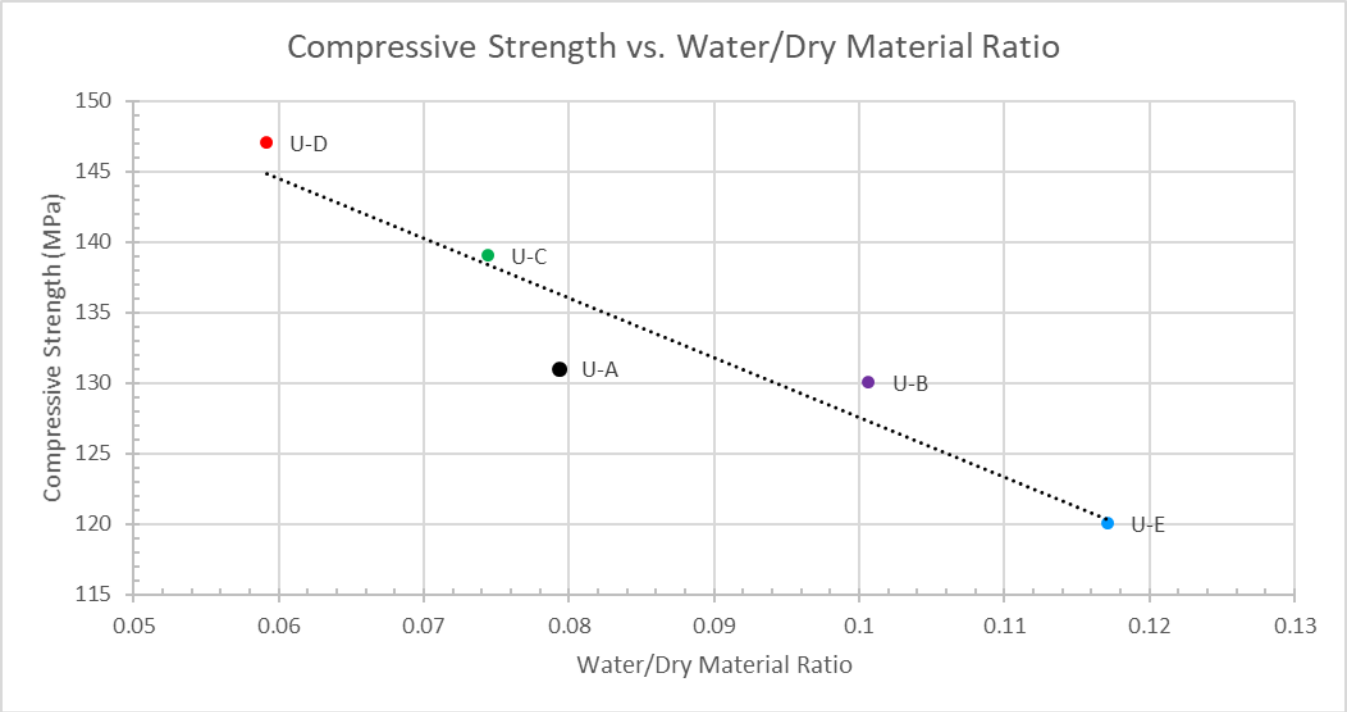

Figure 2.2: Compressive strength vs. water/dry material ratio at 14 days

Graybeal proposed an equation to calculate the modulus of elasticity, shown below, in 2007 [10]. The data from the five materials tested in the 2018 also fitted this model for modulus of elasticity.

$$E_c = 46200\sqrt{f'_c} \quad (psi) \tag{2.1}$$

They conducted direct tension tests on the materials, using the method developed by Graybeal and Baby (2013) [11], which uses prismatic specimens with aluminum grips installed on both ends to allow for testing. The direct tension tests were idealized as having three phases. They were elastic, multi-cracking, and crack localization. The idealized stress-strain response is shown in Figure 2.3.

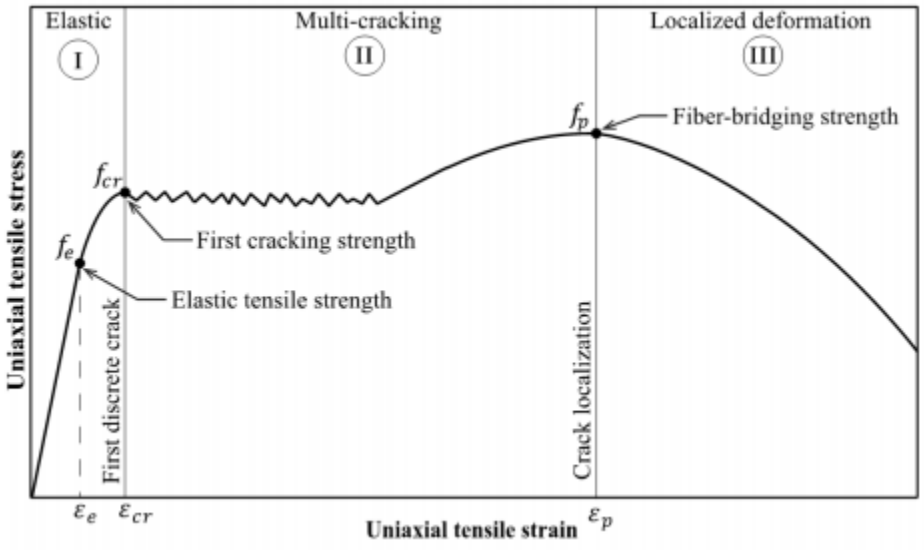

Figure 2.3: Figure 67 from Graybeal [9] Idealized uniaxial tensile response for UHPC

The results from the direct tension tests on the 2% batches of UHPC are shown in Figure 2.4. The tests took place 28 days after casting. In all cases the peak tensile strength occurred after first cracking.

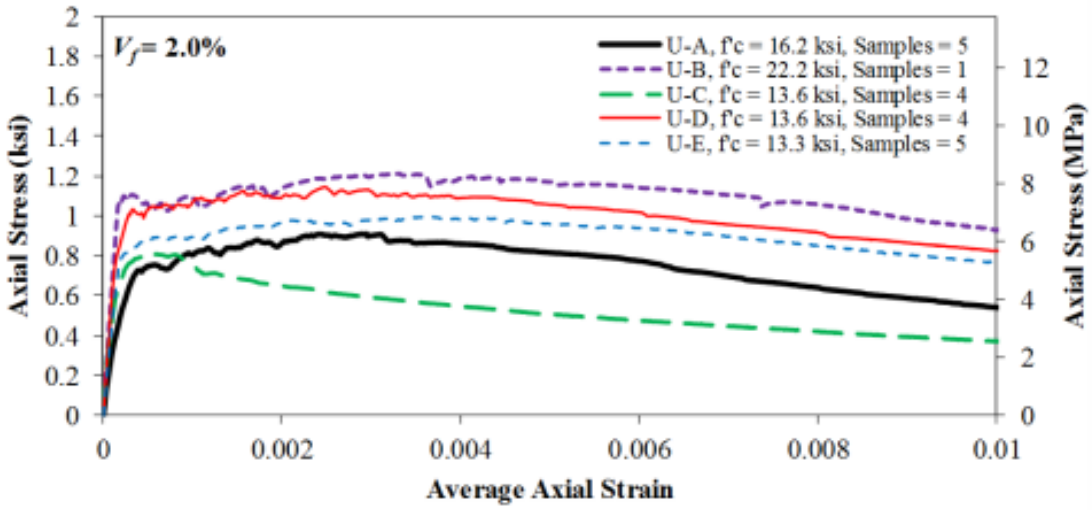

Figure 2.4: Figure 93 from Graybeal [9] Comparison of average tensile stress-strain responses for UHPC with 2% fiber

Based on a 2013 study by Graybeal [11], where UHPC was also tested in direct tension, the following expressions were developed to estimate tensile strength:

$$f_{ct} = 6.7\sqrt{f'_c} \quad (untreated\ specimens) \quad \text{(psi)} \tag{2.2}$$

$$f_{ct} = 8.2\sqrt{f'_c} \quad (steam\ cured\ specimens) \quad \text{(psi)} \tag{2.3}$$

These expressions were not addressed in the 2018 experiments.

In Graybeal's experimental project, no conclusions regarding the fiber content of UHPC were drawn. Instead, results were presented to provide an overview of the way different proprietary UHPC mixes behave.

While the 2018 study by Graybeal included the most recent and extensive material testing, there have been a large number of studies conducted on UHPC that include material properties. Graybeal (2013) [12] includes more material test results of proprietary UHPC. A non-proprietary UHPC mix was used by Azizinamini (2018) [13] to study accelerated retrofits of bridge columns using a UHPC shell. Data about the compressive and flexural strength of UHPC are included in the report. Floyd [14] has overseen multiple studies of the material properties of non-proprietary UHPC at the University of Oklahoma. Since these projects were completed in conjunction with this project, they will be discussed further in Chapter 6.

2.2 Shear Beam Tests

No records were found of pure shear tests conducted on panels. Therefore, the most closely related test information is presented here. Some tests have been conducted on beams made from fiber-reinforced concrete, but they inevitably involve combined shear and bending. They are discussed in this section. One series was also found on fiber-reinforced panels, subjected to pure shear, but those specimens also contained deformed bar reinforcement, which creates difficulties in separating the contributions of the bars and the fibers. They are presented in Section 2.3.

2.2.1 Sharma (1986)

Sharma (1986) [15] tested concrete beams subjected to combined bending and shear loading. The test specimens included both traditional concrete beams and fiber-reinforced concrete beams. All beams were reinforced with rebar in the longitudinal and transverse directions. Sharma determined that the shear strength of the fiber-reinforced concrete was based on transverse reinforcement and fiber content. Equations were developed based on the results of the study to model the contribution of each component.

The shear strength from transverse reinforcement is shown in Equation 2.4. It uses the traditional plastic truss model, with compression struts at 45 degrees, adopted by ACI 318-19 [16] and others.

$$V_s = \frac{A_v f_y d}{s} \tag{2.4}$$

Where:

$V_s = shear\ strength\ from\ shear\ reinforcement$

$A_v = area\ of\ shear\ reinforcement$

$f_y = yield\ strength\ of\ shear\ reinforcement$

$d = depth\ of\ beam$

$s = spacing\ of\ shear\ reinforcement$

The shear stress from the fibers is modeled by Equation 2.5.

$$v_{cf} = \frac{2}{3} f'_t \left(\frac{d}{a}\right)^{0.25} \tag{2.5}$$

Where:

$v_{cf} = shear\ stress\ from\ fibers$

$a = shear\ span\ of\ beam$

$d = depth\ of\ beam$

The tensile strength of steel fiber reinforced concrete, f'_t, is given by:

$$f'_t = 9.5\sqrt{f'_c}\ \ (psi) \tag{2.6}$$

Where:

$f'_t = tensile\ strength\ of\ concrete$

$f'_c = compressive\ strength\ of\ concrete$

The total shear strength is equal to the sum of the contribution from shear reinforcement and fibrous content.

The shear strength from steel fibers is based only on the tensile strength of the concrete, which itself depends on the compressive strength, and dimensions of the specimen. The percentage of fiber content is not taken into account and neither is the material, size, or shape of the fibers.

2.2.2 Narayanan and Darwish (1987)

Narayanan and Darwish (1987) [17] conducted a study similar to Sharma's in which they tested 50 beams in shear, using all fiber reinforced concrete. They established a parameter called the fiber factor, F, that took into account the fiber geometry, volumetric content of fibers in concrete, and bond, as given by Equation (2.7).

$$F = \frac{L}{D}\rho_f \eta_f \tag{2.7}$$

Where:

$F = fiber\ factor$

$L = fiber\ length$

$D = fiber\ diameter$

$\rho_f = volumetric\ fiber\ content\ expressed\ as\ a\ decimal$

$\eta_f = fiber\ bond\ factor$

The bond factor of the fiber is dependent on shape. It is equal to 0.5 for round fibers, 0.75 for crimped fibers, and 1.0 for indented fibers.

They related split cylinder tension strength to compressive strength and fiber factor by:

$$f_{spfc} = \frac{f'_c}{20-\sqrt{F}} + \sqrt{F} + 0.7 \quad (MPa) \tag{2.8}$$

Where:

$f_{spfc} = split\ cylinder\ strength\ of\ concrete$

The split cylinder strength was then used to find the total shear strength of fiber reinforced concrete. Other properties that were relevant are ultimate bond stress factor, ratio of shear reinforcement, and specimen dimensions. The proposed equation is as follows:

$$V_u = e\left[0.24 f_{spfc} + 80\rho\frac{d}{a}\right] + 0.41\tau F \quad (MPa) \tag{2.9}$$

$$e = \begin{cases} 2.8\dfrac{d}{a}, & \dfrac{a}{d} \leq 2.8 \\ 1.0, & \dfrac{a}{d} > 2.8 \end{cases}$$

Where:

$\rho = ratio\ of\ longitudinal\ reinforcement$

$\tau = ultimate\ bond\ stress\ of\ fiber\ matrix, taken\ as\ 4.15\ MPa$

2.2.3 Ashour et al. (1992)

Ashour et al. (1992) [18] conducted an experimental study on high-strength fiber reinforced concrete (HSRC) beams without shear reinforcement. They tested almost 20 specimens with varied percentages of longitudinal reinforcement and fiber content. They found that fiber reinforcing led to more ductile failure mechanisms than that of traditional concrete reinforced with stirrups.

A model for shear strength was developed based on the results of the beam tests. It is shown in the following equation. All variables are as they have been previously defined.

$$V_u = \frac{d}{a}\left[0.7\sqrt{f'_c} + 7F + 17.2\rho\right] \quad (MPa) \tag{2.10}$$

This model is similar to the one developed by Narayanan and Darwish in that they both depend on fiber factor, compressive strength of concrete, longitudinal reinforcement, and the relationship between span and depth of the beam. This is different from the model developed by Sharma that did not include any characteristics of the fiber reinforcement.

2.2.4 Kwak et al. (2002)

Kwak et al. (2002) [19] reviewed results from a total of 139 tests on steel fiber reinforced concrete beams without stirrups but with longitudinal bars to resist bending. The results showed that nominal shear stress at cracking and the ultimate shear strength increased with increasing fiber content. Additionally, as the fiber content increased, the failure mode changed from shear to flexure. The results of the experimental program were used to evaluate the previously mentioned shear equations from Sharma, Narayanan and Darwish, and Ashour et al., as well as develop a new shear equation. The equation developed by Kwak et al. is shown in Equation (2.11).

$$V_u = 2.1 f_{spfc}^{0.7} (\rho \frac{d}{a})^{0.22} + 0.8 v_b^{0.97} \quad (MPa) \tag{2.11}$$

With:

$$v_b = 0.41 \tau F \quad (MPa) \tag{2.12}$$

Where:

$\rho = ratio\ of\ longitudinal\ reinforcement$

$\tau = ultimate\ bond\ stress\ of\ fiber\ matrix, taken\ as\ 4.15\ MPa$

$F = fiber\ factor\ as\ defined\ by\ Nrayanan\ and\ Darwish$

2.3 Pure Shear Panel Tests

2.3.1 Susetyo (2010)

Susetyo (2010) [20] tested steel fiber-reinforced concrete (FRC) panels under in-plane pure shear using a panel testing machine. The panels were made of FRC with varying fiber content and had rebar only in the longitudinal direction. The fibers used were all steel fibers with hooked ends but varied in dimeter and length. The fiber content ranged from 0.5% to 1.5% while the rebar in orthogonal directions were consistently 3.31% and 0.42%. The specimen properties are included in Table 2-2. The specimens are named based on designated compressive strength (C), fiber size (F), and fiber percentage (V).

Table 2-2: Table 1 from Susetyo [20] Shear Panel Test Specimens

ID	Specified f'c (MPa)	Fiber Content (%)	Fiber Type
C1C	50	-	-
C1F1V1	50	0.5	RC80/50-BN
C1F1V2	50	1.0	RC80/50-BN
C1F1V3	50	1.5	RC80/50-BN
C1F2V3	50	1.5	RC80/30-BP
C1F3V3	50	1.5	RC65/35-BN
C2C	80	-	-
C2F1V3	80	1.5	RC80/50-BN
C2F2V3	80	1.5	RC80/30-BP
C2F3V3	80	1.5	RC65/35-BN

The results of the shear tests are shown in Table 2-3. They are, compressive strength (f_c'), shear strength at first cracking (v_{cr}), shear strain at first cracking (γ_{cr}), ultimate shear strength (v_u), shear strain at ultimate (γ_u), final crack width (w_m), and final crack slip (s_m). The results indicated that concrete compressive strength did not have a substantial influence on the shear response of the FRC as there was seemingly no correlation between the two strengths. It was also noted that, based on the data, the fiber content impacted the shear strength more than compressive strength- more fibers led to higher shear strength.

Table 2-3: Table 4 from Susetyo [20] Summary of Results from Shear Panel Tests

ID	f'_c (MPa)	v_{cr} (MPa)	γ_{cr} (mε)	v_u (MPa)	γ_u (mε)	w_m (mm)	s_m (mm)
C1C	65.7	2.01	0.086	5.77	6.01	0.55	57.2
C1F1V1	51.4	2.09	0.197	3.53	2.77	0.55	114.4
C1F1V2	53.4	2.65	0.139	5.17	5.27	0.45	54.7
C1F1V3	49.7	1.83	0.055	5.37	5.10	0.45	57.2
C1F2V3	59.7	1.85	0.070	6.68	6.20	0.45	38.1
C1F3V3	45.5	2.24	0.118	5.59	4.27	0.50	57.2
C2C	90.5	2.57	0.099	6.40	7.00	0.50	66.2
C2F1V3	79.0	2.17	0.131	6.90	5.25	0.70	36.0
C2F2V3	76.5	1.59	0.110	6.31	4.35	0.65	46.6
C2F3V3	62.0	2.10	0.222	5.57	4.97	0.60	40.6

2.3.2 Ishtewi (2012)

Ishtewi (2012) [21] conducted a research project on the shear capacity of steel fiber-reinforced concrete under pure shear at the University of Dayton. The project involved testing 14” x 14” x 2.25” FRC panels under in-plane shear, similar to the work at the University of Toronto, but the tests were conducted in a specially fabricated shear testing frame that was loaded by an MTS machine shown in Figure 2.5. Fiber content was varied based on percentage and type of fibers. There was no longitudinal or transverse reinforcement in the specimens.

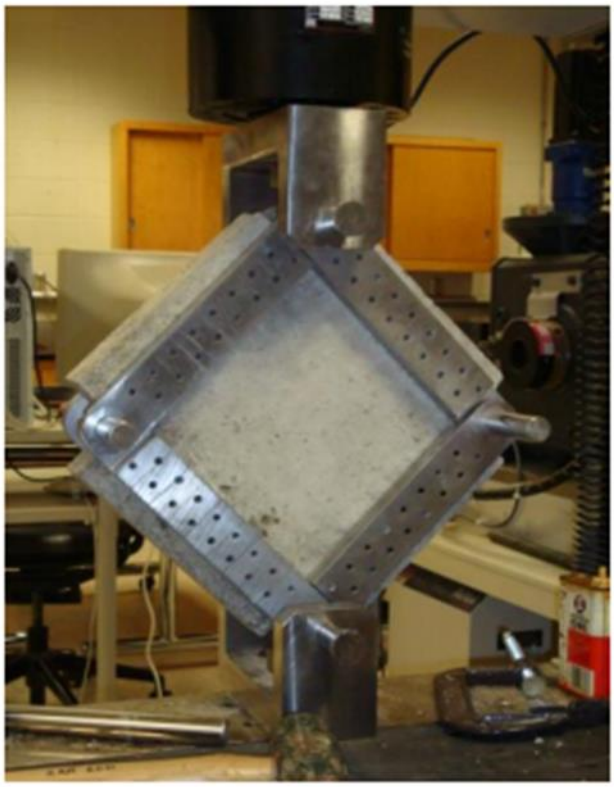

Figure 2.5: Ishtewi shear testing setup [21]

In this research project, Ishtewi determined the contribution to the shear strength of the fibers by finding the shear strength of concrete alone by using the ACI equation used for shear strength of beams, Equation (2.13), then dividing it by the experimental shear strength of the FRC. They found that the contribution from fibers was substantial. This concurs with the conclusion drawn by Susetyo, that fibers have a larger effect than concrete strength on the shear strength of the FRC. Ishtewi et al. compared their results with the proposed models by Sharma, Narayanan and Darwish, and Ashour. They found that Sharma's model was the worst fit and Ashour's model fit the experimental data best. However, the model is designed for beam specimens under a different testing style, and is therefore not ideal. For example, the predictive equations include the shear beam span, but Ishtewi's tests were not conducted on beams and therefore had no dimension that could be interpreted as a span.

$$V_c = 2\sqrt{f_c'}bd \quad (psi) \tag{2.13}$$

Chapter 3: Experimental Test Program

The testing program had two primary objectives:

- To determine the performance of UHPC in pure shear
- To conduct material tests using a mix design developed by the University of Oklahoma but locally materials sourced, for the purpose of determining the effects of obtaining materials from different sources.

The shear tests were carried out in the University of Washington panel element tester, and the material tests consisted of compression cylinders, dog-bone direct tension specimens, and flexural beam tests. The standard mix used 2% steel fibers by volume and materials local to Seattle, Washington, while other specimens were comprised of 1% steel fibers by volume and Seattle-sourced materials, 2% fibers with materials local to Norman, Oklahoma. Each UHPC batch was used to cast a shear panel specimen along with cylinders, beams, and dog-bones to be used in material tests.

The specimens were separated into four test series:

1. Test series 0: Two 2% fiber UW batches used to perfect the mix design and mixing/casting procedure (UW2A, UW2B)
2. Test series 1: Three 2% fiber UW batches (UW2C, UW2D, UW2E)
3. Test series 2: One 1% fiber UW batch (UW1)
4. Test series 3: One 2% OU fiber batch (OU2)

3.1 Mix Design

The UHPC mix design specified by OU is provided in Table 3-1. Note that oz/cwt and w/c refers to the total cementitious materials.

Table 3-1: OU Mix Design

University of Oklahoma Mix Design			
Material	Per yd^3	Unit	Supplier
Type 1 Cement	1179.6	lb	Ash Grove (Chanute, KS)
Slag	589.8	lb	Holcim (Chicago, IL)
Silica Fume	196.6	lb	Norchem (Beverly, OH)
Fine Masonry Sand	1966	lb	Metro Materials (Norman, OK)
Steel Fibers (Dramix OL 13/0.2)	255.2	lb	Bekaert
Superplasticizer (Glenium 7920)	15.77	oz/cwt	BASF
Water	0.2	w/c	
	393.2	lb	

The OU mix design in Table 3-1 was used for batches UW2A and UW2B using 2% fiber content and materials sourced from Seattle. Batch UW2A was found to be too stiff to allow proper deposition and consolidation in the forms. Consequently, the dosage of superplasticizer (Glenium 7920) was increased for the next batch. In batch UW2B, the dosage of superplasticizer proved to be too great, the material was too flowable, and most of the fibers sank, leaving a non-uniform distribution within the cementitious matrix. The superplasticizer dosage was adjusted again, and a retarder was also added. The retarder increased the setting time of the UHPC to provide more workability. The adjusted mix design given in Table 3-2 was used for all remaining specimens. It proved to be both workable and able to support the fibers. The only variations were to the fiber content and the material source, as originally planned, with admixture quantity being reduced proportionately as fiber content was reduced.

Table 3-2: UW Mix Design

University of Washington Mix Design			
Material	Per yd^3	Unit	Supplier
Type 1 Cement	1179.6	lb	Salmon Bay Sand & Gravel (Seattle, WA)
Slag	589.8	lb	Lafarge (Seattle, WA)
Silica Fume	196.6	lb	Salmon Bay Sand & Gravel (Seattle, WA)
Fine Masonry Sand	1966	lb	Salmon Bay Sand & Gravel (Seattle, WA)
Steel Fibers (Dramix OL 13/0.2)	255.2	lb	Bekaert
Superplasticizer (Glenium 7920)	20.7	oz/cwt	BASF
Retarder (Daratard-40)	5.66	oz/cwt	GCP Applied Technologies
Water	0.2	w/c	
	393.2	lb	

3.2 Mixing and Casting Procedure

The mixing and casting procedure used for UHPC strongly affects the quality of the material (Peruchini 2017). The mixing procedure developed by Peruchini [22] was followed, since all available mixing equipment was the same. The general procedure requires a dry mix of cement, slag, and sand, and a separate slurry of sand, silica fume, water, superplasticizer, and retarder. One third of the water and superplasticizer is set aside to be incorporated into the material later. The slurry is then dumped into a pan mixer and the dry mix slowly added in. Once the dry mix is completely incorporated into the slurry, the fibers are slowly added as well as the remaining water and superplasticizer. It is important to save this step for last to avoid clumping. A detailed mix procedure can be found in the Appendix.

The mixing procedure used at OU differed from the one used at UW in multiple ways. First, there was no slurry mix. Instead, all dry materials were mixed together first. Then all of the water with half of the superplasticizer was added to the mixture. The remaining superplasticizer was added as the dry materials formed into a flowable material. Finally, the fibers were incorporated into the cement over the course of two minutes, which is a faster rate than what was used at UW.

Once the UHPC was mixed, the molds were filled as quickly as possible to avoid setting. Smaller molds, such as cylinders, beams, and dog-bones, were rodded and vibrated in accordance with ASTM [23]. The shear panel was too large to fit on the vibrating table and too crowded with rebar to fit a vibrator inside, so it was rodded to achieve uniform consolidation. After casting, all specimens were covered with wet burlap. The materials test specimens were then moved to a lime bath to cure.

3.3 Testing Plan

The following testing plan was developed to collect relevant data from each UHPC batch. Details of the ASTM standards can be found in the Appendix.

Table 3-3: Experimental Testing Plan

University of Washington Testing Plan			
Test	Dimension (in)	Test Day	Reference
Compression Cylinder	4x8	3 @ 3, 28, 56	ASTM C39 [24]
Modulus of Elasticity	4x8	3 @ 56	ASTM C469 [25]
Direct Tension	3.5x2x12	3 @ 56	
Flexural Beam	3x3x11	3 @ 56	ASTM C78 [26]
Pure Shear	35x35x2.75	1 @ 56	

3.3.1 Material Tests

3.3.1.1 Compression

Twelve 4”x8” cylinders were cast with each batch of UHPC to be tested in compression. The tests were conducted in a 400-kip Forney machine, using end caps made of neoprene pads confined in a recess in a steel plate. Figure 3.1 shows a typical compression failure.

Figure 3.1: Typical compression failure

3.3.1.2 Modulus of Elasticity

Cylinders used for modulus of elasticity tests were sulfur capped and tested in a 300-kip capacity Baldwin machine using a conventional testing rig, shown in Figures 3.2 and 3.3, respectively.

Figure 3.2: 300-kip Baldwin testing machine

Figure 3.3: Modulus of Elasticity testing rig

3.3.1.3 Direct Tension

To determine the tensile strength of UHPC, direct tension tests were performed using a dogbone design. As shown in Figure 3.4, the specimens had a reduced section resulting in a 2”x2” failure region. A #3 rebar was embedded in each end of the specimen. The goal was to reduce any accidental end eccentricity by adding a flexible element at each end of the load train. This approach was chosen in preference to Graybeal’s direct gripping method because of concerns about the alignment accuracy that was possible with the test equipment available. Each face of the dogbone was fitted with a linear potentiometer spanning the intended failure region.

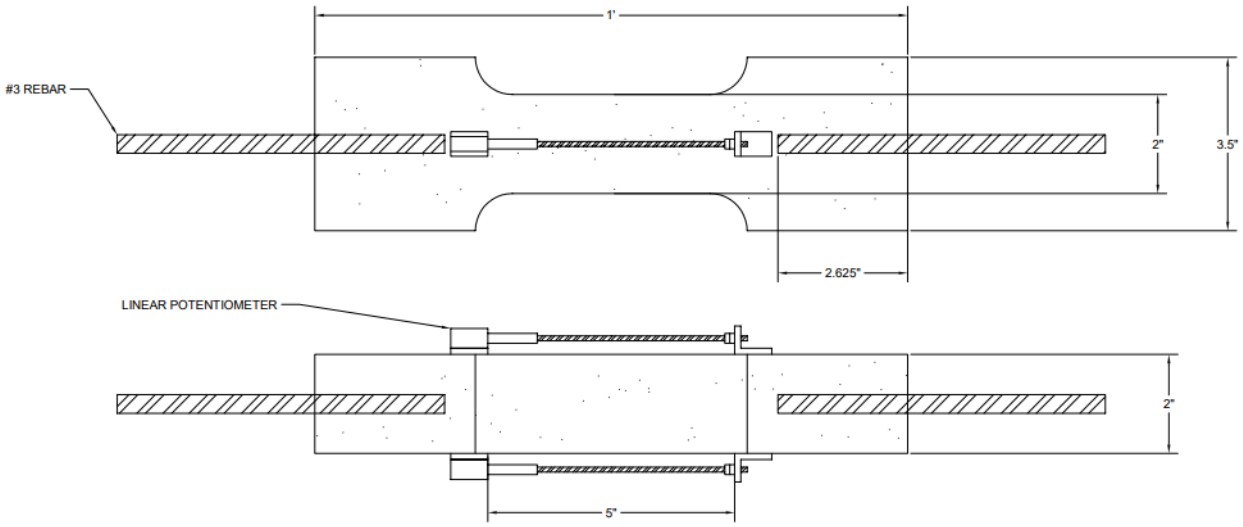

Figure 3.4: Direct tension dogbone specimen drawing

The tension tests were performed using a 100-kip capacity MTS testing frame (Figure 3.5). The specimen was loaded using displacement control at a rate of 0.002 in/min up to first cracking then 0.04 in/min for the remainder of the test. In most cases, failure occurred at approximately the center of the reduced section. Any eccentricity introduced during specimen casting or placement in the test machine was recorded by averaging the potentiometer readings on both faces of the specimen.

Figure 3.5 100-kip MTS testing machine

3.3.1.4 Flexural Beam

For each batch of UHPC, three 3”x3”x11” beams were tested in four-point loading, with a 9” span, using the 300-kip Baldwin. They were fitted with instrumentation on top and bottom to obtain strain readings. On the top face, a 60 mm strain gage from Texas Measurements (PL-60-11-3LJC-F) was adhered directly to the concrete. On the bottom face, a linear potentiometer was positioned to span across the desired gage length. Additional potentiometers were situated vertically next to each side of the beam to capture vertical displacement. The typical flexural beam setup is shown below.

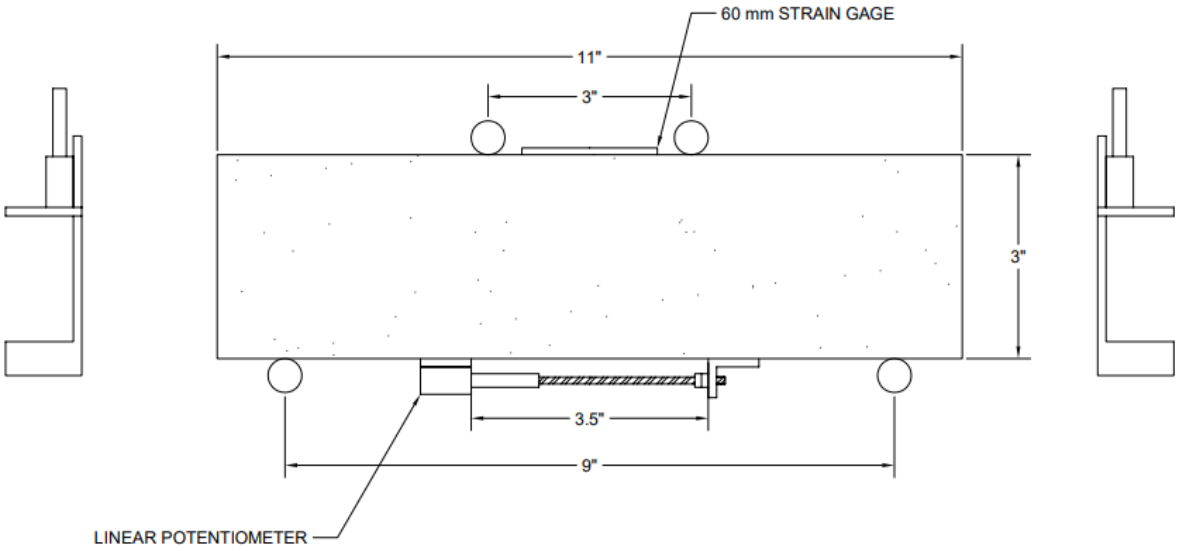

Figure 3.6: Flexural beam testing setup

3.3.2 Pure Shear Test

3.3.2.1 Panel Element Tester

One of the two objectives of the testing program was to evaluate the response of UHPC specimens subject to pure shear. This was done by testing square panels in the University of Washington Panel Element Tester, shown in Figure 3.7. In the panel tester, the panel is loaded by 20 vertical and 20 horizontal links. Of these 40 links, 37 are connected to hydraulic cylinders and 3 are fixed (denoted with a yellow base). The fixed links act as supports. At each attachment point, one horizontal and one vertical link are pin-connected to a steel block that is attached to reinforcing bars embedded in the specimen. The actuators can be controlled in groups, thereby allowing any combination of shear and direct stress to be applied to the panel.

To avoid out-of-plane movements, tension arms are used to attach the shear keys to a back frame. Pure shear loading (shown with green arrows on Figure 3.7a) was obtained by retracting group 3 and group 4 actuators while advancing group 1 and group 2 actuators using a hydraulic pump and load maintainer. Details on how the panel tester is operated, including additional equipment, is available in the Appendix.

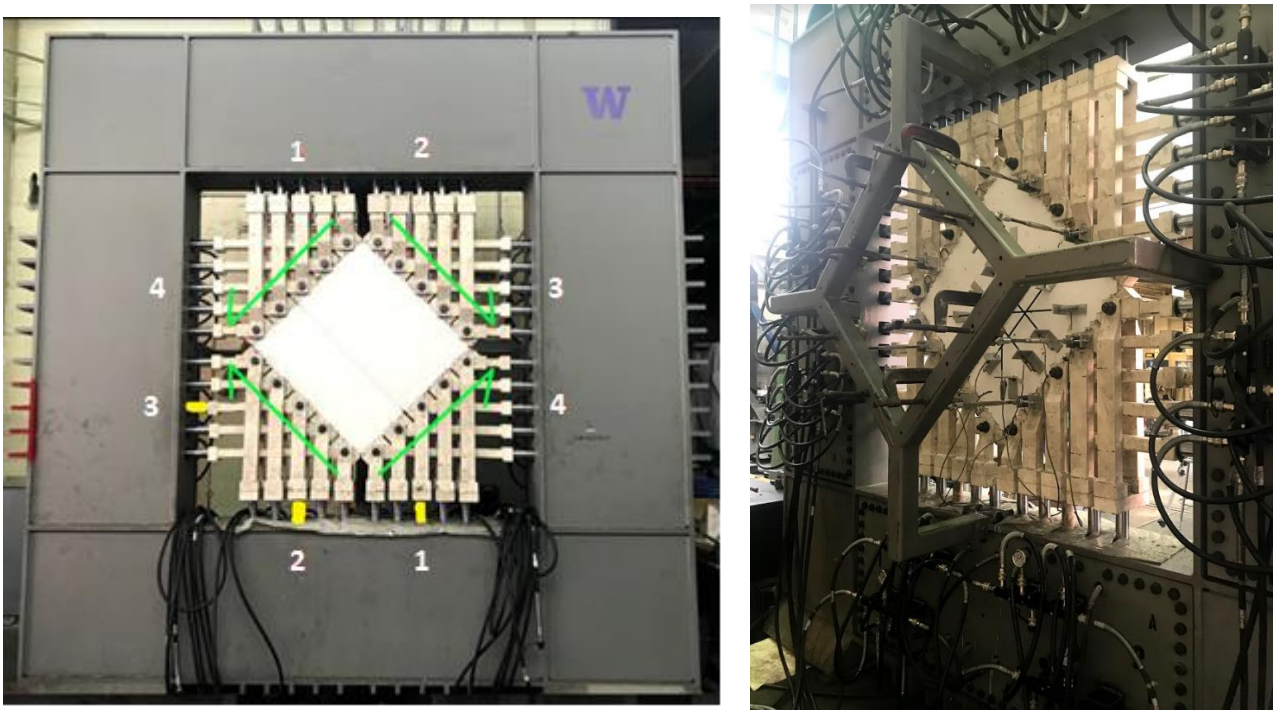

Figure 3.7: UW Panel Element Tester (a) front and (b) back

3.3.2.2 UHPC Specimen

The UHPC specimens were designed to meet the dimensional constraints of the UW Panel Element Tester. To ensure accurate dimensions, the shear keys used to connect the specimen to the machine were also used as formwork for casting. This resulted in a specimen of size 35x35x2.75 (in). Although the goal was to test pure UHPC, with no rebar, rebar was required to attach the shear keys to the concrete specimen and ensure that failure did not occur outside of the intended test region. This is shown in Figure 3.8. The rebar must also be symmetrical to avoid any out-of-plane eccentricity when loaded. Therefore, the panel was designed to have two layers of rebar in the y-

direction and one in the x-direction, with a small test region made of pure UHPC with no rebar (Figure 3.8). To promote failure in the test region, the panel thickness was reduced by 0.25 inches on the top and bottom, to a net thickness of 2.25', and a 2.5" long crack initiator was added to each end of the region (Figure 3.9). The same specimen design was used for every batch of UHPC.

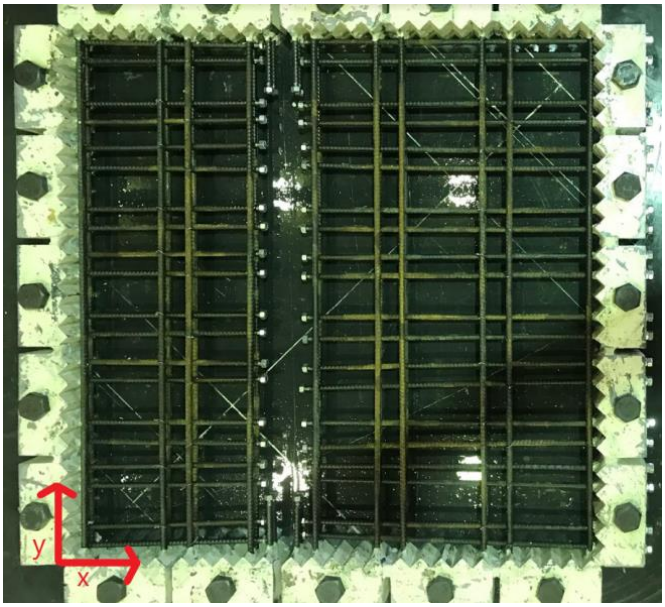

Figure 3.8: Rebar layout

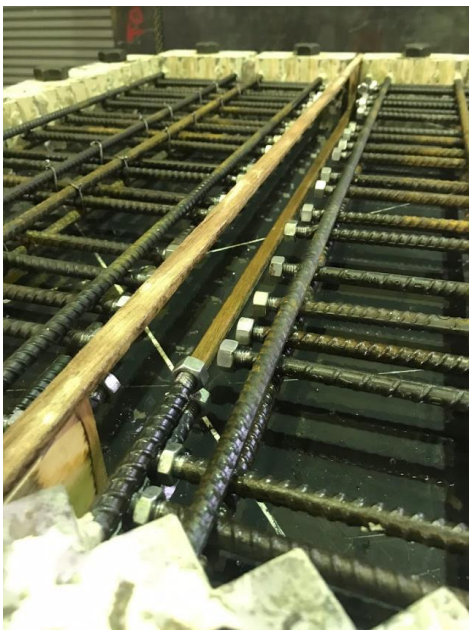

Figure 3.9: Test region failure promotion

Each rebar was threaded on both ends so that nuts could be used to secure its position. One 3/8"-16 hex full nut was tightened at the inner end of each embedded rebar. On the outside of the shear keys, one washer, one 3/8"-16 hex full nut, and one 3/8"-16 hex jam nut was used. Initially, two full nuts were used in the Test Series 0 panels to avoid failure by stripping the thread of a single nut, which had previously occurred in similar panel tests. This design added too much extra length to the specimen making it difficult to fit in the panel tester. To avoid this problem, while still protecting the specimen from unwanted failure, the second nut was switched to a jam nut. Detailed panel drawings are included in Figure 3.10. Note that shear key units are millimeters since the panel tester and shear keys were originally designed in metric. Rebar lengths are given in English units.

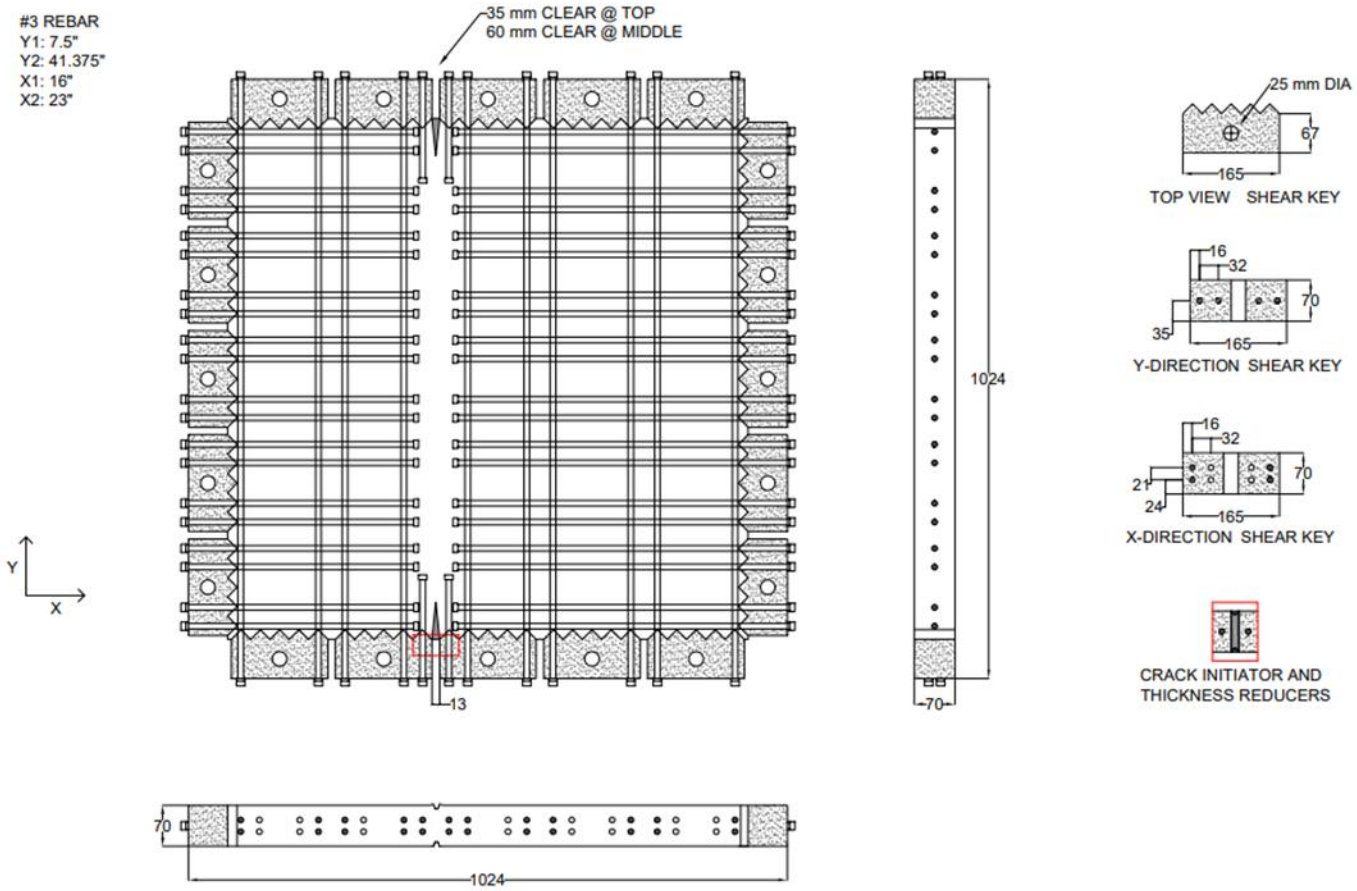

Figure 3.10: Panel specimen drawing with reinforcement and shear key details

3.3.2.3 Instrumentation

Instrumentation was added to the panel and connected to a data acquisition system (DAQ) in order to record loads and displacements. To track displacement, LED Optotrak targets and linear potentiometers were used. The LED targets were taped to the front face of the panel in a 5x5 grid with dimensions approximately 540 mm x 540 mm. The Optotrak camera was set up directly in front of the panel to get a clear reading of the targets. A level was used to verify that the camera was oriented horizontally to simplify data processing. The camera took photos at a frequency of 5 Hz, each time recording the x, y, and z position of each target. These measurements were processed to calculate global strain for the outer square, along with local strain in each of the smaller 16 squares. The Optotrak setup and camera can be viewed in Figure 3.11. It was kept consistent for all tests.

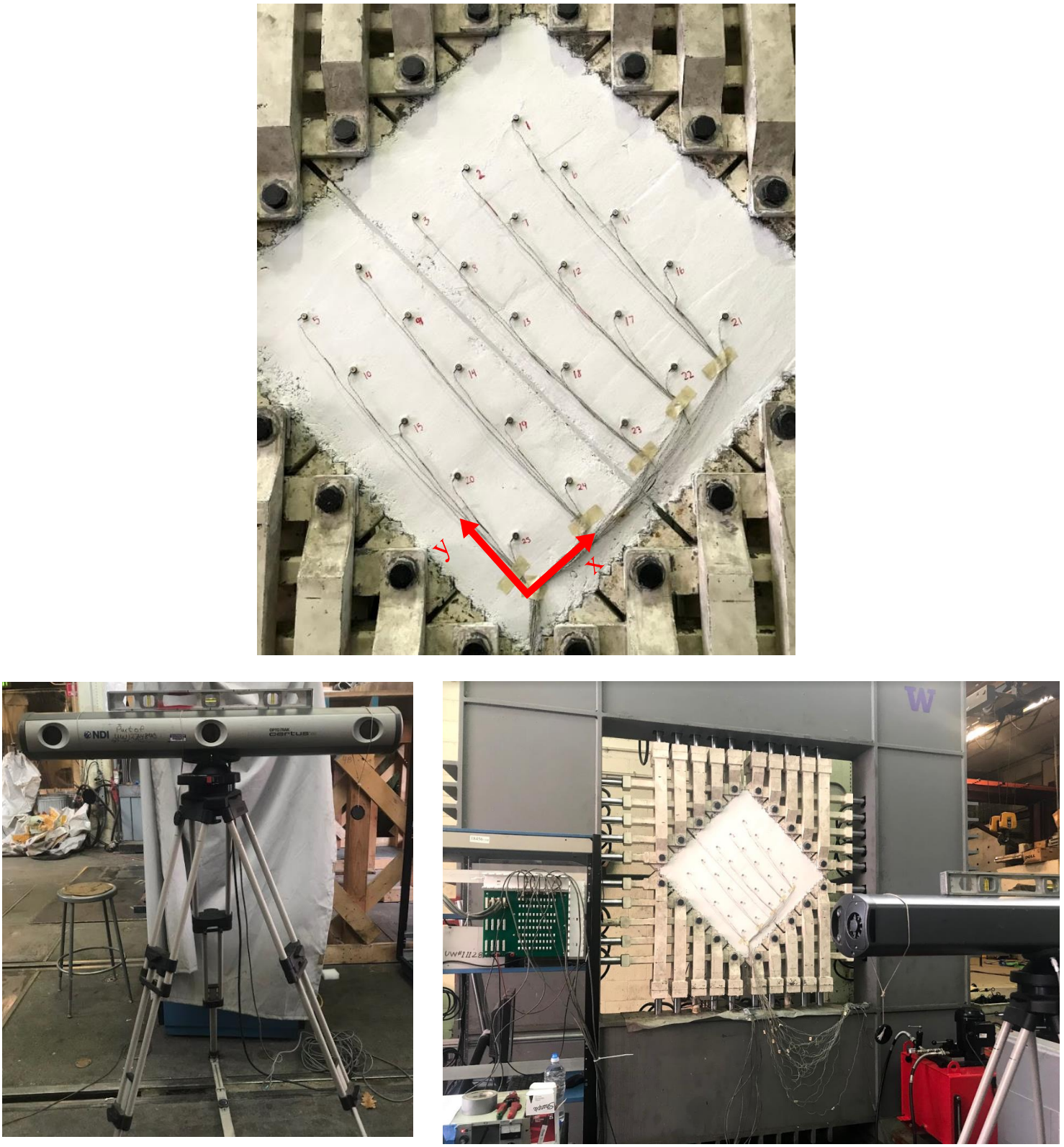

Figure 3.11: (a) Optotrak targets (b) Optotrak camera (c) test setup

As a backup to the Optotrak readings, potentiometers were used on the back face of the panel. Eight potentiometers were used to create a 405 mm x 405 mm grid, as shown in Figure 3.12: two x-direction, two y-direction, two across the failure to read slip, one vertical, and one horizontal. This layout ensures that all global strains can be determined from the resulting data.

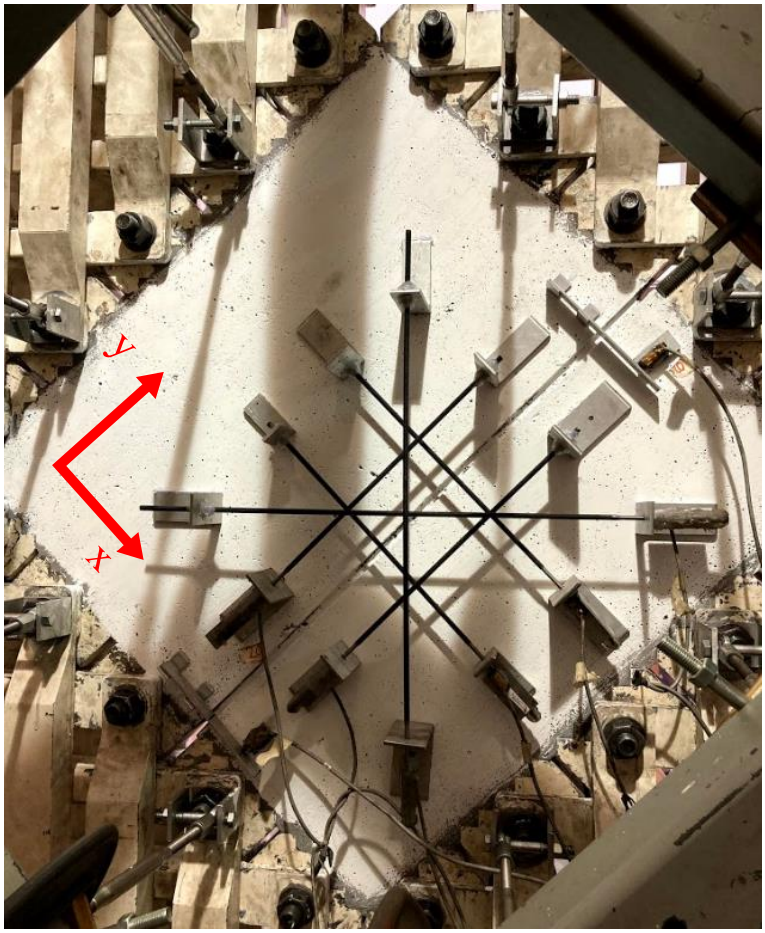

Figure 3.12: Linear potentiometer layout

Pressure sensors were used to record hydraulic oil pressure throughout the test. Two were attached directly to the load maintainer; one on the advance line and one on the retract line. While only one is necessary to record pressure data, both advance and retract were measured to continuously confirm that the ratio between them was correct. Maintaining a constant ratio is necessary because the actuators have different effective areas in tension and compression. A third pressure sensor was hooked up to the back of the panel tester to verify that the oil was circulating through the machine properly and there were no leaks.

3.3.2.4 Test Procedure

Once the panel, pump, load maintainer, instrumentation, and DAQ were set up (see Appendix for detailed steps) the test was performed. First, the hydraulic pump was set to 7000 psi. This pressure was transferred to the load maintainer. Next, the load maintainer valves were opened at a slow rate until reaching 1000 psi. Once this pressure was reached, the load maintainer held the pressure constant while both faces of the panel were inspected for cracks. This process continued, in intervals of 1000 psi, until first cracking was observed. After cracking, the intervals between marking cracks were reduced to 500 psi. The pressure was increased until the panel split in two pieces along the reduced area section, at which point the oil pressure to the load maintainer was turned off. The same testing procedure was used for each panel. Figure 3.13 shows the typical panel failure with cracks marked.

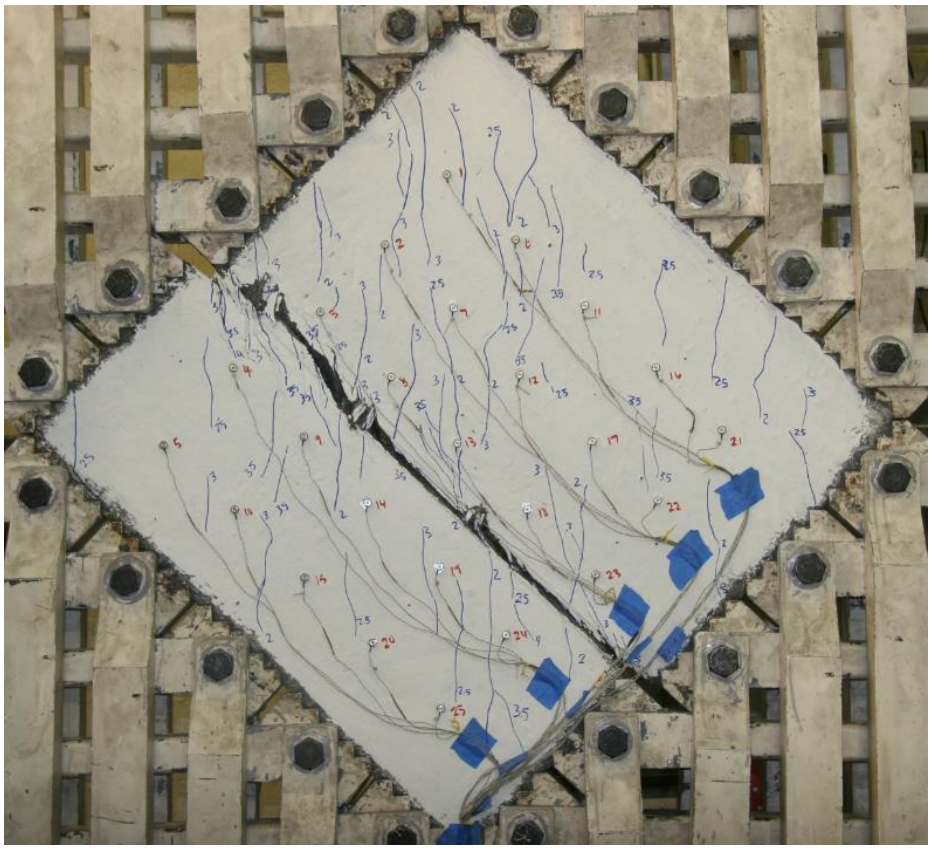

Figure 3.13: Typical pure shear failure

3.4 Data Processing

This section presents the equations used to process the raw data from testing. Information regarding the instrumentation that resulted in the raw data is also included.

3.4.1 Material Tests

3.4.1.1 Compression

The compression cylinder tests provided the load reading at the time of UHPC failure. This value was then divided by the cross-sectional area of the cylinder to determine the compressive strength of the UHPC.

$$f_c' = \frac{P}{A} \tag{3.1}$$

Where:

$f_c' = compressive\ strength$

$P = load$

$A = cross - sectional\ area$

3.4.1.2 Modulus of Elasticity

The modulus of elasticity tests resulted in load and displacement readings for the duration of the test. The load data were divided by the cross-sectional area of the cylinder to determine the stress. The displacement data were divided by the gage length of the LVDT to determine the corresponding strain for each stress value. The stress and strain recordings were plotted to show the compression stress-strain curve for UHPC, and then used to find the modulus of elasticity.

$$E = \frac{\sigma}{\varepsilon} \tag{3.2}$$

Where:

$E = modulus\ of\ elasticity$

$\sigma = stress$

$\varepsilon = strain$

3.4.1.3 Direct Tension

The direct tension tests resulted in load and displacement readings for the duration of the test. The load data were divided by cross-sectional area at the reduced section of the dogbone to determine the stress. The peak load was used to find the tensile strength. The displacement was divided by the gage length of the potentiometer to give strain. Since there was a potentiometer on each side of the dogbone, the strains from both were averaged. The stress and strain data were used to plot the tensile stress-strain curve for UHPC.

$$f_t = \frac{P}{A} \tag{3.3}$$

Where:

$f_t = tensile\ strength$

$P = load$

$A = cross - sectional\ area\ of\ dogbone$

3.4.1.4 Flexural Beam

The modulus of rupture equation that was used was derived for linear elastic behavior. This assumption is accurate for first cracking but it is likely not reliable after cracking when the fibers are engaged instead of the cementitious component. However, the linear elastic equation was used for pre- and post-cracking strength since that is what was used in the research from OU, so that the results could be compared.

$$M = \frac{P}{2} \times \frac{L}{3} \tag{3.4}$$

$$S = \frac{bd^2}{6} \tag{3.5}$$

$$f_r = \frac{M}{S} = \frac{PL}{bd^2} \tag{3.6}$$

Where:

$f_r = flexural\ strength\ (modulus\ of\ rupture)$

$M = moment$

$S = elastic\ section\ modulus$

$P = load$

$L = span\ length$

$b = width\ of\ beam$

$d = depth\ of\ beam$

The tensile strength of the UHPC was found from the flexural beam tests assuming plastic behavior, which is likely more representative for UHPC since the fibers provide the great majority of the tension strength after initial cracking. This tensile strength from flexural testing can be compared with the tensile strength from direct tension testing. It is derived here assuming that the ratio of compressive strength to tension strength is high enough to characterize the neutral axis as lying at the top of the beam.

$$M = \frac{P}{2} \times \frac{L}{3} \tag{3.4}$$

$$Z = \frac{bd^2}{2} \tag{3.7}$$

$$f_t = \frac{M}{Z} = \frac{PL}{3bd^2} \tag{3.8}$$

Where:

$f_t = tensile\ strength$

$M = moment$

$Z = plastic\ section\ modulus\ for\ unequal\ tension\ and\ compression\ strengths$

$P = load$

$L = span\ length$

$b = width\ of\ beam$

$d = depth\ of\ beam$

3.4.2 Pure Shear Test

The shear stress of the UHPC was determined based on the shear panel tests. The pressure was read by pressure sensors throughout the duration of the test. The force in the horizontal and vertical actuators was found by multiplying the pressure by the area of the corresponding actuator. Since the advance and retract lines were calibrated using the appropriate ratio, either advance or retract pressure and actuator area can be used. The force was converted to shear force by multiplying by

number of actuators on each side of the panel (5) and finding the diagonal component of the force. Finally, the shear stress was found by dividing shear force by the cross-sectional area of the failure region. This process is shown in the following equations.

$$F = p_{act} A_{act} \tag{3.9}$$

$$V = 5\sqrt{2} \times F \tag{3.10}$$

$$v = \frac{V}{A_f} \tag{3.11}$$

Where:

$F = force$

$p_{act} = pressure\ of\ either\ advance\ or\ retract\ line$

$A_{act} = area\ of\ either\ advance\ (3.19\ in^2)\ or\ retract\ (6.49\ in^2)\ actuator$

$V = shear\ force$

$v = shear\ stress$

$A_f = cross - sectional\ area\ of\ failure\ region$

The crack opening displacements and shear strains were found from the Optotrak readings. However, the Optotrak system records data on its own system and is separate from the DAQ on which the potentiometers and pressure sensors were recorded. It was therefore necessary to synchronize the two data streams. This was done by plotting the displacements from the Optotrak and potentiometers, then applying a time shift in the Optotrak data so that the two plots matched. With this shift applied, the load data and Optotrak displacement data correspond to one another and thereafter the potentiometer data was no longer used.

The Optotrak displacements were used to obtain strains. Shear strains were of the greatest interest. They were obtained for the panel as a whole by using the four outermost corner markers, on a grid of approximately 20” x 20”. In addition, the local strains within each 5” x 5” sub-grids were obtained from the corner markers of the sub-grid. This allowed the strains in the failure region to be computed using the finer sub-grid. Three typical sub-grids adjacent to and spanning the failure region are shown in Figure 3.14. The accompanying equations for crack width, crack slip, and

shear strain follow. Effects from rigid body rotation were accounted for by subtracting any global rotation from the individual target displacements.

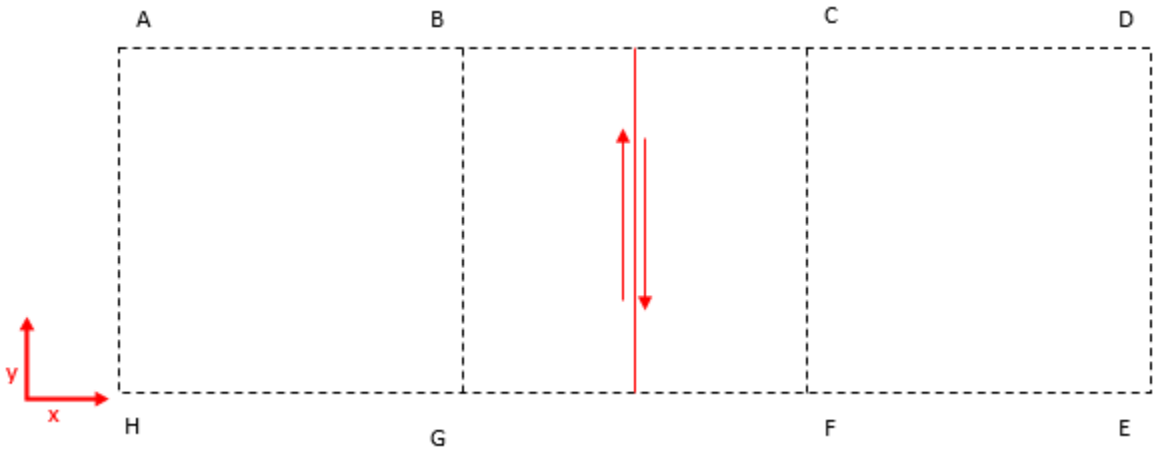

Figure 3.14: Typical Optotrak target grids with failure

Crack Width:

$$w_1 = C_x - B_x \quad (3.12)$$

$$w_2 = F_x - G_x \quad (3.12)$$

The crack width was found for each row of targets resulting in a total of 5 individual crack width results. The five were averaged to find one value for crack width.

Crack Slip:

$$s_1 = B_y - C_y \quad (3.13)$$

$$s_2 = G - F_y \quad (3.13)$$

The crack slip was found for each row of targets resulting in a total of 5 individual crack slip results. The five were averaged to find one value for crack slip.

Shear Strain:

Shear strain was found for each individual grid, but the strain for grids outside of the failure region were negligible.

The shear strain is defined by:

$$\gamma = \frac{du}{dy} + \frac{dv}{dx} \tag{3.14}$$

Where:

$\gamma = shear\ strain$

$\frac{du}{dy} = rate\ of\ change\ in\ x - displacement\ with\ respect\ to\ y - axis$

$\frac{dv}{dx} = rate\ of\ change\ in\ y - displacement\ with\ respect\ to\ x - axis$

The sample equation is shown for the grid that includes the failure region (BCFG).

$$\gamma = \frac{1}{2}\left[\left(\frac{\Delta G_x - \Delta B_x}{B_y - G_y} + \frac{\Delta G_y - \Delta F_y}{F_x - G_x}\right) + \left(\frac{\Delta F_x - \Delta C_x}{C_y - F_y} + \frac{\Delta B_y - \Delta C_y}{C_x - B_x}\right)\right] \tag{3.15}$$

3.4.3 Instrumentation Resolution and Accuracy

The Optotrak accuracy is 0.1 mm and resolution is 0.01 mm [27]. Therefore, strains obtained from small displacements are subject to round-off errors. This should be taken into account when reviewing test results at small initial crack opening. The Optotrak camera is also subject to outside sources of error. It records null results if someone stands between the camera and targets (e.g. during crack marking). These null data points need to be removed from the record. Vibrations from the floor can theoretically cause data errors, but, because the lab floor is a 12” thick slab on grade, such vibrations are expected to be negligible. Careful observation of the record shows no signs of such vibrations. Impacts to the camera or tripod can clearly cause problems. These are expected to be rare and easily identifiable from the record.

Chapter 4: Experimental Results

The program included seven shear panel specimens, each with its own material test series. The results are summarized in Table 4-1. Specimens UW2A through E were fabricated using UW materials and 2% fiber. Specimen UW1A used UW materials and 1% fiber, while Specimen OU2 used OU materials and 2% fiber.

Specimens UW2A and UW2B were cast first, and posed considerable difficulty in mixing and depositing the concrete. During the process, the mix had to be adjusted, and the resulting materials were poor quality. Consequently, those two specimens were treated as trial specimens, and the results were not used in subsequent comparisons for the purpose of identifying trends. For all the other specimens, the mixing and depositing of the concrete was satisfactory. Thus, the nominally identical specimens UW2C through E were used as a reference group, and specimens UW1 and OU2 were used to investigate the effects of changing one variable at a time. In a few specimens, the material test series was not completed, or the instrumentation in the panel tests malfunctioned. Those deviations are noted in the detailed descriptions that follow.

Table 4-1: Summary of UHPC Results

UHPC Strength Results (MPa)					
Batch	Compression	EMod	Tension	Flexural	Shear
UW2A	N/A	N/A	N/A	N/A	N/A
UW2B	124	36400	4.52	17.2	7.33
UW2C	129	N/A	N/A	N/A	8.89
UW2D	139	39600	8.23	19.7	9.75
UW2E	134	39200	4.89	16.8	9.91
UW1	133	36600	4.66	12.9	7.38
OU2	133	42100	6.68	18.2	9.29

4.1 Test Series 0: Trial Panels

4.1.1 UW2A

The first trial panel, UW2A, was subject to multiple complications. This was the first attempt to make the concrete more flowable than the initial sample batch, therefore the dosage of superplasticizer was increased to twice the prescribed amount of 15.77 oz/cwt, or 31.54 oz/cwt. The concrete was no longer able to suspend the fibers and they sank to the bottom of the formwork for the cylinders, beams, dogbones, and panel. While the concrete still exhibited a material compressive strength that was quite high, other properties, such as the tension strength were adversely affected by the poor distribution of fibers.

In addition to the concrete complications, which affected the compression, modulus of elasticity, direct tension, flexural beam, and shear panel tests, the Optotrak suffered technical difficulties during the shear panel test. This rendered the target data useless, leaving only the potentiometer data. That data addressed the same global quantities as the Optotrak, but, because there were only six instruments compared with the 25 Optotrak markers, it was less detailed. Furthermore, the mounting brackets for the potentiometers were prone to falling off when the concrete cracked near them.

No data are reported for Specimen UW2A, because the material was poor and the instrumentation malfunctioned. The batch did, however, provide important experience in mixing the material and was instrumental in subsequently developing a successful UHPC mix design.

4.1.2 UW2B

The next attempt at refining the UHPC mix design was batch UW2B. The dosage of superplasticizer that was used was 1.15x the original amount, or 18.14 oz./cwt. During mixing this seemed like the perfect compromise and the smaller, solid, material specimens were successfully cast. However, casting the panel, which is not only bigger but is crowded with reinforcing bars, proved to be a challenge. The UHPC set quickly and did not flow well between rebars. This experience led to the addition of retarder to the mix for the purpose of slowing the set. In all subsequent specimens, 5.66 oz./cwt of Daratard-40 chemical retarder was used, which led to

material that was flowable enough to consolidate well in the forms, but not so flowable that the fibers sank.

During panel testing first cracking occurred at a shear stress of roughly 3.5 MPa. As the loading increased, cracking continued to take place at a 45 degree angle to the intended failure line, or slot. Failure was initiated at the bottom right crack initiator where a crack first formed around 5.5 MPa and opened up around 7 MPa. The failure did not propagate through the failure region in a completely concentrated manner. However, as slip increased, the failure continued along the slot and the panel broke into two separate pieces.

The following set of figures is used for each panel test specimen. They are explained in detail for the first UHPC batch, but not the others.

The first figure (Figure 4.1) is a summary of material test results, and includes three sub-plots. The first is a plot of Compressive Strength vs time. Compression tests were generally performed three times per batch, but in some cases only twice. The data points are shown by circle markers, with linear interpolation between them.

The second sub-plot shows the Modulus of Elasticity. Three tests were done per batch, so there are three sets of data. All the cylinders were loaded to the same strain of 0.0015 for consistency.

Next, tensile stress vs strain for three samples is shown. In this case, the data was cut off at a strain of 0.01 to focus on the region of response that engaged the steel fibers. Taking the gauge length of the potentiometers into account (5”), this was a crack opening of just over 1 mm.

The final plot shows the load vs. displacement data for one of the UW2B flexural beam tests. The initial slope of the curve, before first cracking, is not linear as it should be and the slope of the line is about an order of magnitude too low. Additionally, the beam deflections shown in the data were much higher than what was physically observed during testing. Therefore, it can be concluded that the flexural beam instrumentation was not functioning as intended. It is believed that the problems with the vertical deflections might have been caused by potentiometer supports that were too

flexible. The loads were recorded from the pressure cell in the test machine, but the test used such a low fraction of the machine capacity that the procedure led to stepping, rather than a smooth curve. This problem could be fixed with the use of a load cell calibrated to read low loads. Since the displacement data for the flexural test was unreliable, and the load data exhibited serious stepping, it will not be included in the results for the remaining UHPC batches, or in any future analysis.

Photos of the material test failures can be found in the Appendix.

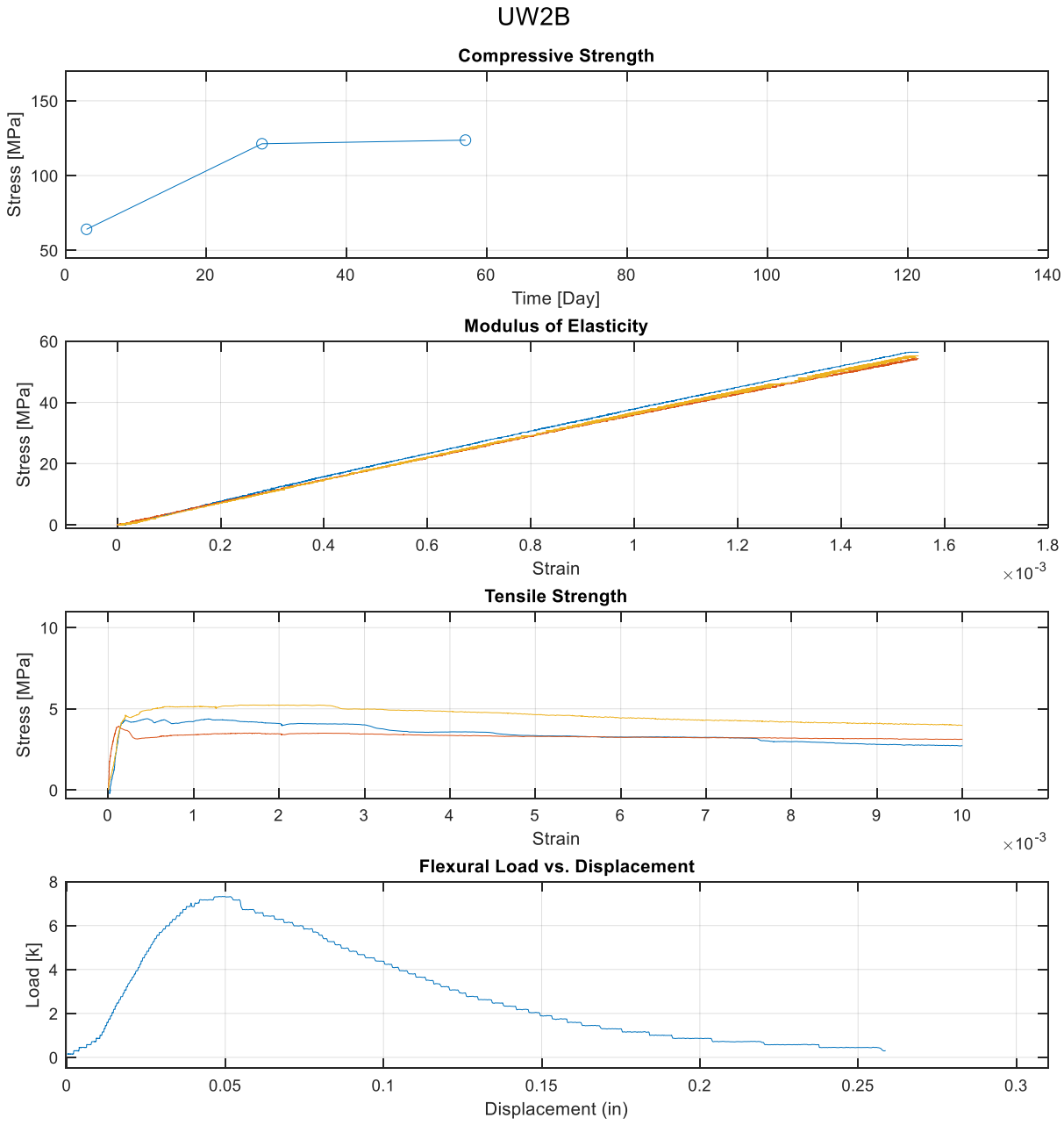

Figure 4.1: UW2B material tests results: (a) Compressive Strength, (b) Modulus of Elasticity, (c) Tensile Strength, and (d) Flexural Load vs. Displacement

The following figures, Figure 4.2 to Figure 4.6, refer to the pure shear panel tests. Figure 4.2 shows the stress vs time of the test. The constant portions of the plot indicate time that was spent inspecting and marking cracks on the specimen. The final data point occurs at the instant of failure. All data shown in the ensuing figures was cut off at the same time corresponding to failure. Three milestones are marked on the plot: first cracking, crack localization, and failure. First cracking is defined as the moment at which cracking first became noticeable upon visual inspection. Crack localization is the point at which individual cracks coalesced to form a single crack along the failure line. Failure is the exact moment the panel separated, before the actuators showed a large jump in free movement. The portion of testing where actuators experienced free movement will be referred to as post-failure, and is not shown on the graph. These markers are included on all other plots when applicable.

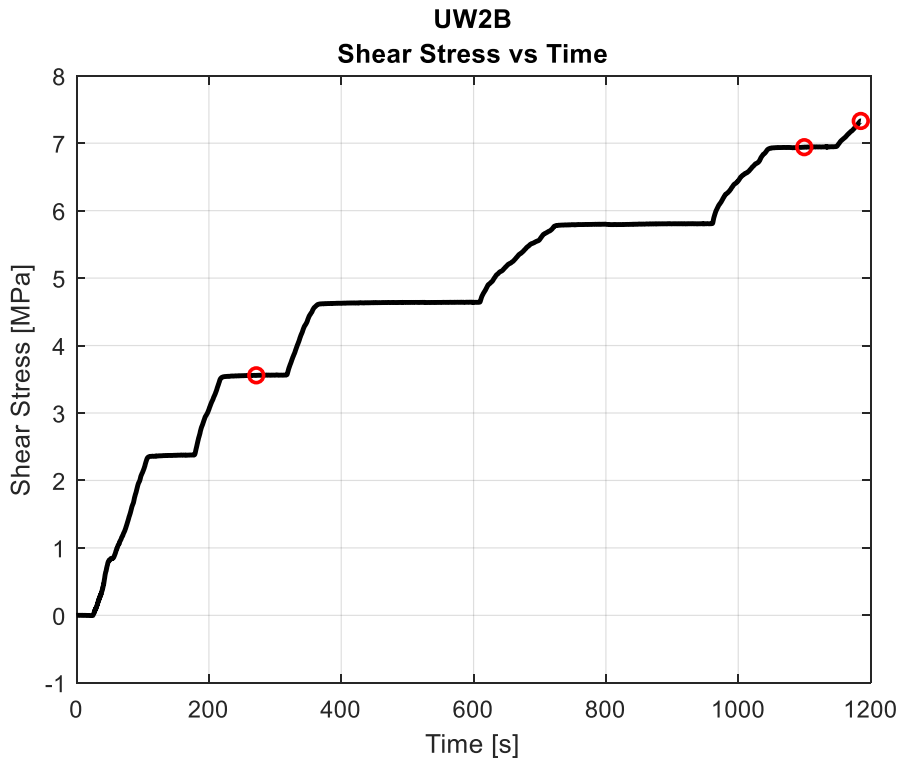

Figure 4.2: UW2B Shear Stress vs Time with first cracking, crack localization, and failure marked

Figure 4.3 is based on the Optotrak LED Targets. The figure shows the initial position of targets in blue and the final position, directly before failure, in red. The intended failure line runs parallel to the y-axis, roughly at the 200 mm position in the x-direction. The figure is rotated 45 degrees clockwise from the testing position so that the local x- and y-axes align with the global coordinate system.

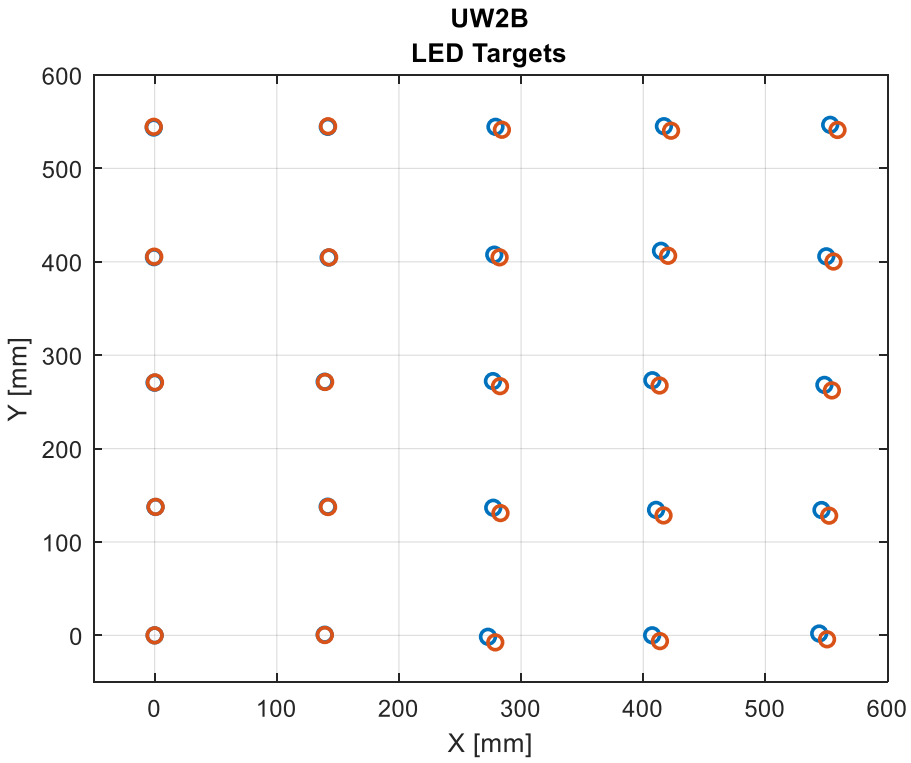

Figure 4.3: UW2B LED targets initial vs final position

The next group of plots, Figure 4.4, shows the shear stress vs crack width, shear stress vs crack slip, and crack width vs crack slip. The crack width is considered crack opening in the x-direction and crack slip is the relative movement of the two parts of the panel in the y-direction. Markers indicating first cracking, crack localization, and failure are also included.

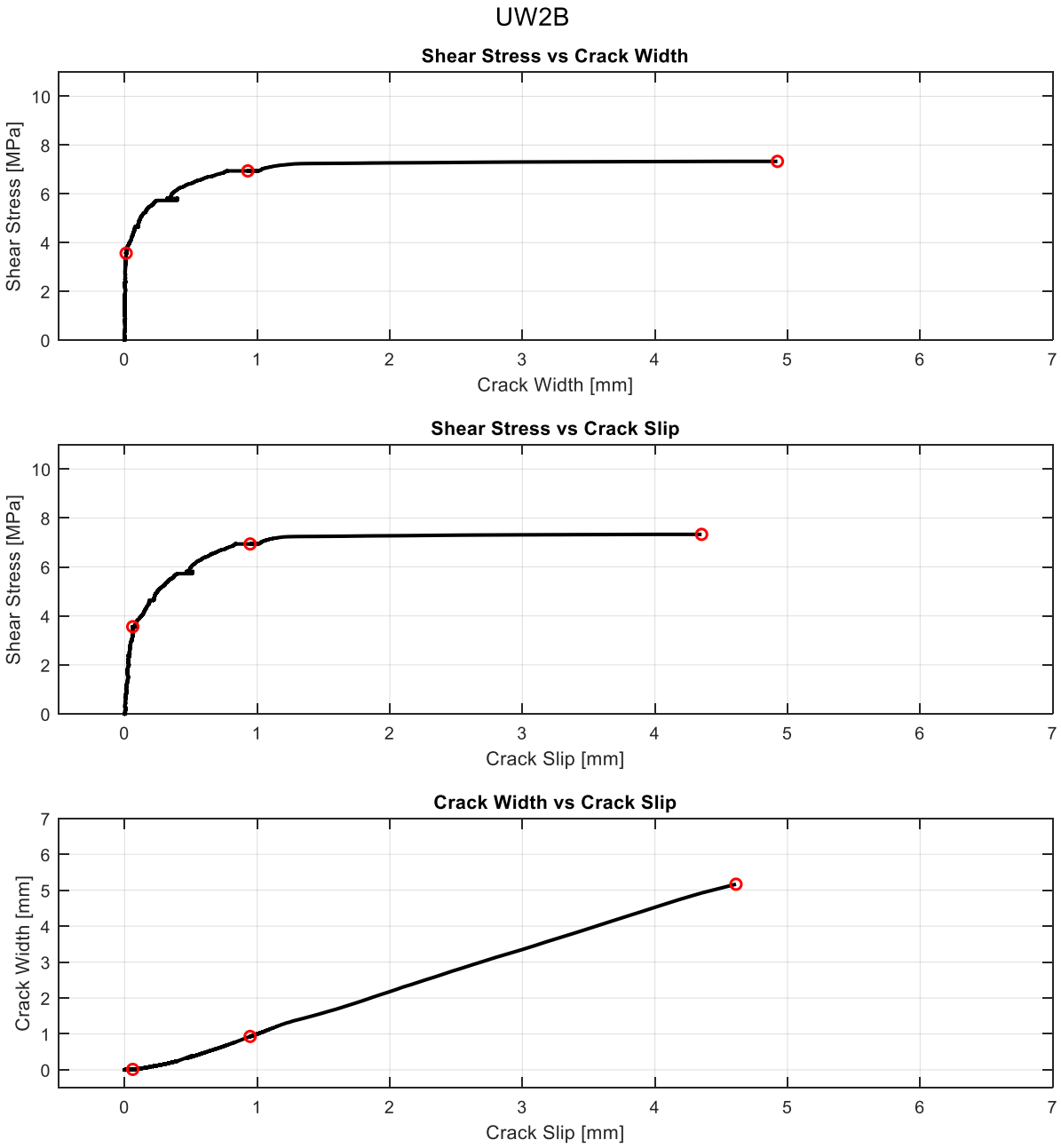

Figure 4.4: UW2B Shear Stress vs Crack Width, Shear Stress vs Crack Slip, Crack Width vs Crack Slip with first cracking, crack localization, and failure marked

Figure 4.5 provides a graded representation of the x-, y-, and shear strain experienced by the specimen at the point of failure. Each parameter was calculated between sets of four Optotrak targets. This resulted in sixteen smaller grids within the global grid of targets with their own characteristics. Each type of strain is reported in the same scale so that the color gradient is consistent across all three figures.

Finally, test photos corresponding to five phases are included in Figure 4.6. The phases are as follows: (a) start of test, (b) first cracking, (c) crack localization, (d) failure, and (e) post-failure. Phases (b), (c), and (d) can be traced back to the markers on Figure 4.2 and Figure 4.4.

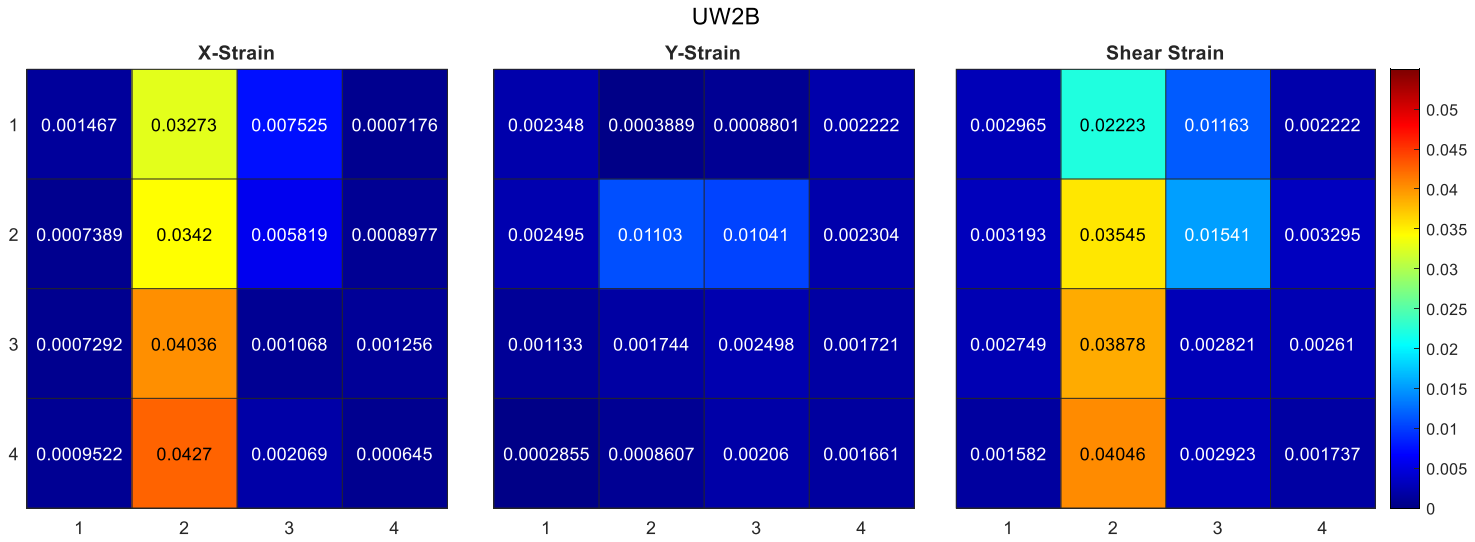

Figure 4.5: UW2B X-Strain, Y-Strain, and Shear Strain for individual target grids

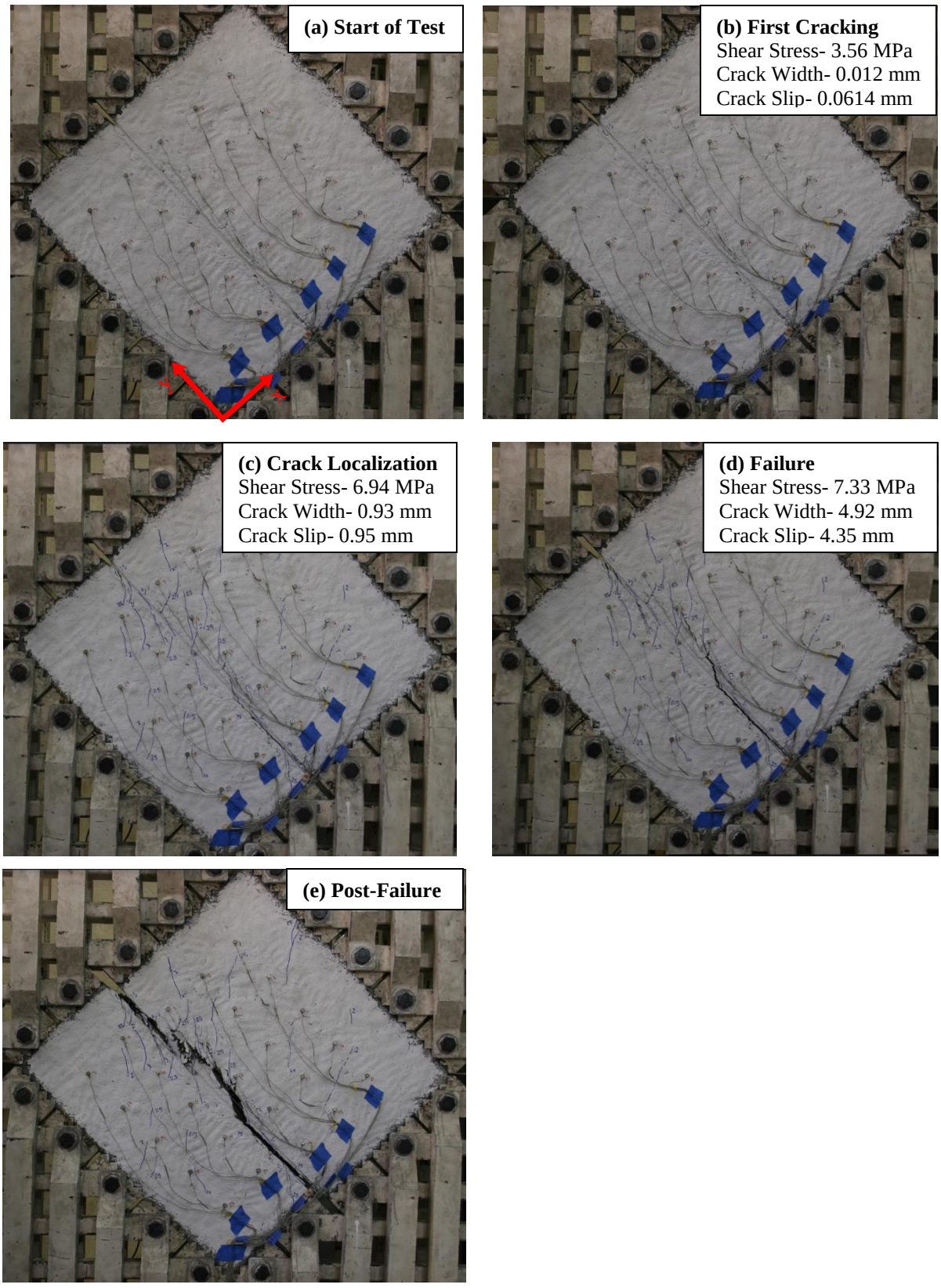

Figure 4.6: UW2B test photos of (a) start of test, (b) first cracking, (c) crack localization, (d) failure, and (e) post-failure

4.2 Test Series 1: 2% Fibers using UW Materials

The standard UHPC batch used 2% fiber content. Three of these batches were made using UW materials in order to collect enough data to get an accurate idea of the typical UHPC behavior. All mixing, casting, and testing procedures were identical for batches UW2C, UW2D, and UW2E.

4.2.1 UW2C

Due to outside circumstances, material tests were not completed for the UW2C batch with the exception of compression tests. Figure 4.7 shows these results.

During panel testing first cracking occurred at a stress of roughly 3.2 MPa. As the loading increased, hardly any additional cracking took place. Failure happened abruptly at 8.9 MPa and looked completely concentrated. The failure line perfectly followed the intended line with very few cracks concentrated around the line.

The same six figures were reproduced using the UW2C test results, with the exception of the Modulus of Elasticity and direct tension test results. Figure 4.8 through Figure 4.12 reference the pure shear panel test. For a detailed description of each figure and any plots, see Section 4.1.

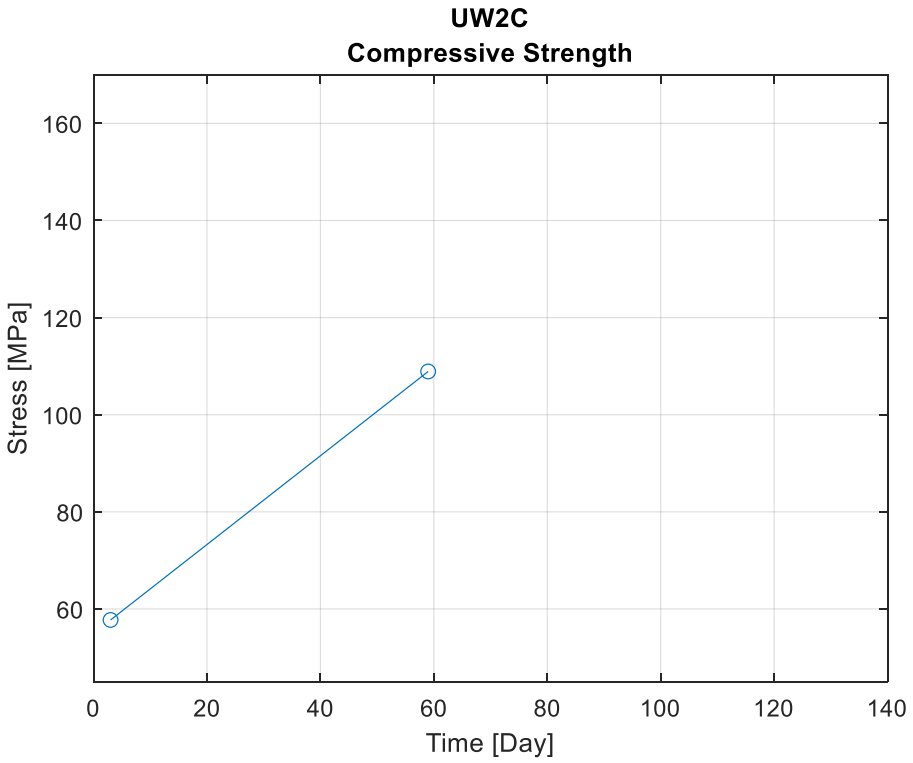

Figure 4.7: UW2C material tests results: (a) Compressive Strength, (b) Modulus of Elasticity, and (c) Tensile Strength

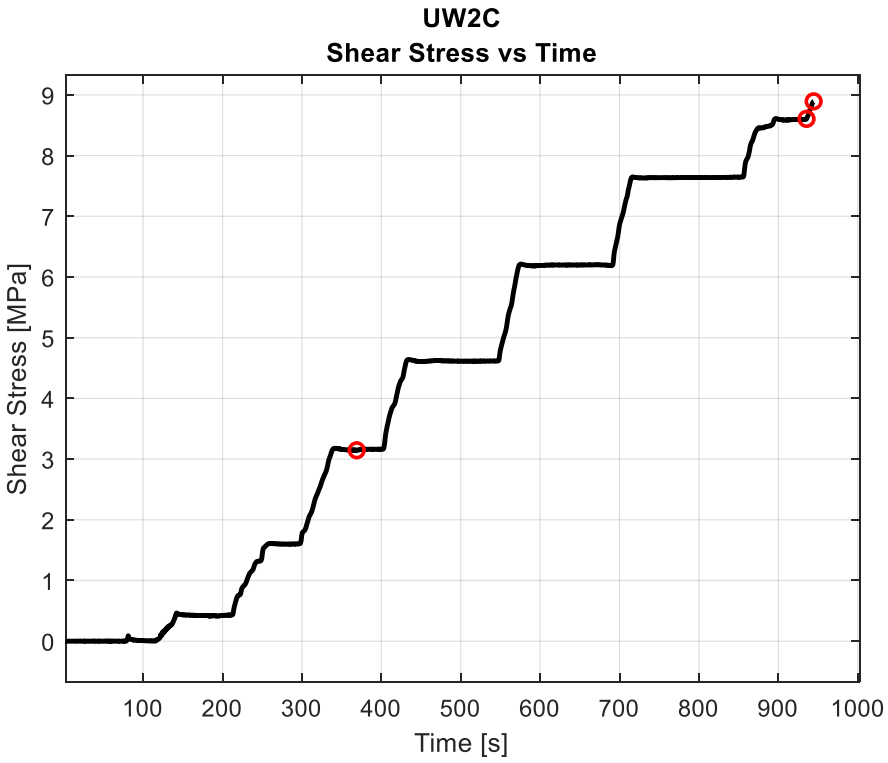

Figure 4.8: UW2C Shear Stress vs Time with first cracking, crack localization, and failure marked

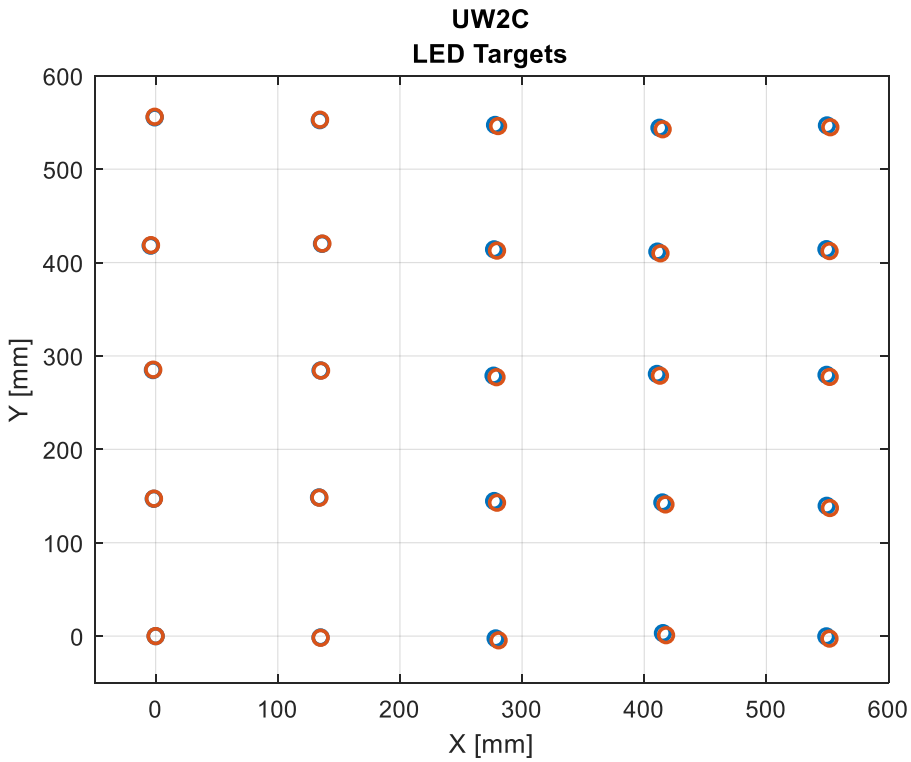

Figure 4.9: UW2C LED targets initial vs final position

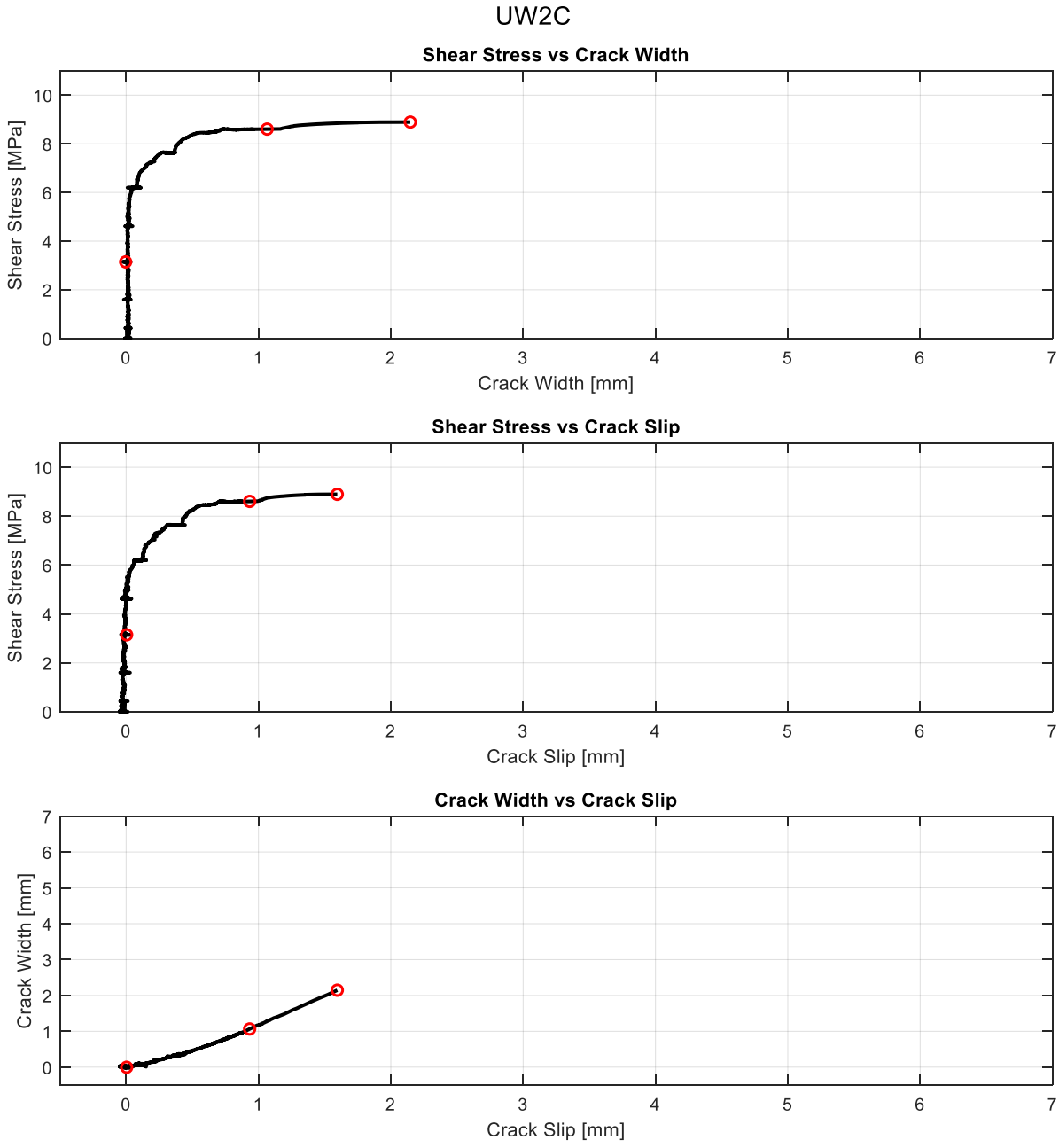

Figure 4.10: UW2C Shear Stress vs Crack Width, Shear Stress vs Crack Slip, Crack Width vs Crack Slip with first cracking, crack localization, and failure marked

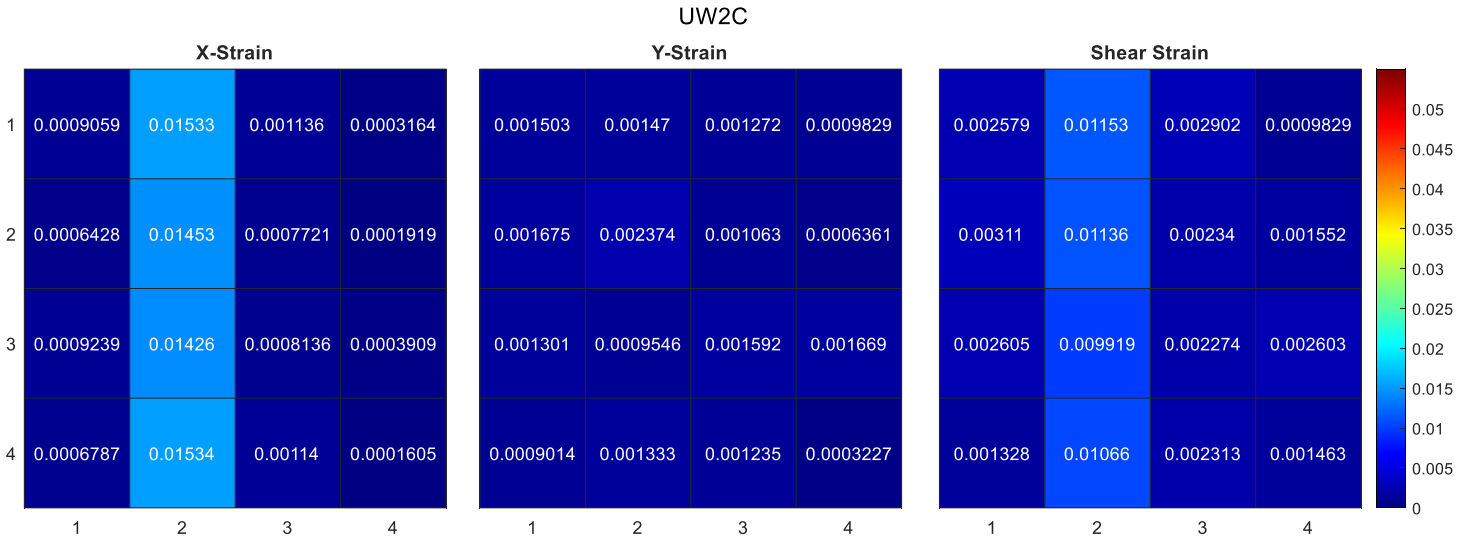

Figure 4.11: UW2C X-Strain, Y-Strain, and Shear Strain for individual target grids

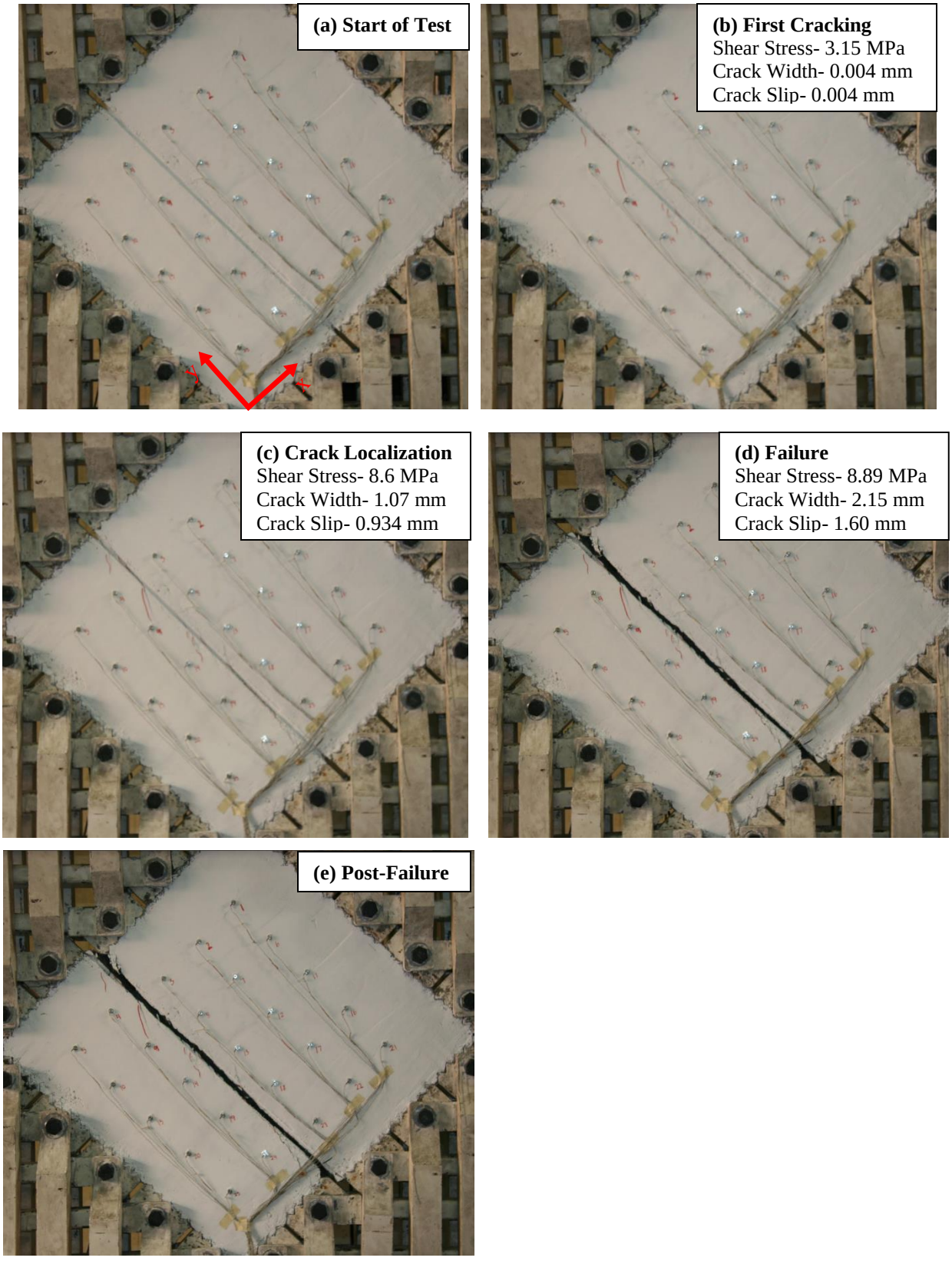

Figure 4.12: UW2C test photos of (a) start of test, (b) first cracking, (c) crack localization, (d) failure, and (e) post-failure

4.2.2 UW2D

During panel testing first cracking did not occur until a stress of 4.7 MPa. As the loading increased, cracking continued to take place at 45 degree angles to the designated failure line. Failure was initiated at the top left crack initiator where a crack was first formed around 8 MPa and began opening not long after. The upper left side of the panel continued to open more, while the bottom right side stayed intact. Finally, the failure reached the right side of the panel through 45 degree cracking in the middle of the panel. Although the failure was initiated along the intended failure line, it ended up following a path parallel to the line. Based on the location of the failure, it appears to have happened along the line of nuts at the ends of the embedded bars instead of along the slot intended to initiate shear failure.

The same seven figures were reproduced using the UW2D test results. Figure 4.13 contains the material test results while Figure 4.14 through Figure 4.18 reference the pure shear panel test. For a detailed description of each figure and any plots, see section 4.1.

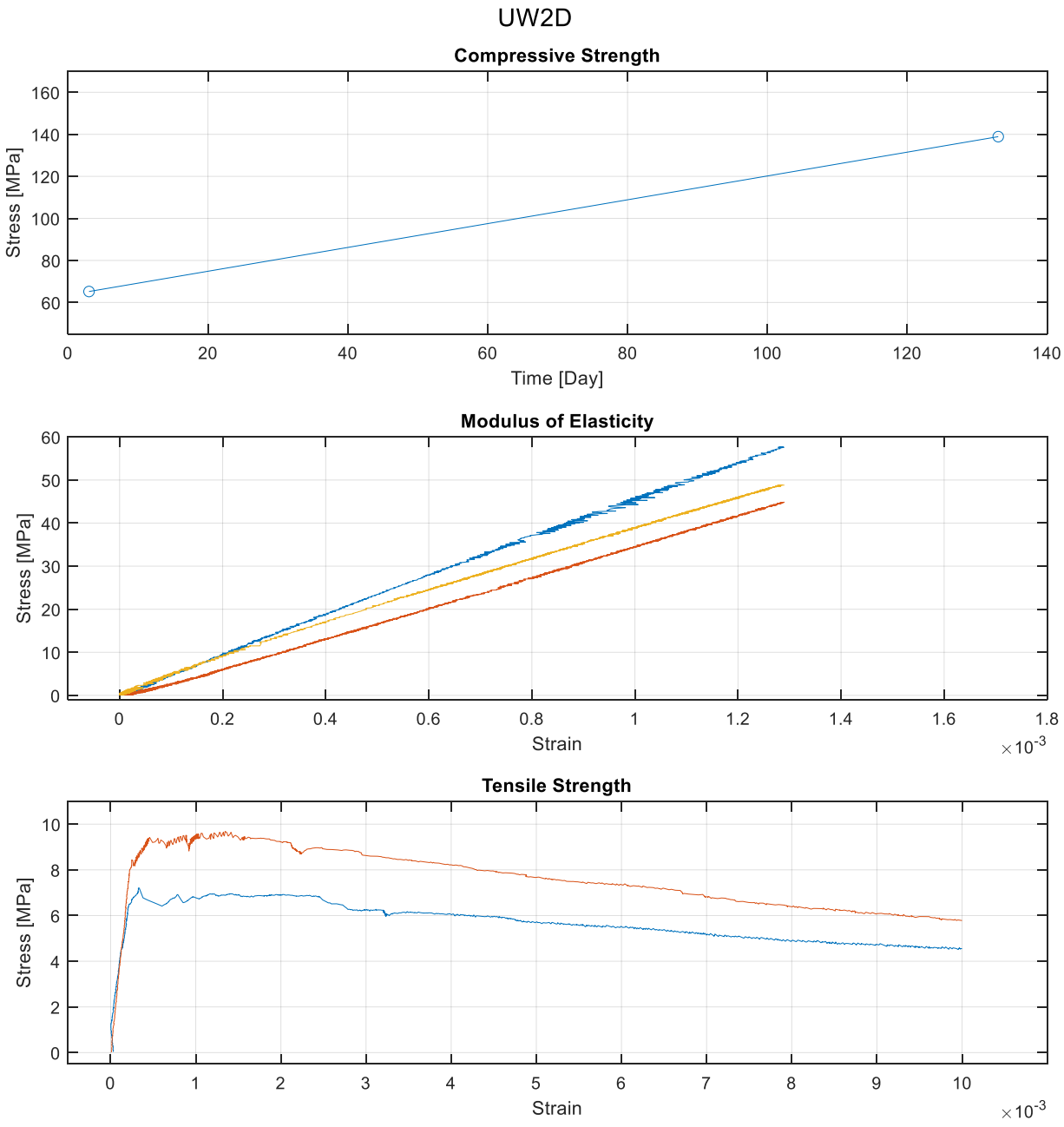

Figure 4.13: UW2D material tests results: (a) Compressive Strength, (b) Modulus of Elasticity, and (c) Tensile Strength

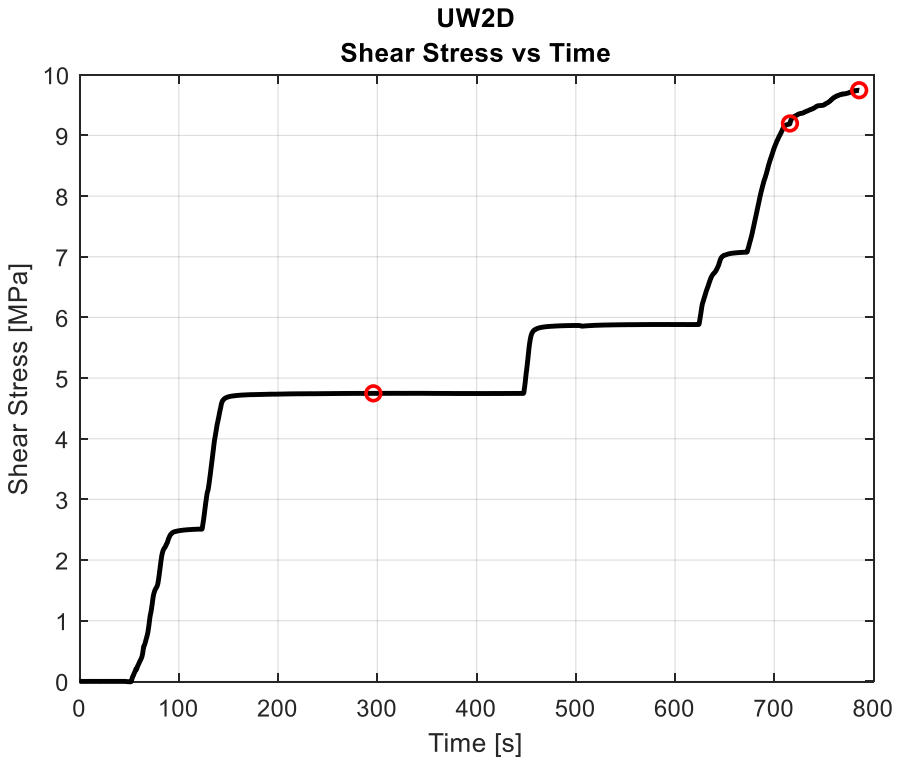

Figure 4.14: UW2D Shear Stress vs Time with first cracking, crack localization, and failure marked

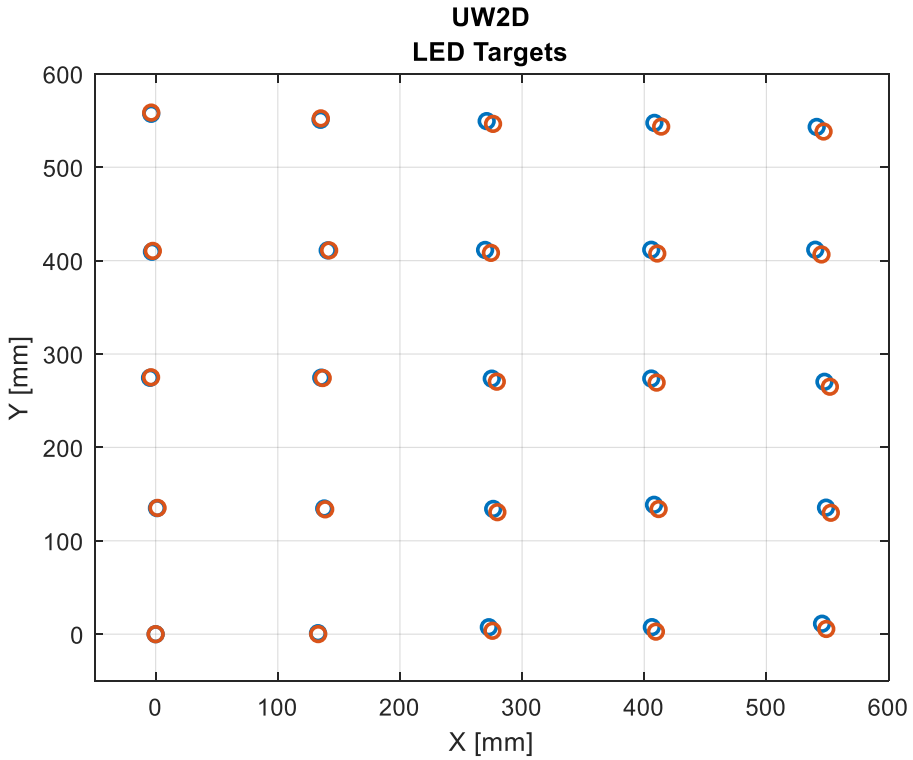

Figure 4.15: UW2D LED targets initial vs final position

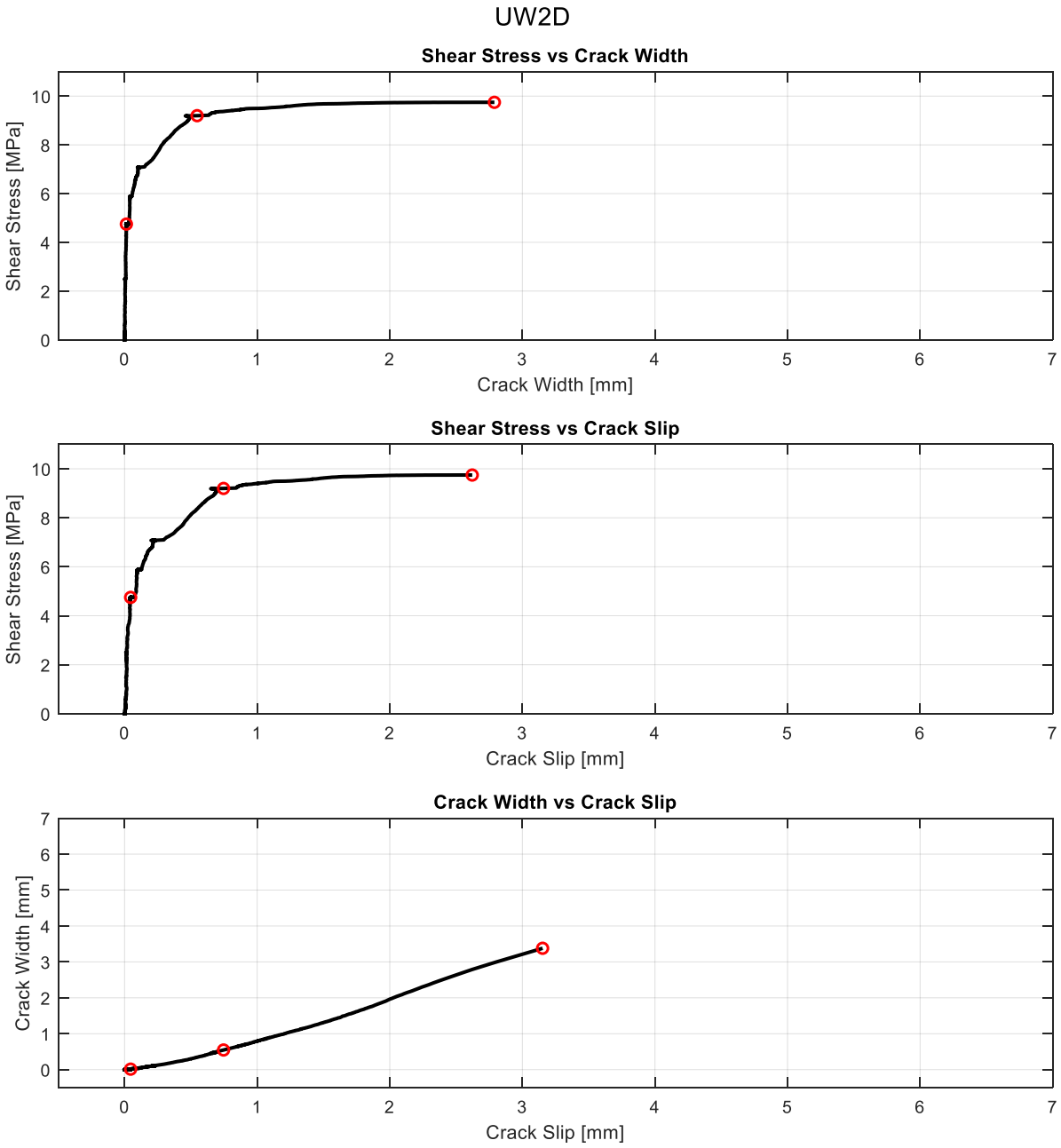

Figure 4.16: UW2D Shear Stress vs Crack Width, Shear Stress vs Crack Slip, Crack Width vs Crack Slip with first cracking, crack localization, and failure marked

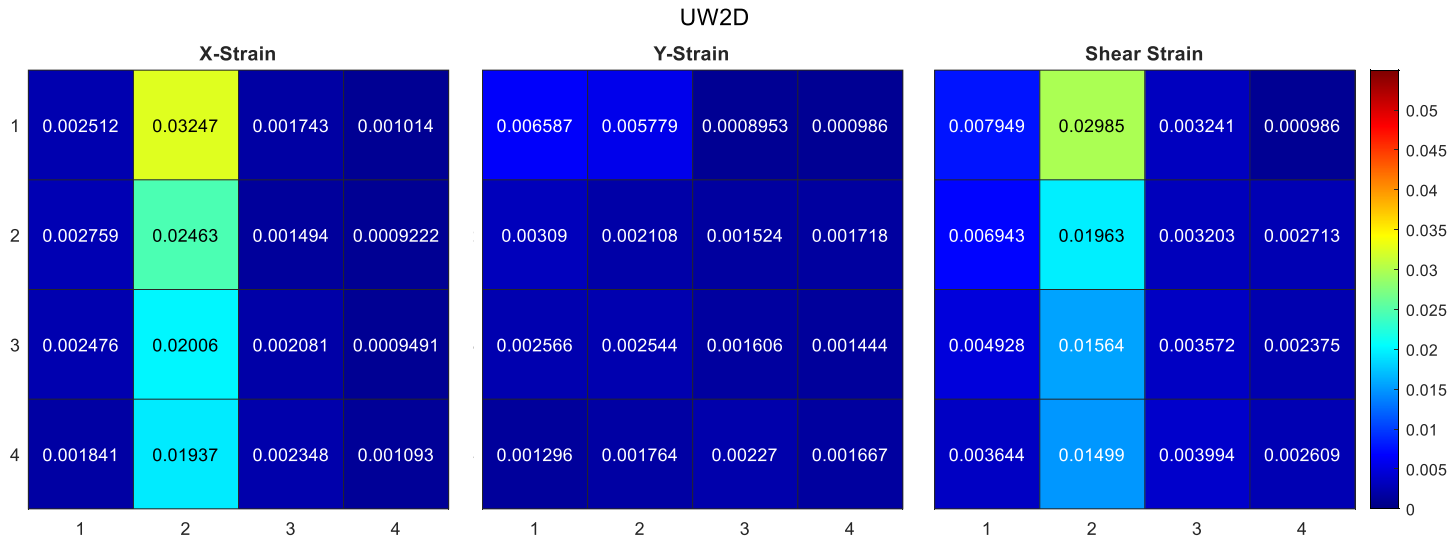

Figure 4.17: UW2D X-Strain, Y-Strain, and Shear Strain for individual target grids

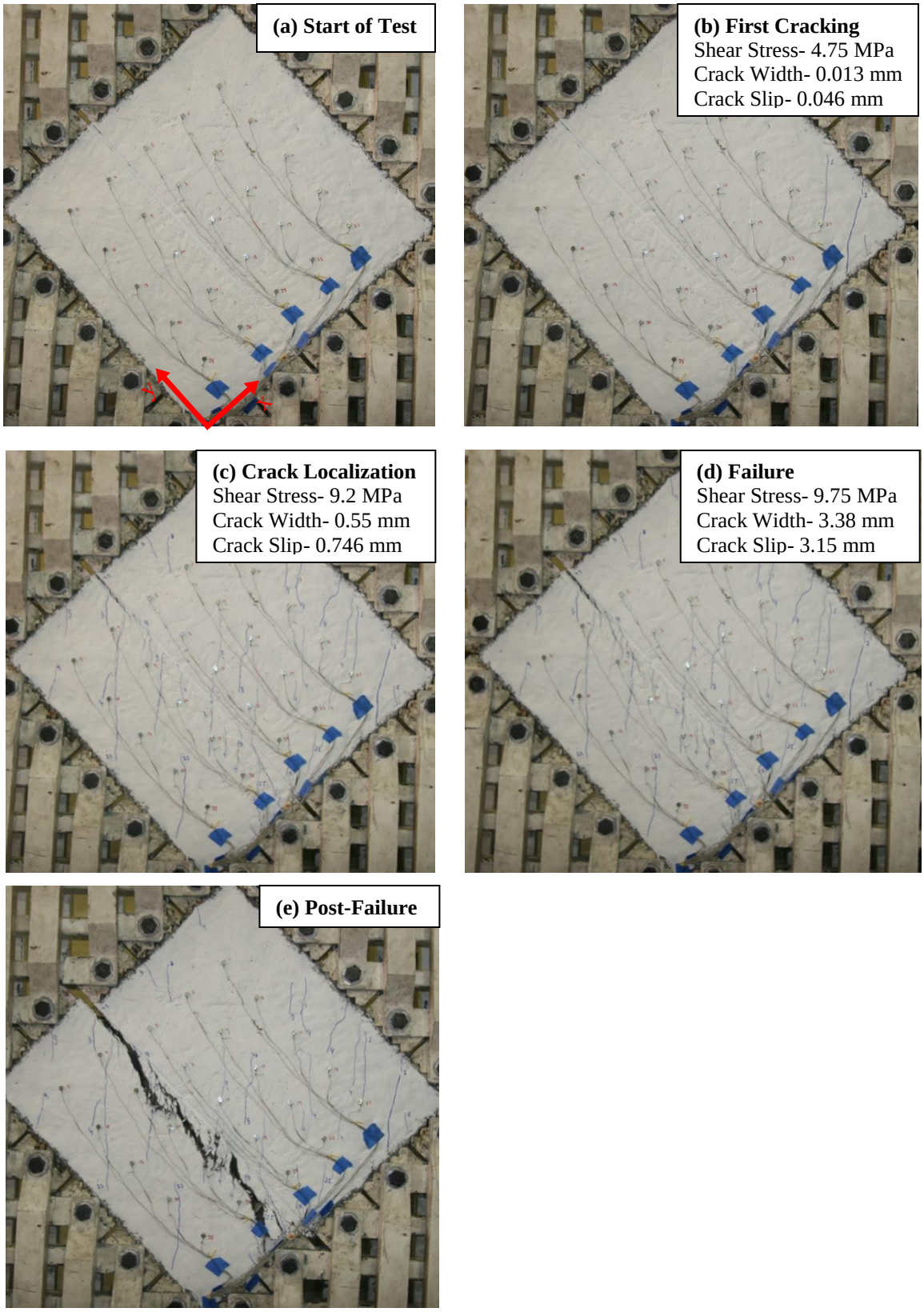

Figure 4.18: UW2D test photos of (a) start of test, (b) first cracking, (c) crack localization, (d) failure, and (e) post-failure

4.2.3 UW2E

During panel testing first cracking occurred at a stress of roughly 3.5 MPa. As the loading increased, cracking continued to take place at 45 degree angles. Failure began in the middle of the panel in cracks that intersected the intended failure line. These cracks were first formed around 5.7 MPa and opened more at 9 MPa. Since the failure began in the middle of the panel, it did not perfectly follow the intended failure line. However, the failure found its way to the crack initiators on both ends of the panel. The result was a slightly curved line rather than a straight, rigid, separation.

The same seven figures were reproduced using the UW2E test results. Figure 4.19 contains the material test results while Figure 4.20 through Figure 4.24 reference the pure shear panel test. For a detailed description of each figure and any plots, see section 4.1.

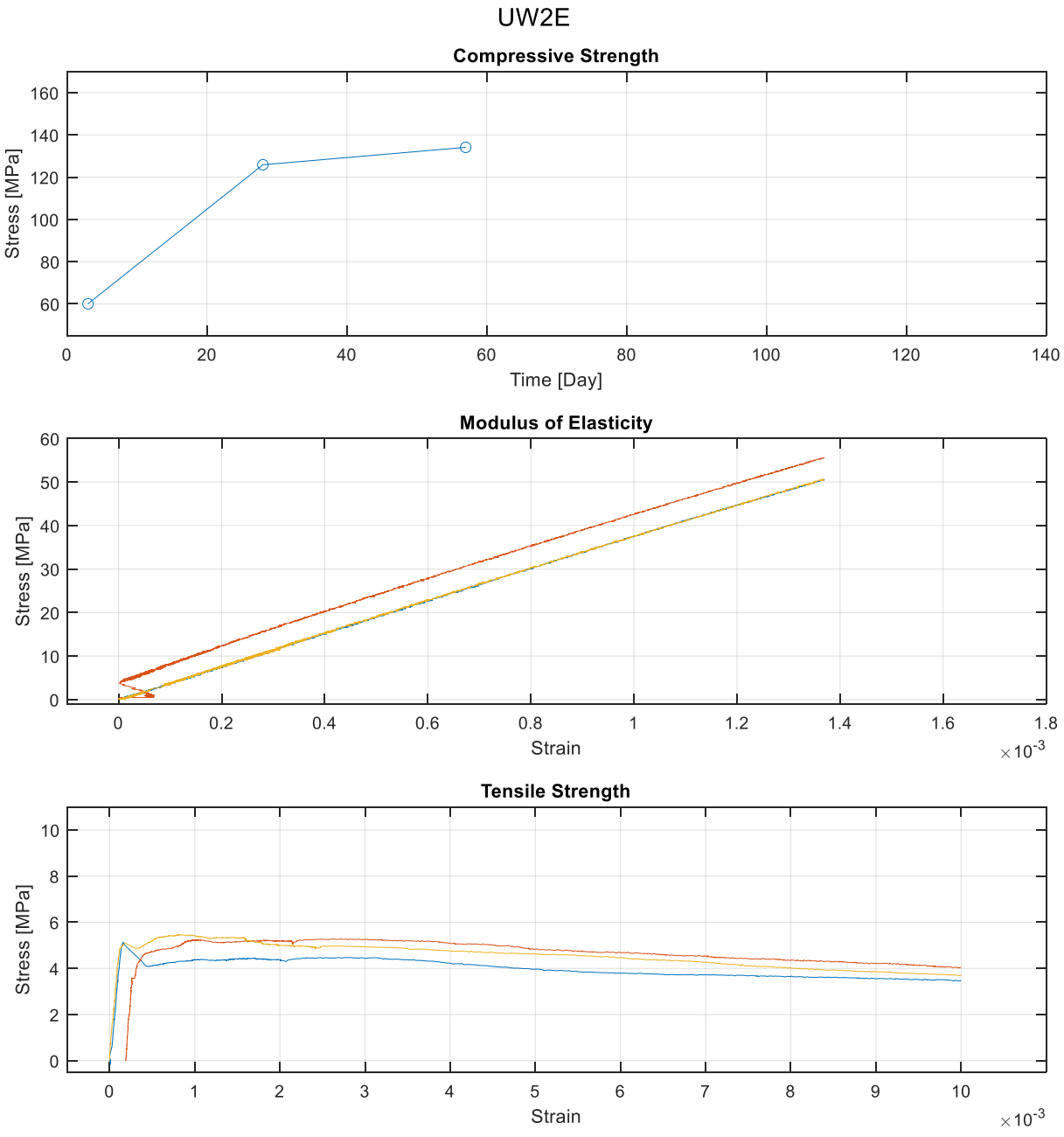

Figure 4.19: UW2E material tests results: (a) Compressive Strength, (b) Modulus of Elasticity, and (c) Tensile Strength

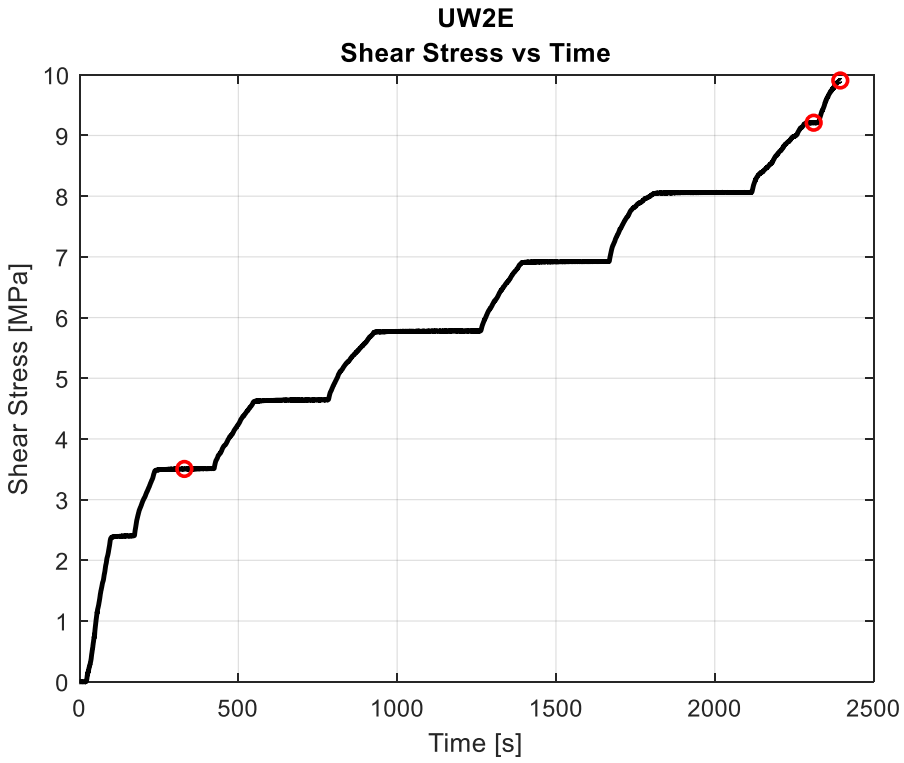

Figure 4.20: UW2E Shear Stress vs Time with first cracking, crack localization, and failure marked

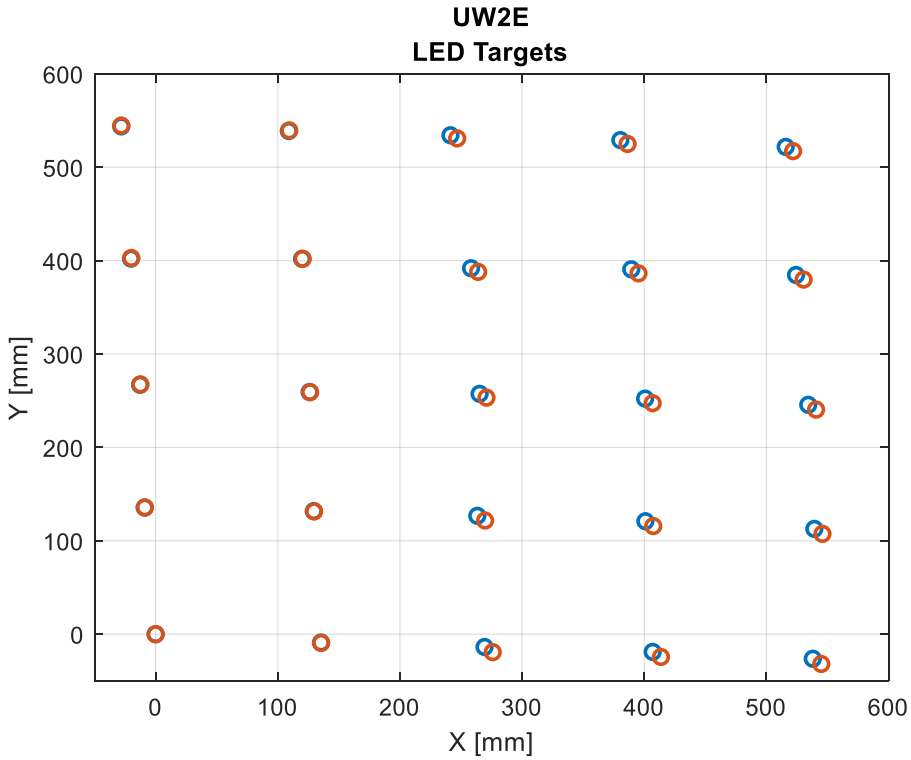

Figure 4.21: UW2E LED targets initial vs final position

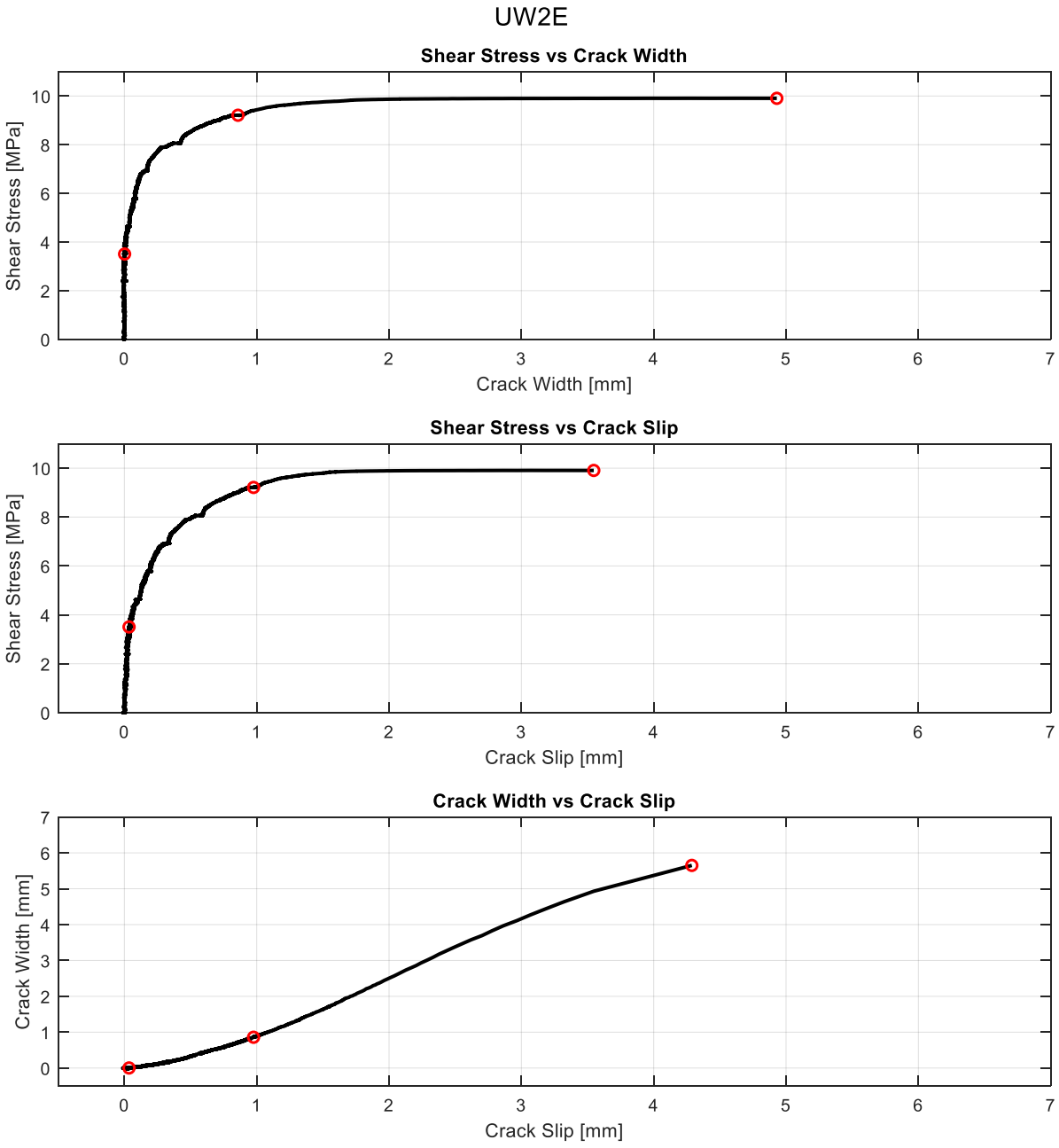

Figure 4.22: UW2E Shear Stress vs Crack Width, Shear Stress vs Crack Slip, Crack Width vs Crack Slip with first cracking, crack localization, and failure marked

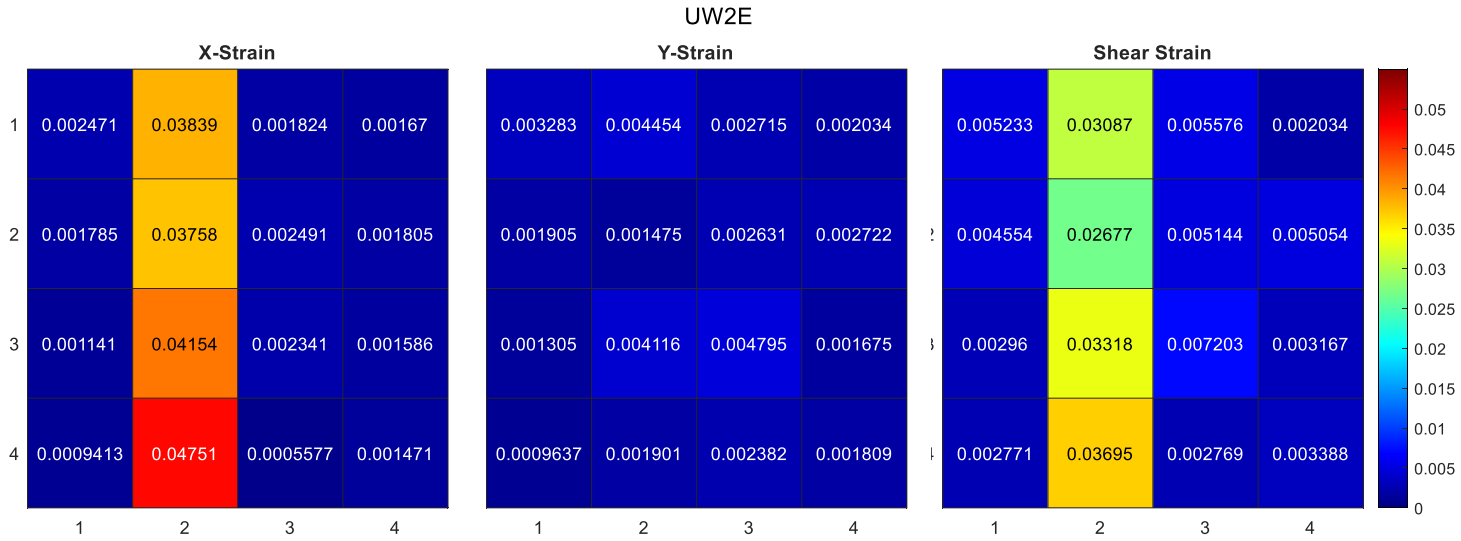

Figure 4.23: UW2E X-Strain, Y-Strain, and Shear Strain for individual target grids

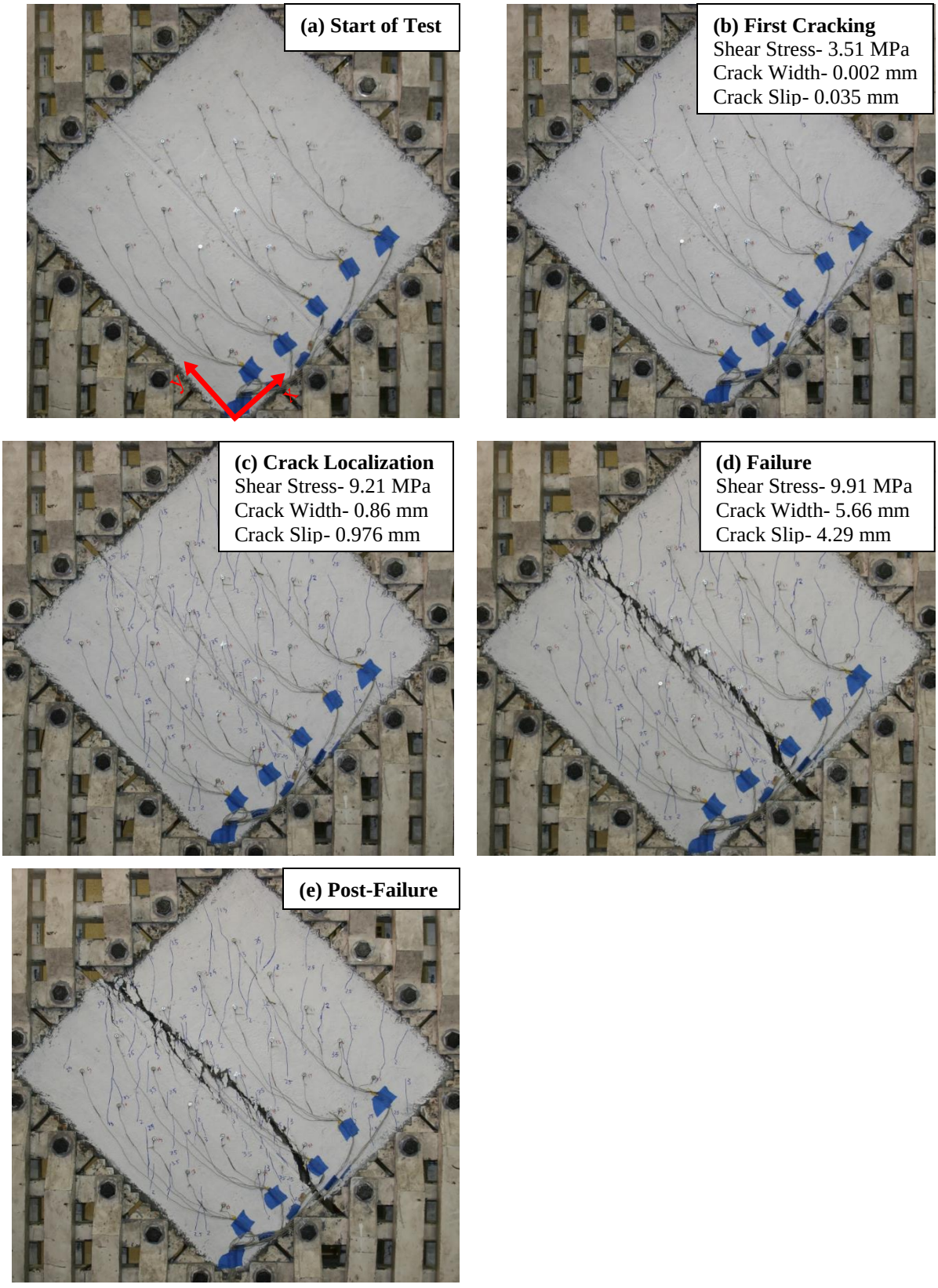

Figure 4.24: UW2E test photos of (a) start of test, (b) first cracking, (c) crack localization, (d) failure, and (e) post-failure

4.3 Test Series 2: 1% Fibers using UW Materials

4.3.1 UW1

The only UHPC batch in Test Series 1 was batch UW1. This batch used the finalized UHPC mix design that was used for all subsequent batches, but with half as many fibers. It was observed that mixing and casting was exponentially easier with the fewer fibers. UHPC flowed easily between rebar but was still thick enough to keep fibers suspended. The mix time was also decreased since there were fewer fibers to incorporate into the concrete.

During testing, explosive failure was seen in the compression tests. Additionally, for each test performed, more concrete and fewer fibers were seen at the failure interface. This is consistent with the expectation of having a small percentage of fibers in the batch.

During panel testing, first cracking occurred at a stress of roughly 2.3 MPa in 45 degree cracks that spanned across the panel. As the loading increased, cracking continued to take place at 45 degree angles. By the time a stress of 6.8 MPa was reached, a large number of cracks were running at an angle of about 30 degrees to the slot. Failure ultimately began when these cracks opened more. The failure started in the middle of the panel and propagated to the perimeter, where it was forced back to the crack initiators.

The same seven figures were reproduced using the UW1 test results. Figure 4.25 contains the material test results while Figure 4.26 through Figure 4.30 reference the pure shear panel test. For a detailed description of each figure and any plots, see section 4.1.

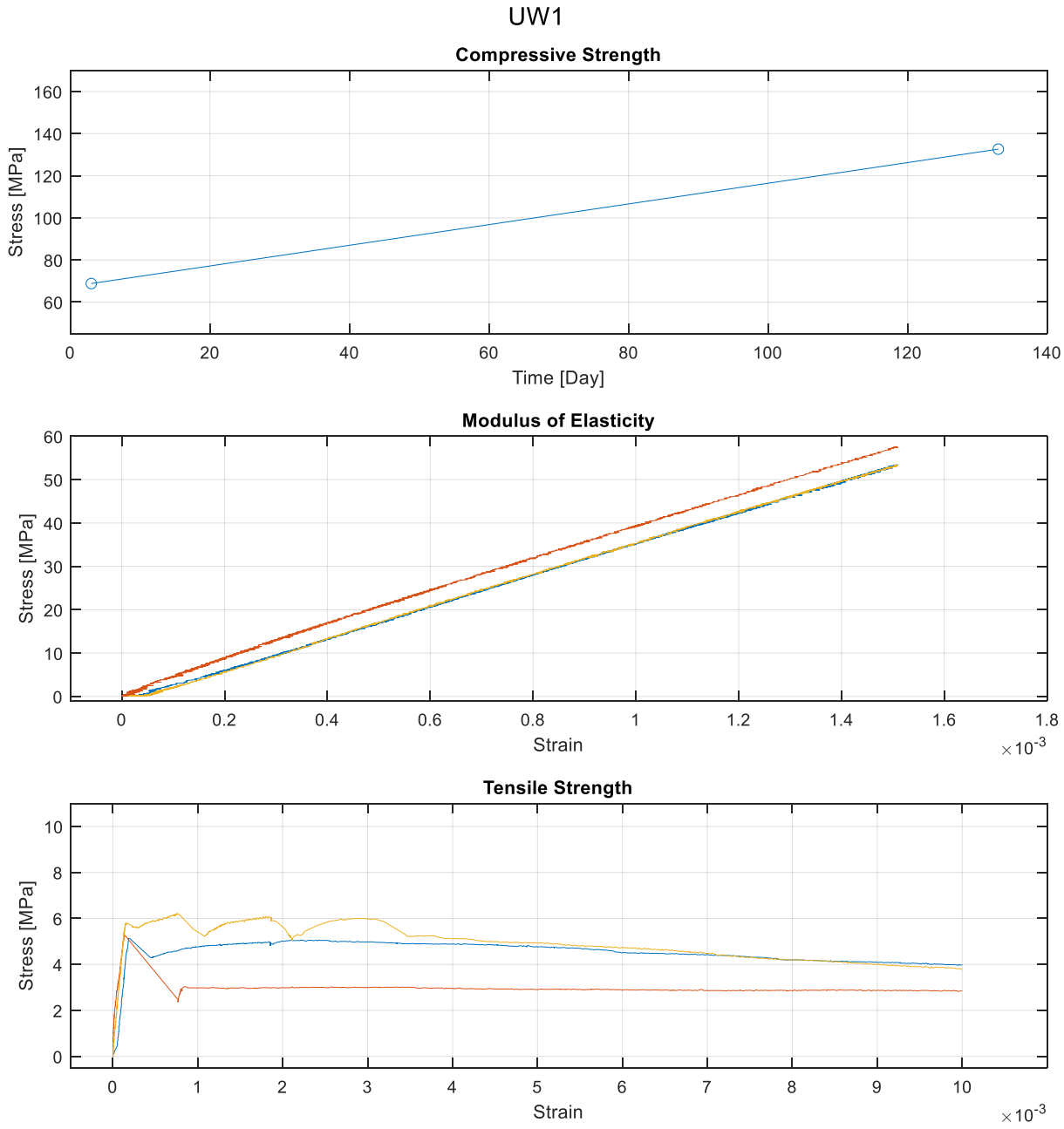

Figure 4.25: UW1 material tests results: (a) Compressive Strength, (b) Modulus of Elasticity, and (c) Tensile Strength

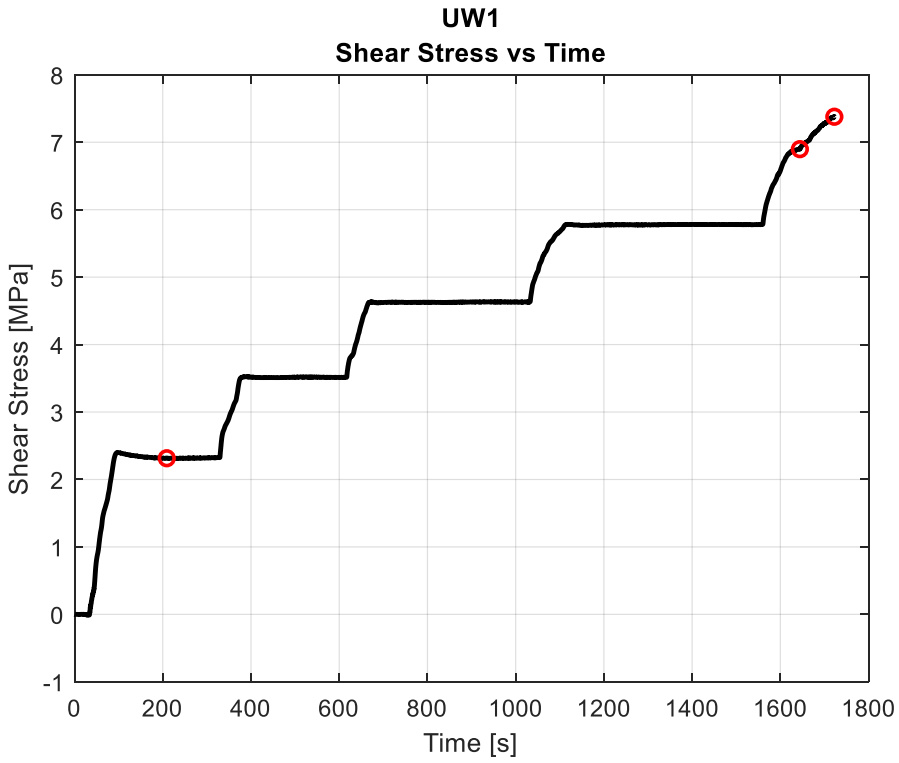

Figure 4.26: UW1 Shear Stress vs Time with first cracking, crack localization, and failure marked

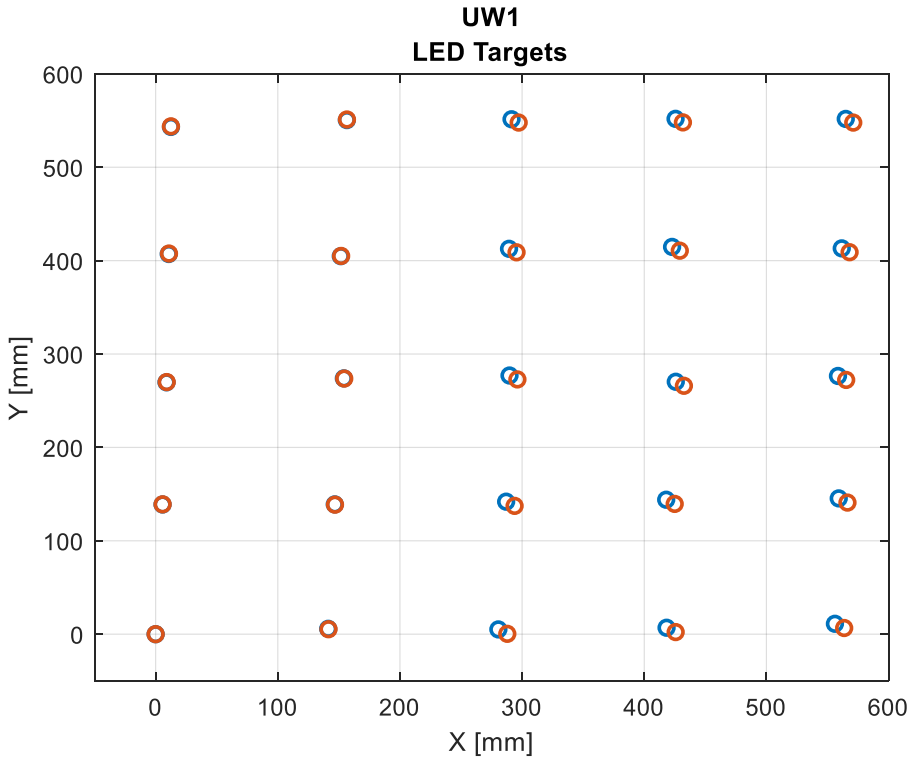

Figure 4.27: UW1 LED targets initial vs final position

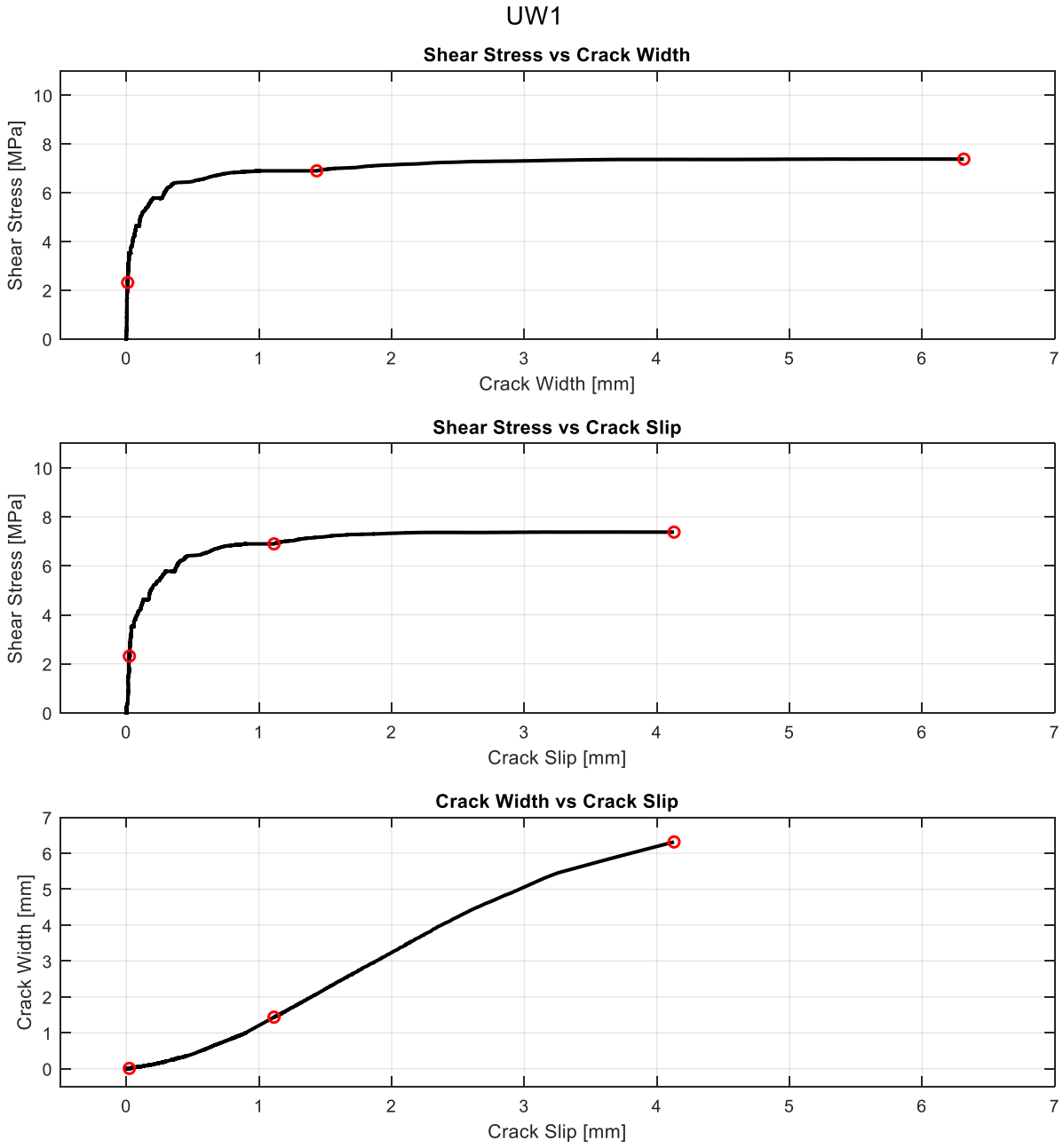

Figure 4.28: UW1 Shear Stress vs Crack Width, Shear Stress vs Crack Slip, Crack Width vs Crack Slip with first cracking, crack localization, and failure marked

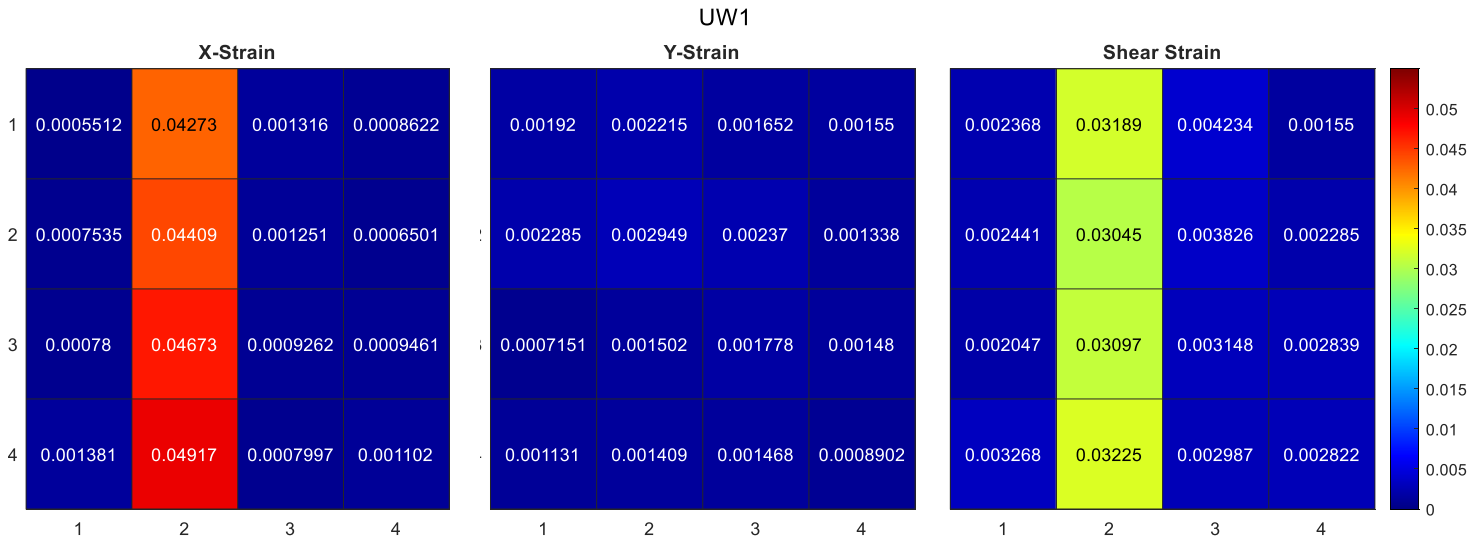

Figure 4.29: UW1 X-Strain, Y-Strain, and Shear Strain for individual target grids

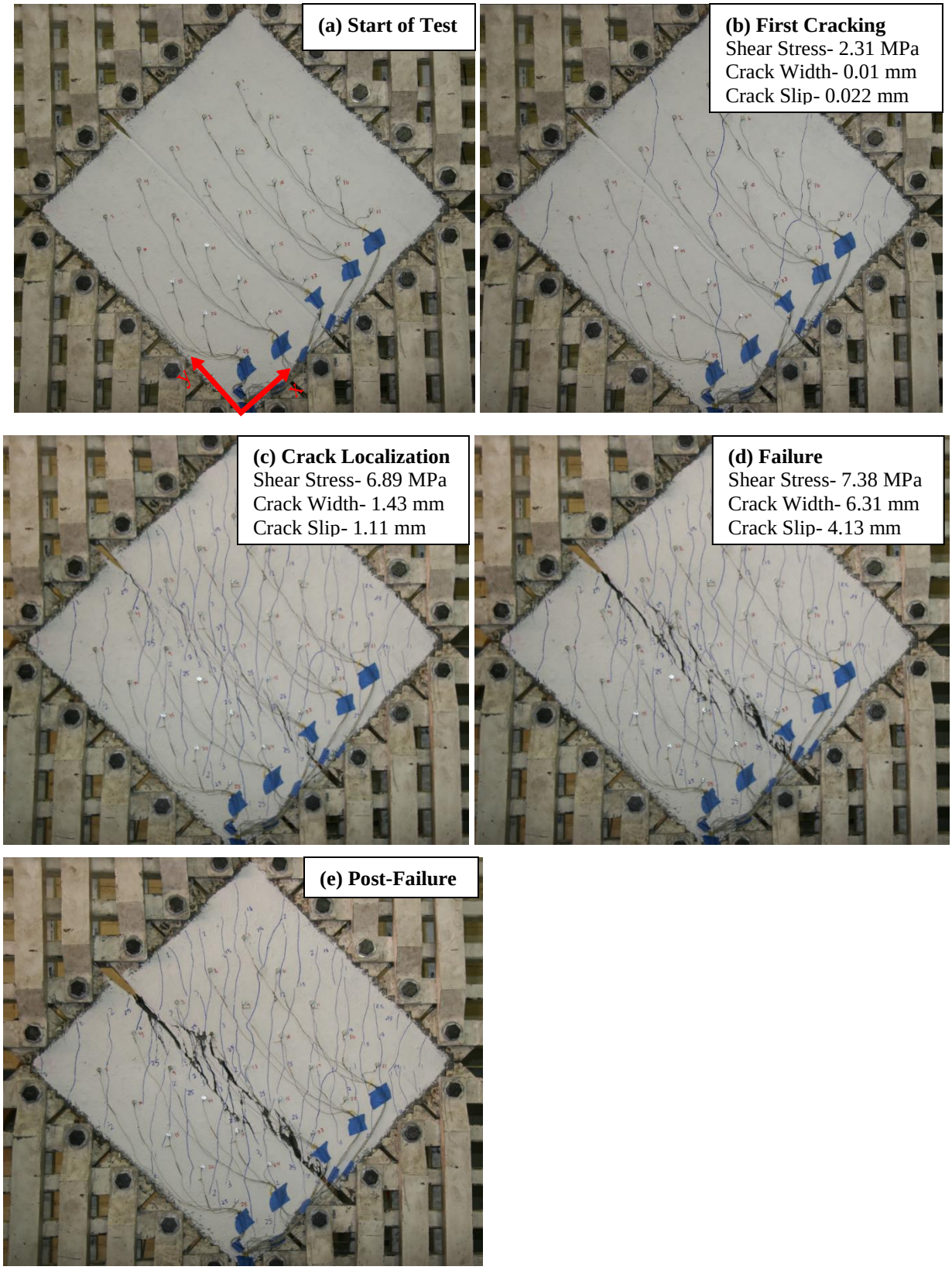

Figure 4.30: UW1 test photos of (a) start of test, (b) first cracking, (c) crack localization, (d) failure, and (e) post-failure

4.4 Test Series 3: 2% Fibers using OU Materials

The final test series included one UHPC batch, OU2, that was comprised of 2% fibers and materials local to the University of Oklahoma instead of the University of Washington. While the mixing, casting, and testing procedures were identical to previous panels, the difference in materials could result in new findings. Although most of the materials are standard no matter where they are bought, the sand from OU was noticeably finer than the sand from UW. Figure 4.31 shows the UW sand (left) and the OU sand (right).

Figure 4.31: UW sand vs. OU sand

4.4.1 OU2

No changes were noticed during the mixing and casting of the OU2 batch that could have been the result of finer sand. While the OU sand had a higher absorption than the UW sand, this was accounted for by adjusting the amount of water in the UHPC to keep the same free water-to-cement ratio.

During panel testing, first cracking did not occur until a stress of roughly 4.6 MPa. As the loading increased, cracking continued to take place at 45 degree angles. At 5.7 MPa a crack formed along

the bottom right side of the slot. The crack increased in length and slowly opened leading up to an abrupt failure at 9.3 MPa. Although the failure was abrupt, it was not completely rigid as the line became less distinct as it met the other end of the panel.

The same seven figures were reproduced using the OU2 test results. Figure 4.32 contains the material test results while Figure 4.33 through Figure 4.37 reference the pure shear panel test. For a detailed description of each figure and any plots, see section 4.1.

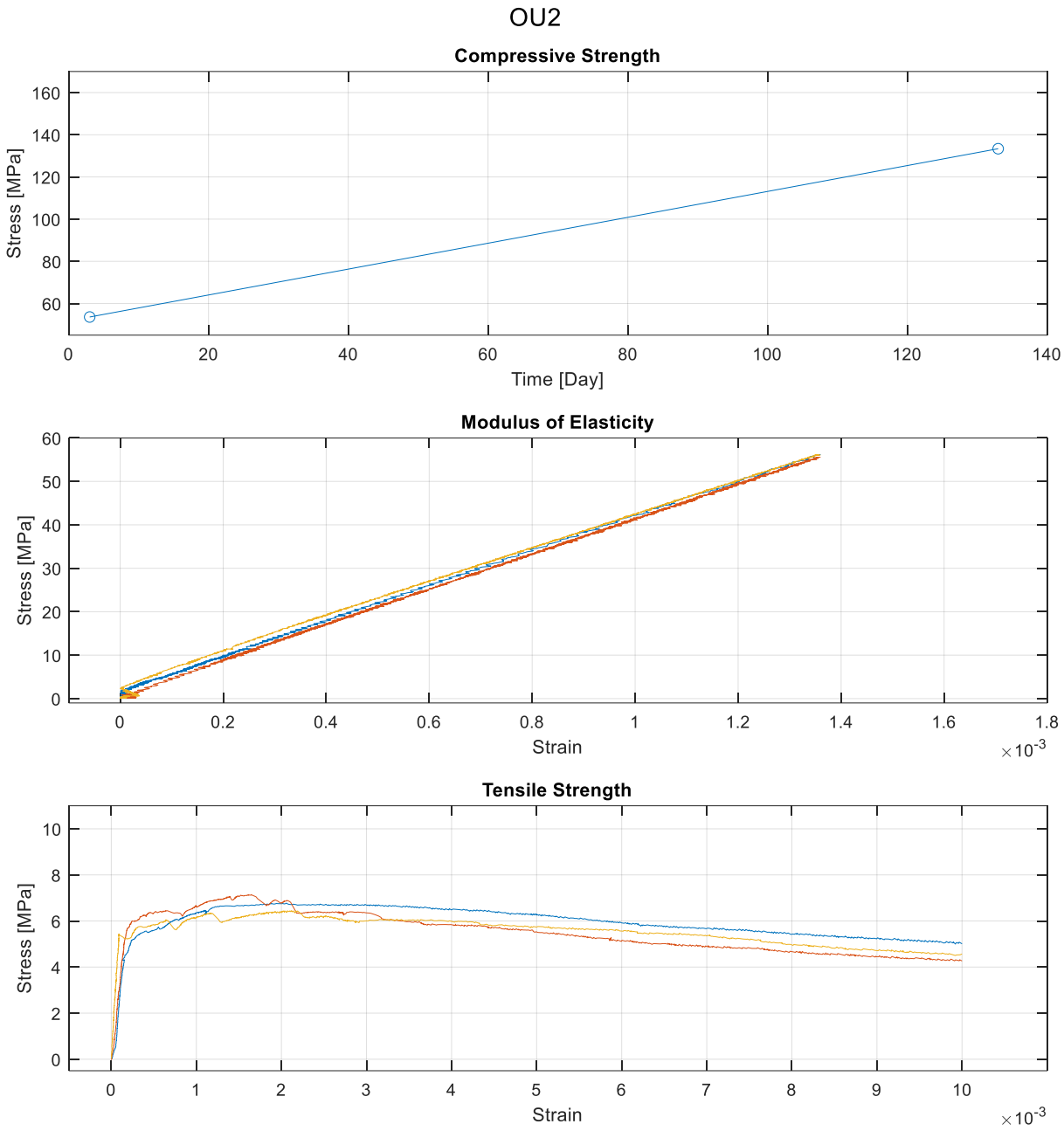

Figure 4.32: OU2 material tests results: (a) Compressive Strength, (b) Modulus of Elasticity, and (c) Tensile Strength

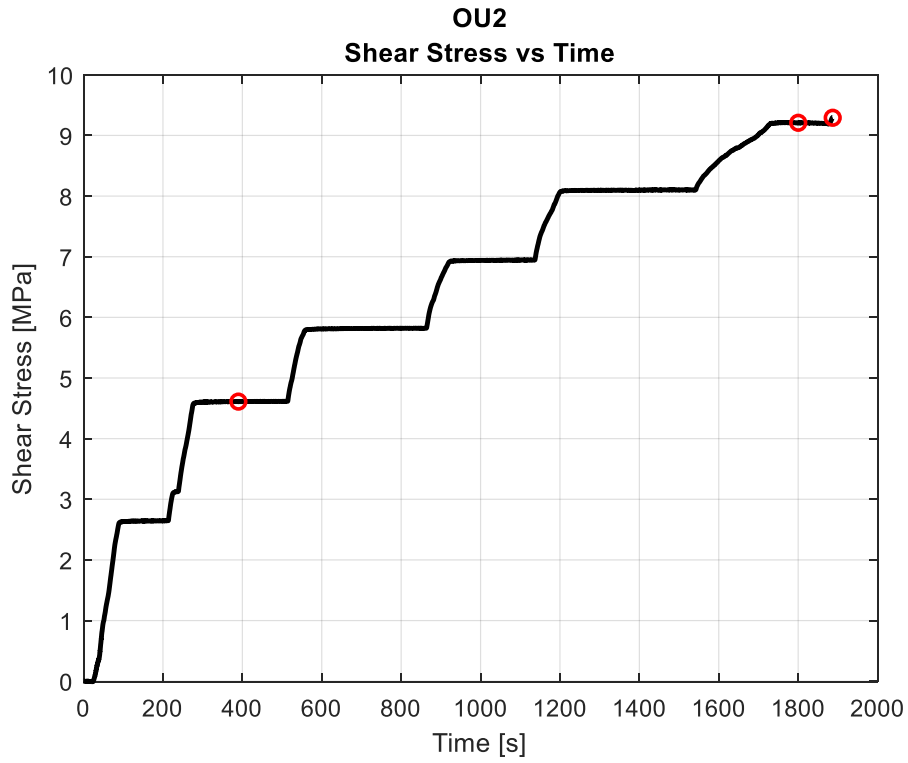

Figure 4.33: OU2 Shear Stress vs Time with first cracking, crack localization, and failure marked

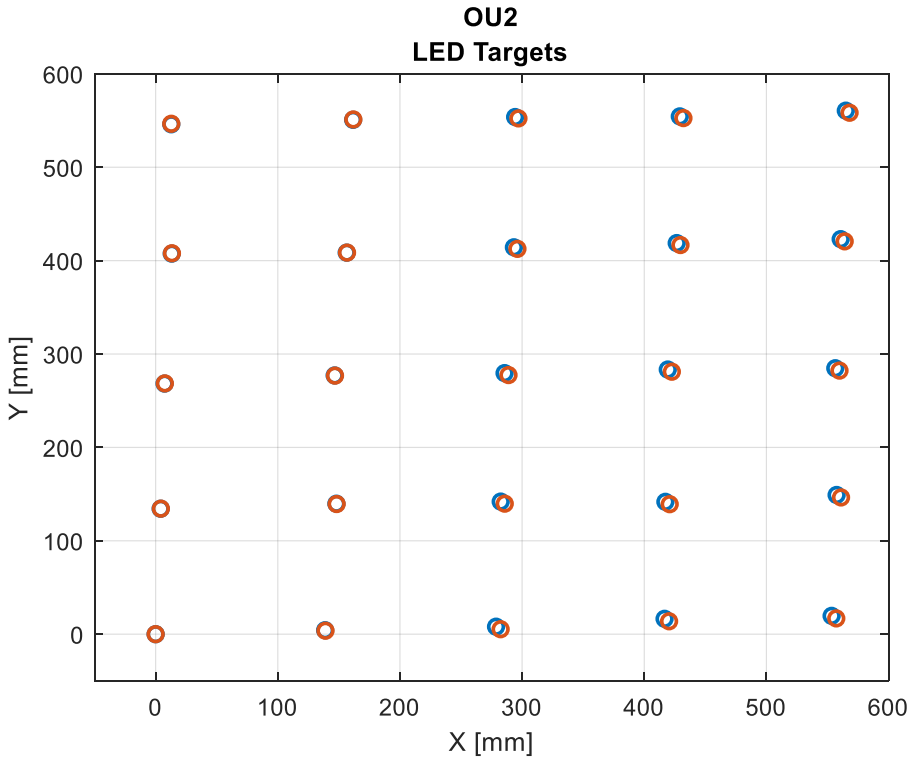

Figure 4.34: OU2 LED targets initial vs final position

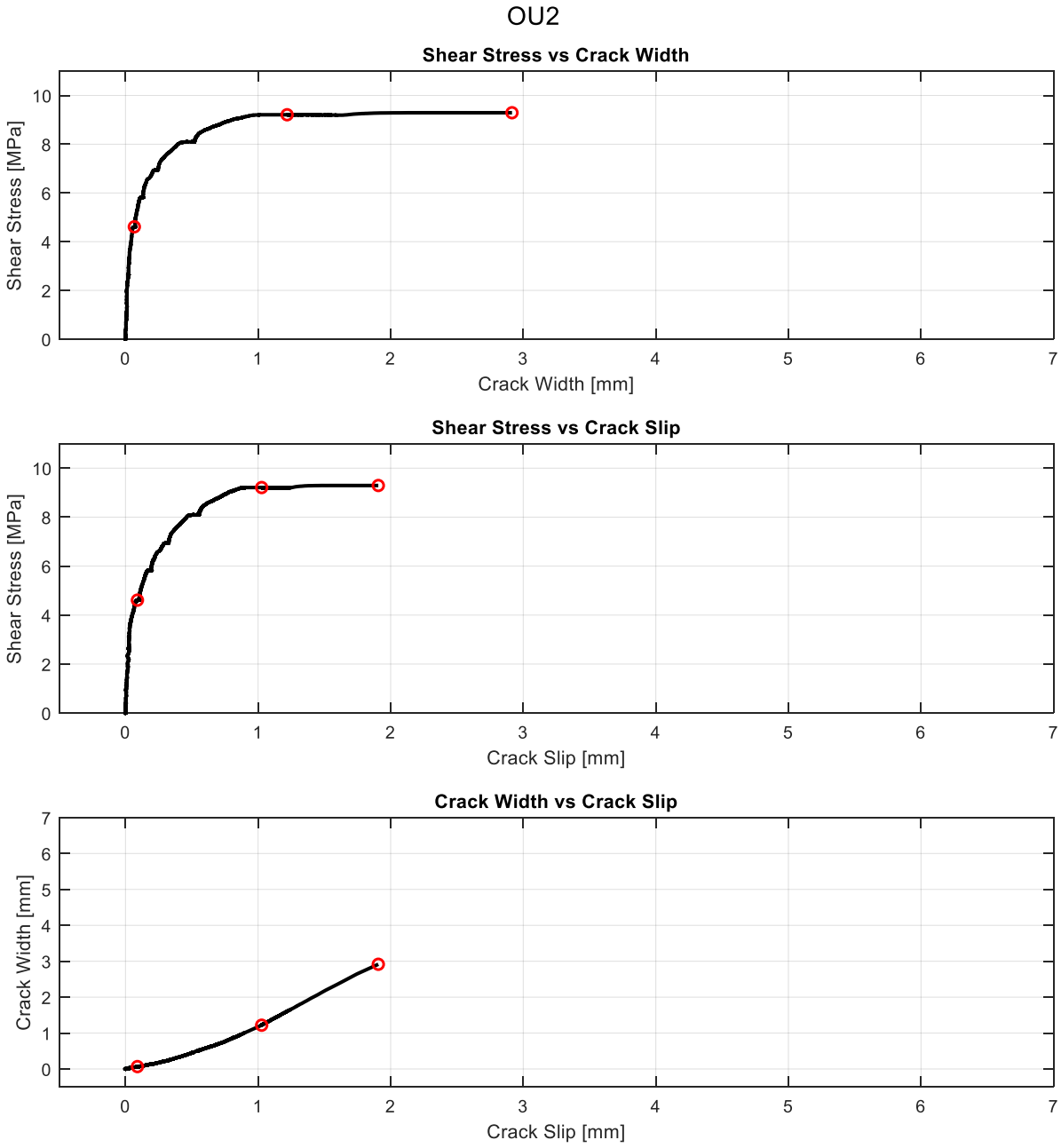

Figure 4.35: OU2 Shear Stress vs Crack Width, Shear Stress vs Crack Slip, Crack Width vs Crack Slip with first cracking, crack localization, and failure marked

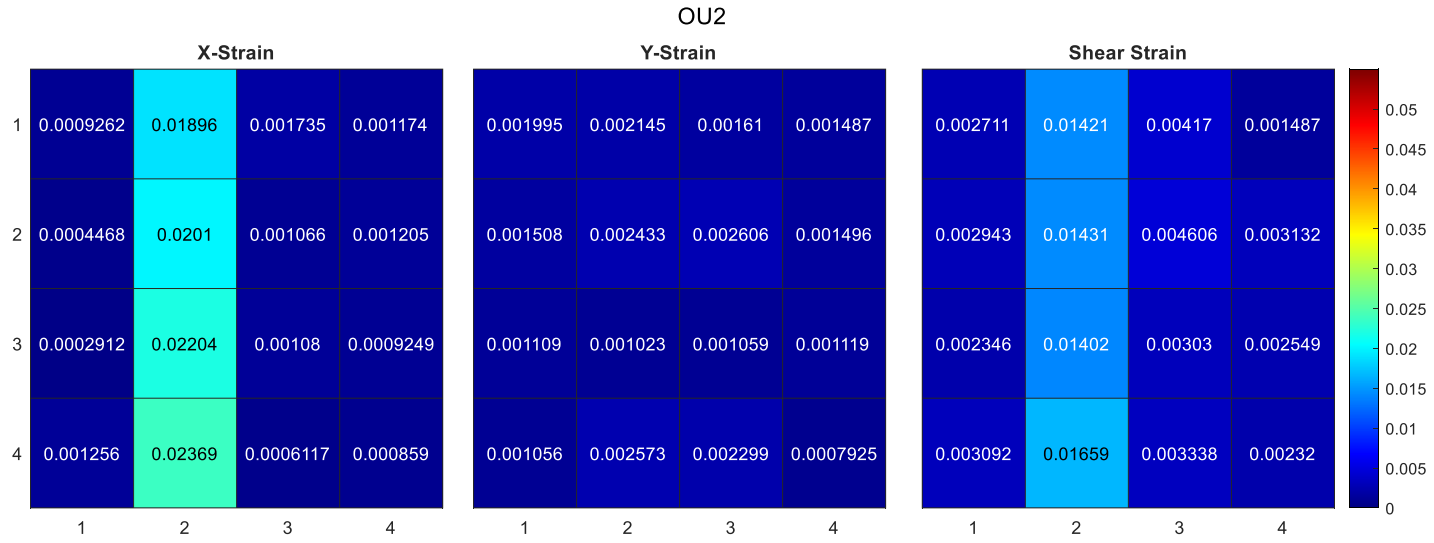

Figure 4.36: OU2 X-Strain, Y-Strain, and Shear Strain for individual target grids

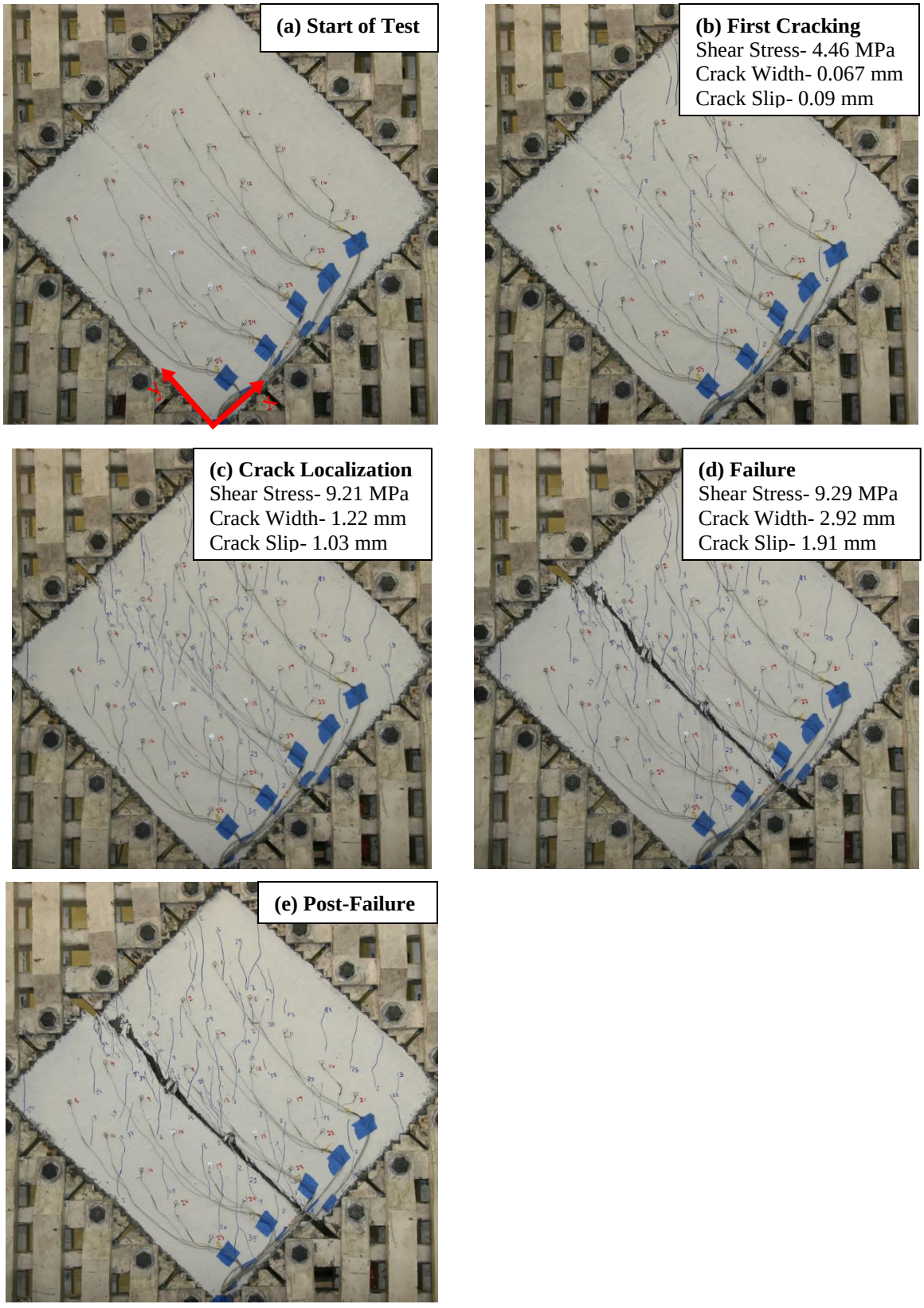

Figure 4.37: OU2 test photos of (a) start of test, (b) first cracking, (c) crack localization, (d) failure, and (e) post-failure

Chapter 5: Analysis of Results

The experimental results from the UHPC tests were analyzed to determine the influence of fiber content and local materials on strength and behavior. Although results were recorded for trial panel UW2B, when compared against other 2% panels it was clear that the poor consolidation of the batch corrupted the results. The UW2B results found in Chapter 4 serve as an example of how poorly consolidated UHPC behaves, but since this parameter is not in the scope of the project the results for that panel will not be discussed any further. Therefore, the following analysis includes only Test Series 1, 2, and 3. First, separate plots were prepared for each test type (compression, tension, and shear), and all results for all batches are shown on each plot. Next, results are analyzed by fiber content and material source rather than by batch. Last, results are analyzed based on the influence of fiber content and material source location.

5.1 UHPC Results by Individual Batch

The following table is adapted from Table 4-1 to show only the relevant UHPC results. The results for individual test specimens within each batch were averaged to report one result, per batch, for each test type.

Table 5-1: Summary of Relevant UHPC Results

UHPC Strength Results (MPa)					
Batch	Compression	EMod	Tension	Flexural	Shear
UW2C	129	N/A	N/A	N/A	8.89
UW2D	139	39500	8.23	19.7	9.75
UW2E	134	39200	4.89	16.8	9.91
UW1	133	36600	4.66	12.9	7.38
OU2	133	42100	6.68	18.2	9.29

To compare material test results, compressive strength, modulus of elasticity, and tensile strength were plotted for each UHPC batch on one figure. A second figure showing shear stress vs. crack width, shear stress vs. crack slip, shear stress vs. shear strain, and crack width vs. crack slip for

each shear panel test was also produced. Each batch uses the same color, according to the legend, for all plots. Figure 5.1 includes material test results and Figure 5.2 includes shear panel test results.

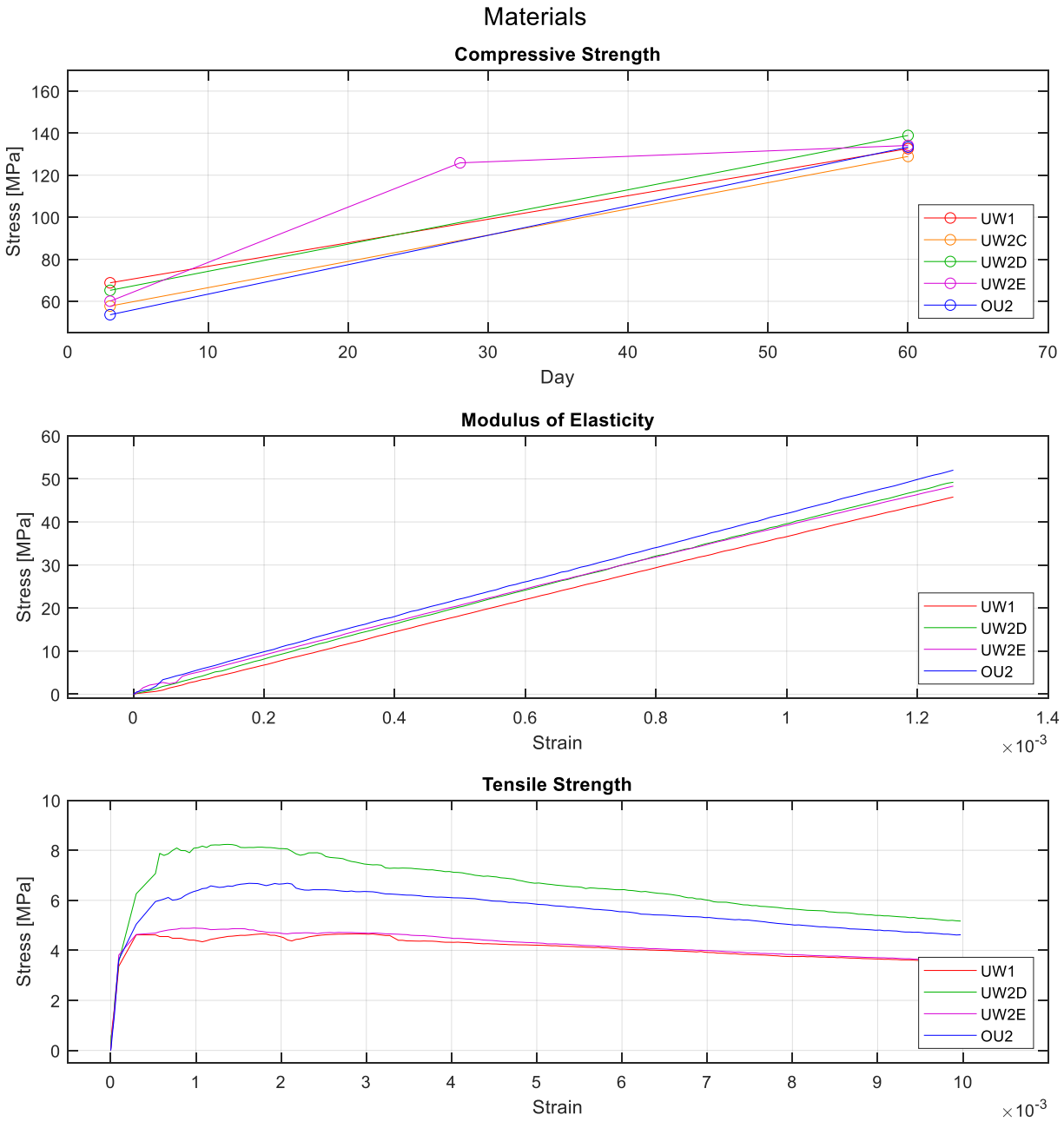

Figure 5.1: Material test results shown by UHPC batch

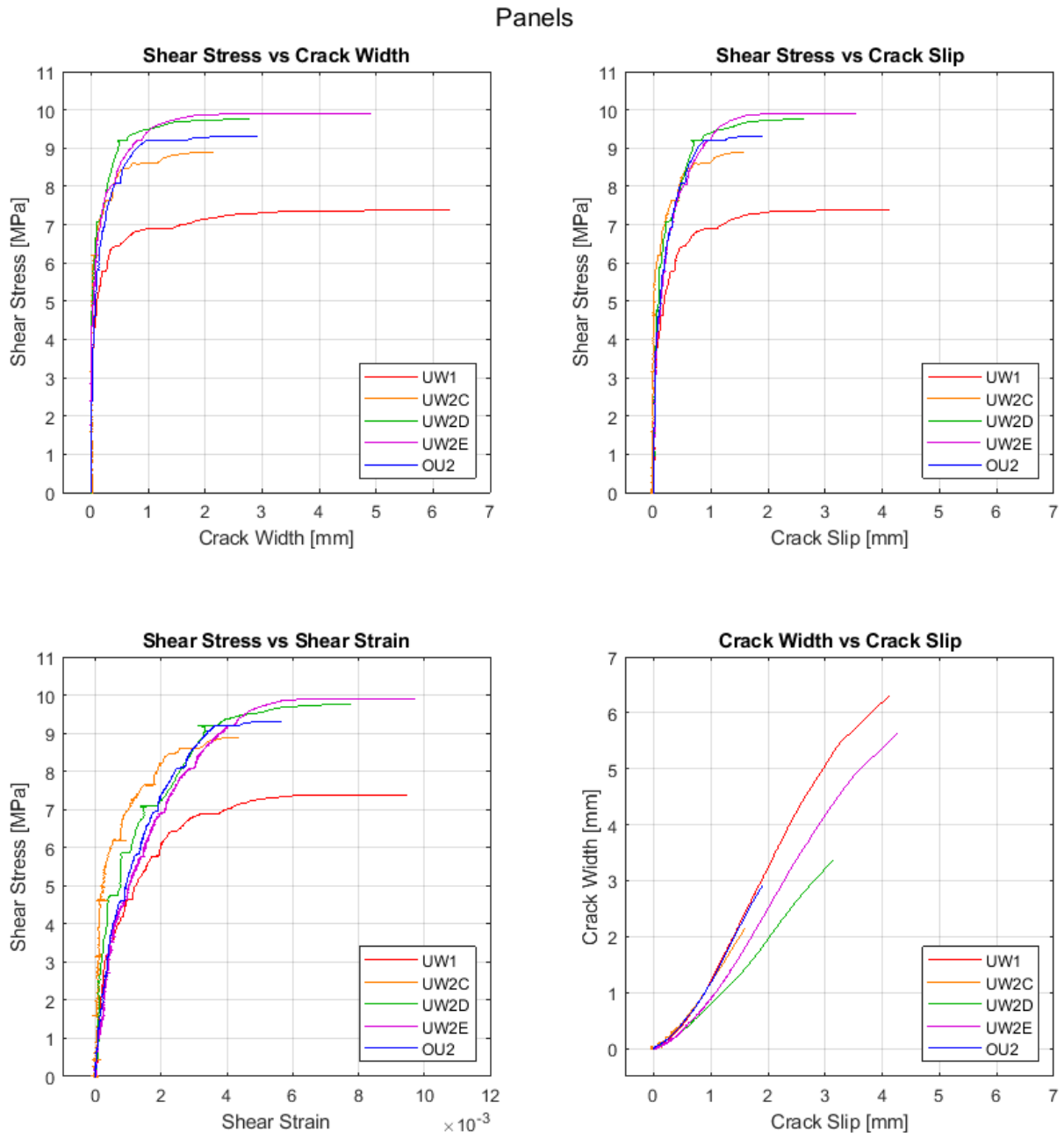

Figure 5.2: Shear panel test results shown by UHPC batch

5.2 UHPC Results by Test Series

Table 5-2 shows the UHPC strength results by test series. The test series are as follows:

Test Series 1: 2% fibers using UW materials (UW2C, UW2D, and UW2E)

Test Series 2: 1% fibers using UW materials (UW1)

Test Series 3: 2% fibers using OU materials (OU2)

The strengths for the three batches in Test Series 1 were averaged to report one value for each series in the summary table.

Table 5-2: Summary of UHPC Results by Test Series

UHPC Strength Results (MPa)					
Test Series	Compression	EMod	Tension	Flexural	Shear
1	134	39400	6.56	18.3	9.52
2	133	36600	4.66	12.9	7.38
3	133	42100	6.68	18.2	9.29

The same figures for material test results and shear panel test results were recreated using a different color scheme to highlight the different variables. In each plot, black represents Test Series 1, red represents Test Series 2, and blue represents Test Series 3. Figure 5.3 shows material test results and Figure 5.4 shows shear panel test results. In each figure, the individual results for Test Series 1 were plotted rather than showing the average curve for all of the Test Series 1 batches.

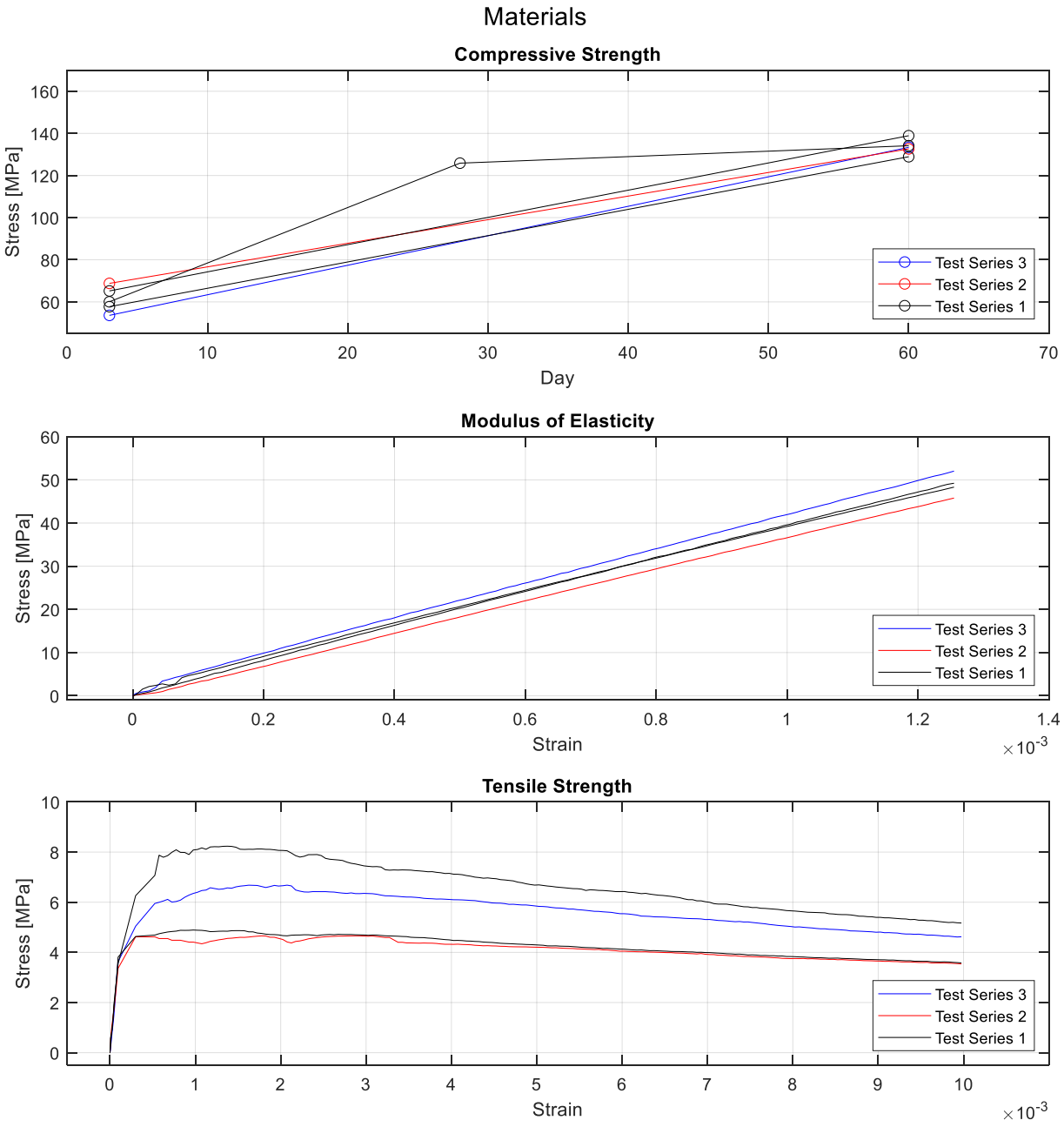

Figure 5.3: Material test results shown by test series

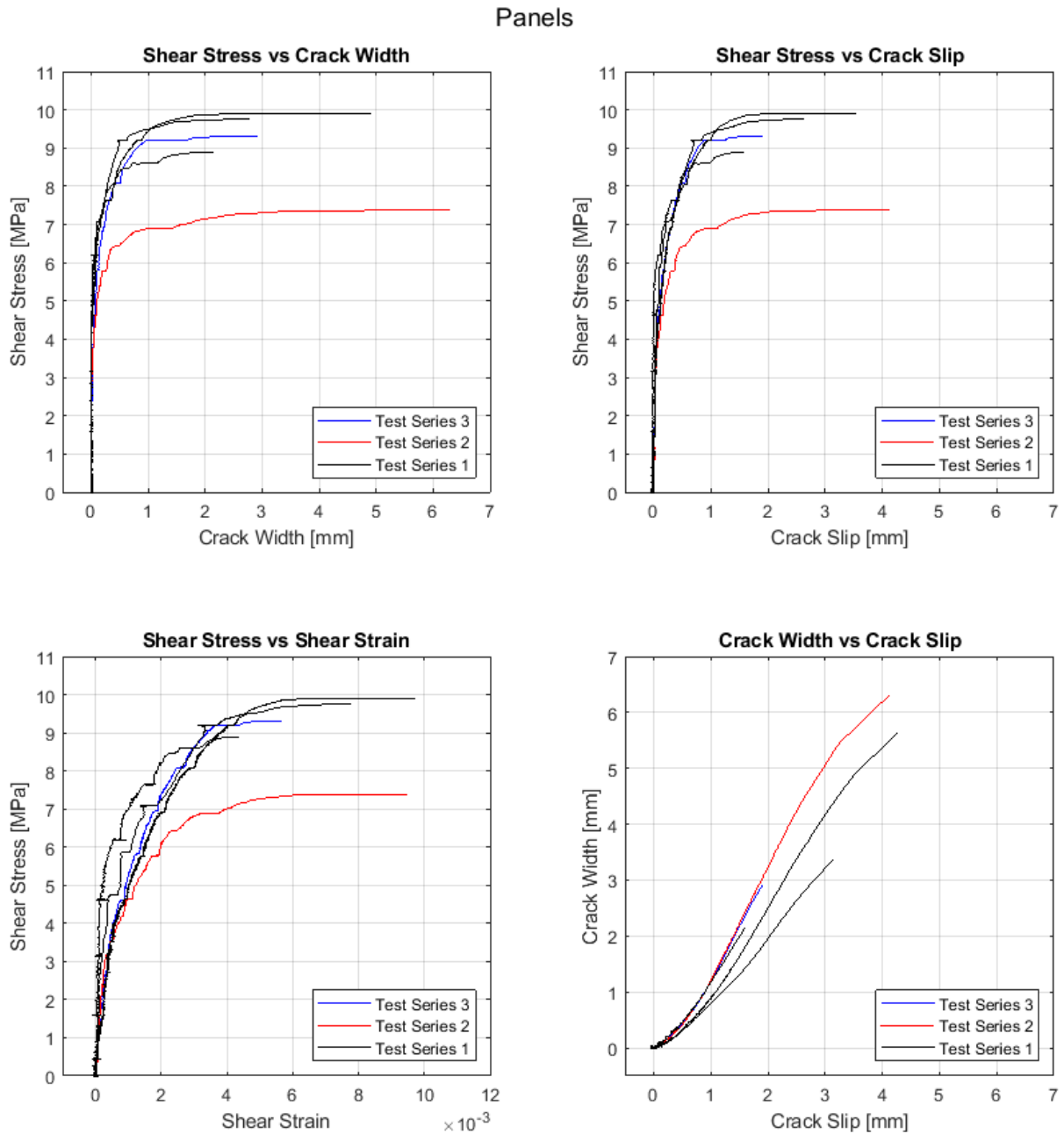

Figure 5.4: Shear panel test results shown by test series

5.3 Influence of Fiber Content

This section will discuss the effect of fiber content on UHPC behavior and strength by comparing the results of Test Series 1, with 2% fibers, and Test Series 2, with 1% fibers. The results from Test Series 1 were averaged to report one result. The results of Test Series 3 will not be referenced since the materials were sourced from a different location and therefore fiber influence cannot be isolated.

5.3.1 Material Test Results

The following bar graph, Figure 5.5, shows the material test results normalized to 2% fiber content to show how 1% fiber content results compare. The 2% results are in black and the 1% results are in a diagonal stripe pattern. This figure, as well as Figure 5.3, will be referenced throughout this section.

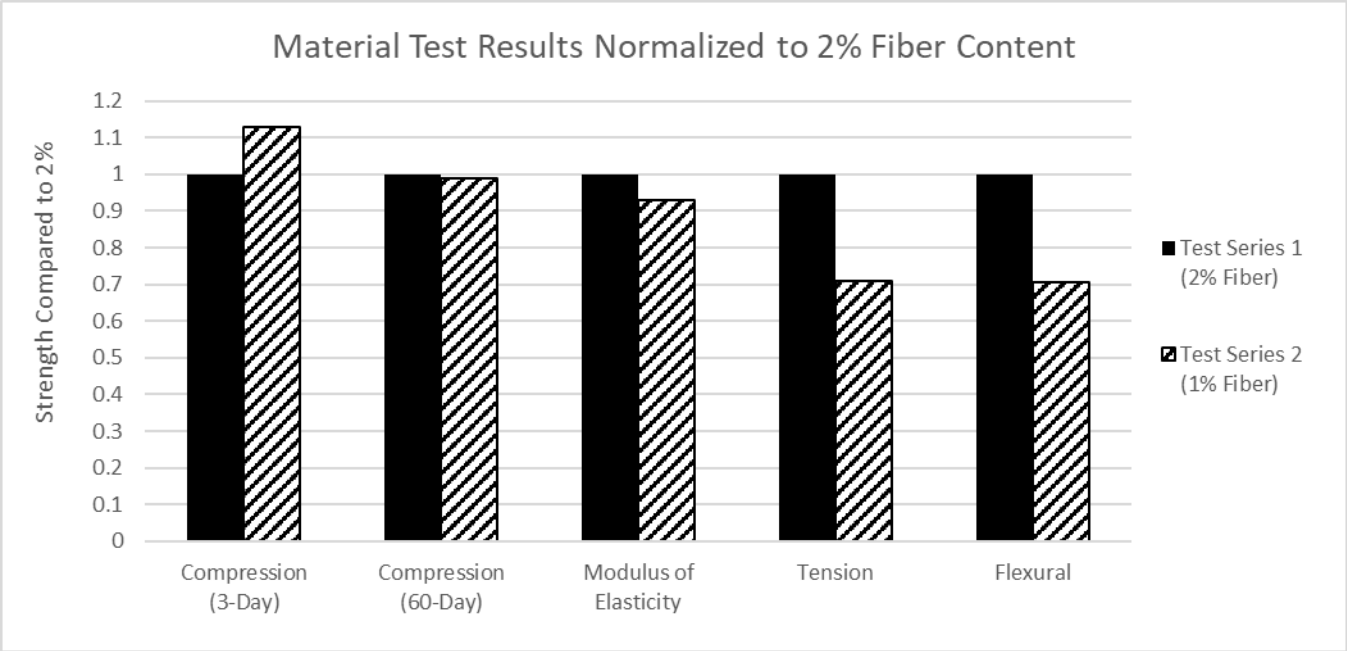

Figure 5.5: Material test results normalized to 2% fiber content

5.3.1.1 Compression and Modulus of Elasticity

Compression tests were only performed 3 days after casting and on test day for all but one UHPC batch. Therefore, strength gain over time cannot be fully assessed. UHPC strength typically levels off after the 28 day mark, but since only one sample supports this claim it cannot be verified.

The 3-day compressive strength of Test Series 1 was 12% weaker than Test Series 2. The strengths were 61 MPa and 69 MPa, respectively. By day 60, the strengths were essentially equal, at 133 MPa. However, the modulus of elasticity of Test Series 1, 39398 MPa, was 7% higher than that of Test Series 2, 36582 MPa. Based on these results, no pattern can be found to connect fiber content and compressive strength or modulus of elasticity.

5.3.1.2 Direct Tension

The tensile strength plot in Figure 5.3 shows that Test Series 1 and 2 exhibited the same pattern in direct tension testing. The pattern shows that peak strength was reached after first-cracking, which typically occurred before $1x10^{-3}$ strain. From $1x10^{-3}$ to $4x10^{-3}$ strain, roughly, concrete and fibers were both engaged. After about $4x10^{-3}$ strain it can be assumed that mainly fibers contributed to the tensile strength of the UHPC since the cracking was large enough to separate the cementitious material.

The peak strength for Test series 2 was only 70% the strength of Test Series 1. This indicates that fiber content has a big impact on tensile strength. This is consistent with the concept that, at the peak load, extensive cracking has already taken place and the majority of the tension force is resisted by the fibers.

5.3.1.3 Flexural Beam

Figure 5.5 shows that the flexural strength of Test Series 2 was roughly 70% the strength of Test Series 1. This is consistent with the ratio of tensile strength which indicates that the flexural and tensile response of UHPC heavily depend on fiber content. However, the strength with 1% fiber was more than half of the strength with 2% fiber.

5.3.2 Shear Test Results

The shear tests were analyzed by looking at the three phases described in Chapter 4; first cracking, crack localization, and failure. First cracking is defined as the moment cracking first became noticeable upon visual inspection. Crack localization is the point at which individual cracks coalesced and the failure line began to open. Failure is the exact moment the panel separated, before the actuators showed a large jump in free movement. The first two measured depend on human observation, so are not objective or uniquely defined. A tabulated record of the stress, crack width, and crack slip at each point of the test for Test Series 1 and Test Series 2 is shown in Table 5-3. Stress units are MPa and crack units are mm.

Table 5-3: Summary of Shear Test Results by Fiber Content

Summary of Shear Test Results by Fiber Content									
	First Cracking			Crack Localization			Failure		
Test Series	Shear Strength (MPa)	Crack Width (mm)	Crack Slip (mm)	Shear Strength (MPa)	Crack Width (mm)	Crack Slip (mm)	Shear Strength (MPa)	Crack Width (mm)	Crack Slip (mm)
1	3.8	0.0063	0.0283	9.00	0.827	0.885	9.52	3.73	3.01
2	2.31	0.01	0.022	6.89	1.43	1.11	7.38	6.31	4.13

Figure 5.6 shows the recorded stress and crack opening data. Test Series 1, 2% fiber content, is shown in solid black. Test Series 2, 1% fiber content, is shown in a black dashed line. This figure, as well as Figure 5.4, are relevant to this section.

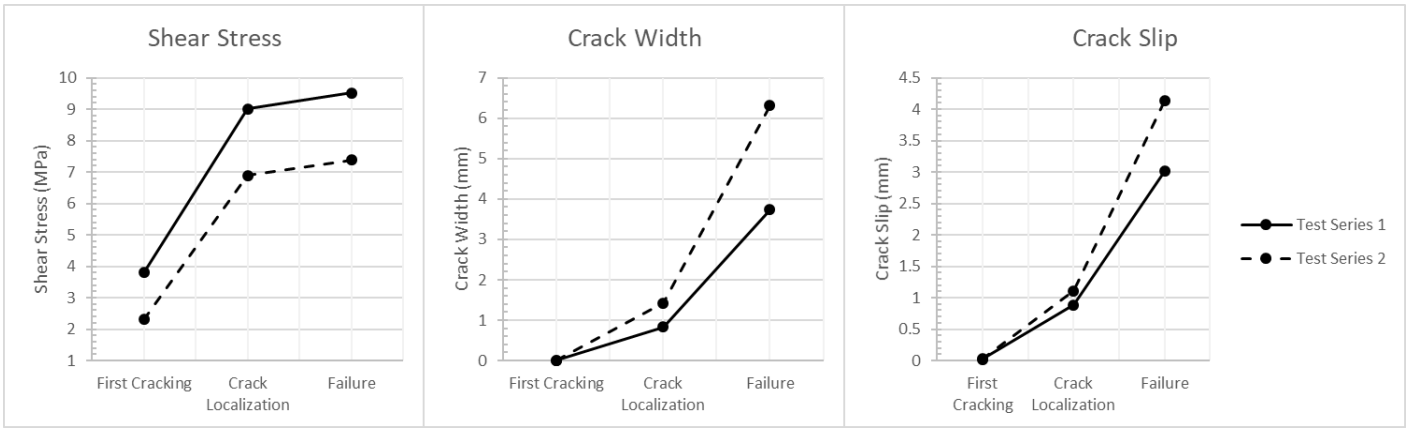

Figure 5.6: Shear test results by fiber content

Throughout each stage of testing, the 1% fiber panel consistently showed lower strength and higher crack opening than the 2% panels. The final shear strength of Test Series 1 was 9.52 MPa while Test Series 2 was only 7.38 MPa. This is a reduction of about 22% in shear strength, similar to difference in tensile and flexural strength between the test series. Not only did the 1% panel fail at a lower strength than the 2%, but it also saw first cracking occur at a much lower value. The difference in the first cracking strengths was about 40% of the Test Series 1 results. First cracking was determined based on visual inspection and is subject to human error. Therefore, this metric may not be a reliable comparison between fiber content.

Although the strengths of the test series' varied, the failure patterns were similar. First cracking occurred at around 30-40 percent of the peak strength and crack localization occurred at about 94 percent of the peak strength. Additionally, the crack width at crack localization was about 22 percent of the failure width, and crack slip was about 28 percent the failure slip. This shows that the panels behaved similarly even though they had different result ranges.

The only difference in pattern of failure is shown between the crack width and slip for each test series. In Test Series 1, the final slip is 80% the size of the width. For Test Series 2, the crack slip is only 65% the size of the width.

5.4 Influence of Material Source

This section will discuss the effect of material source on UHPC behavior and strength by comparing the results of Test Series 1, with UW materials, and Test Series 3, with OU materials. Both had 2% fiber content.

5.4.1 Material Test Results

The following bar graph, Figure 5.7, shows the material test results normalized with respect to UW materials. The UW results are in black and the OU results are in a grid pattern. This figure, as well as Figure 5.3, will be referenced throughout this section.

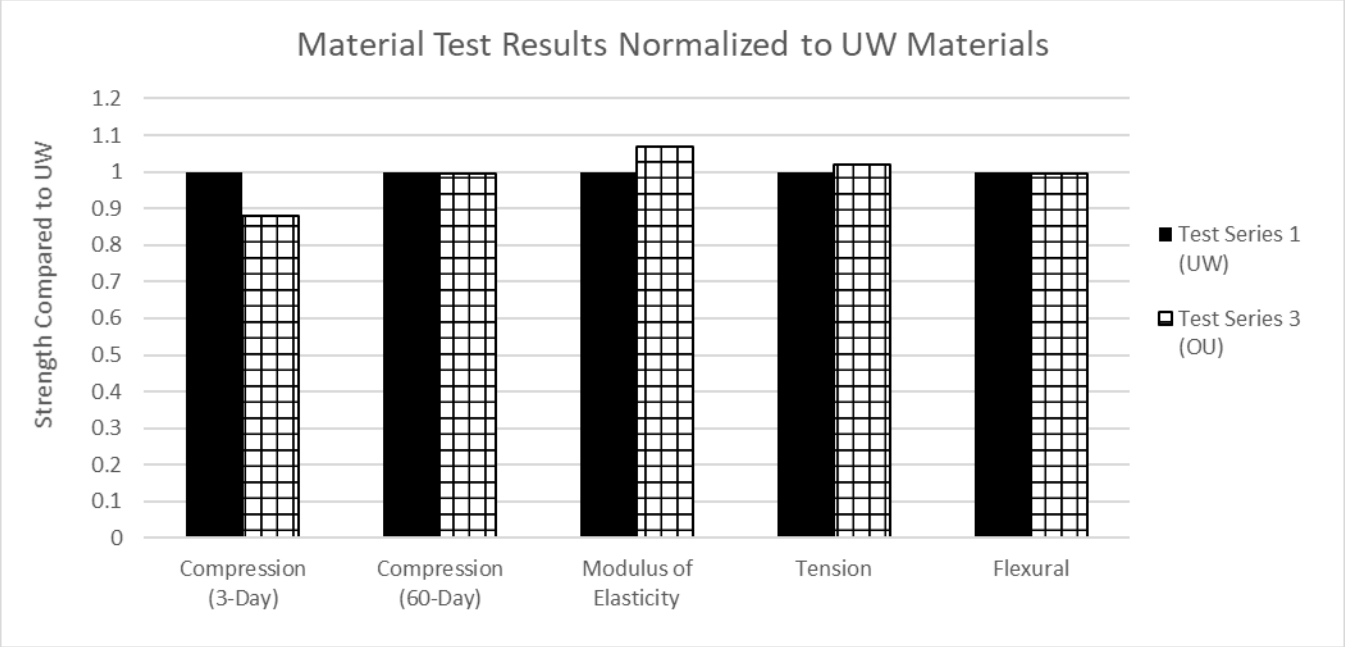

Figure 5.7: Material test results normalized to UW materials

5.4.1.1 Compression and Modulus of Elasticity

Figure 5.7 shows that the materials from the different sources led to results that were essentially identical, and that no consistent trends could be seen. The only real exception to this observation lies in the 3-day compression test. However, the exact age (in hours) at that test was not recorded for either UHPC batch, and hence maturity was likely somewhat different as well as material sourcing. Therefore, non-systemic differences between results are more likely for that test than

others. Within the limitations of these tests, the sourcing of materials has no influence on the material properties measured.

5.4.1.2 Direct Tension

The Tensile Strength plot in Figure 5.3 shows that Test Series 1 and 3 exhibited the same pattern in direct tension testing. The pattern shows that peak strength was reached after first-cracking, which typically occurred before $1x10^{-3}$ strain. From $1x10^{-3}$ to $4x10^{-3}$ strain, roughly, concrete and fibers were both engaged. After about $4x10^{-3}$ strain, it can again be assumed that mainly fibers contributed to the tensile strength of the UHPC since the cracking was large enough to separate the cementitious material.

The average peak strength for Test Series 1 and 3 were almost exactly the same at 6.6 MPa. This indicates that material sourcing did not affect the direct tension results.

5.4.1.3 Flexural Beam

Figure 5.7 shows that the flexural strength of Test Series 3 was equal to the strength of Test Series 1. These results once again support the concept that the material source does not affect UHPC behavior.

5.4.2 Shear Test Results

The shear tests were analyzed by looking at the three phases described in Chapter 4; first cracking, crack localization, and failure. A tabulated record of the stress, crack width, and crack slip at each point of the test for Test Series 1 and Test Series 3 is shown in Table 5-4. Stress units are MPa and crack units are mm.

Table 5-4: Summary of Shear Test Results by Material Source

Summary of Shear Test Results by Material Source									
	First Cracking			Crack Localization			Failure		
Test Series	Shear Strength (MPa)	Crack Width (mm)	Crack Slip (mm)	Shear Strength (MPa)	Crack Width (mm)	Crack Slip (mm)	Shear Strength (MPa)	Crack Width (mm)	Crack Slip (mm)
1	3.8	0.0063	0.0283	9.00	0.827	0.885	9.52	3.73	3.01
3	4.46	0.067	0.09	9.21	1.22	1.03	9.29	2.92	1.91

Figure 5.8 shows the recorded stress and crack opening data. Test Series 1, UW materials, is shown in solid black. Test Series 3, OU materials, is shown in a black dashed line. This figure, as well as Figure 5.4, are relevant to this section.

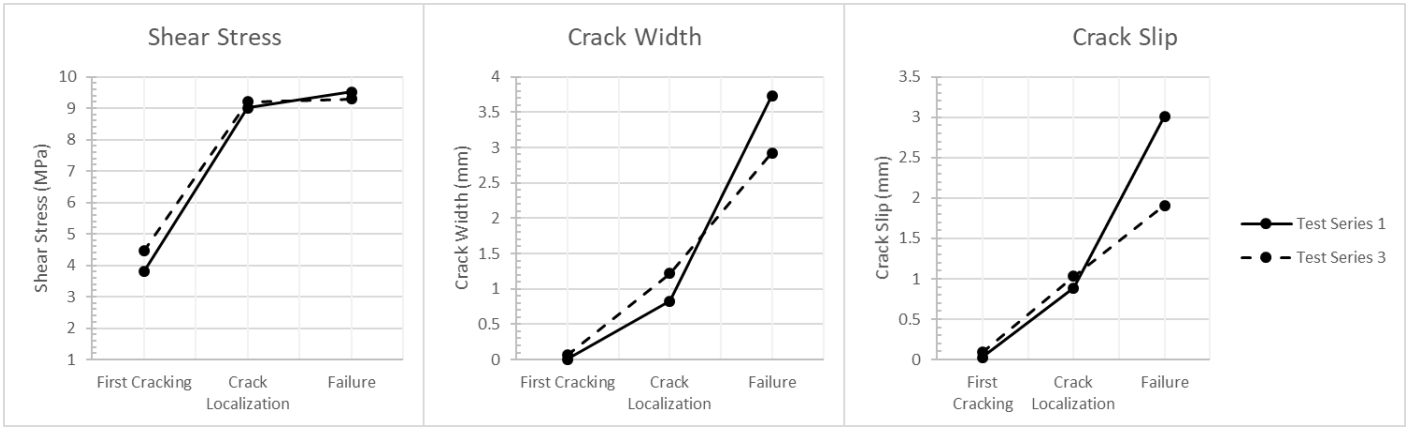

Figure 5.8: Shear test results by material source

There are very few distinguishable differences in the shear test results for Test Series 1 and Test Series 3. Upon failure, Test Series 1 had a slightly higher peak strength at 9.52 MPa compared to Test Series 3's 9.29 MPa. This difference of 2.5% is not statistically significant, especially with only one OU panel tested. Therefore, the effect of material sources is negligible in shear response of UHPC.

Chapter 6: Comparison of Results

In this chapter, the previously discussed results are compared with the results of UHPC experiments conducted at other institutions and assessed in the context of widely accepted standards available in literature. The goal is to determine any effects on performance caused by differences in the mix designs and mixing procedures used by the different institutions, and to compare results with those obtained by others in previous research. The effort focuses on the material tests, because no pure shear tests by other researchers were identified. In their place, simple comparisons were made with shear tests results on fiber-reinforced concrete (FRC) panels.

6.1 Material Test Results

Results from experiments at University of Washington and The University of Oklahoma are heavily utilized in this section. First, the results of this project itself are included. However, in order to easily compare with other results, they are referred to using different nomenclature. Test Series 1 and Test Series 2, which are UW materials with 2% fibers and UW materials with 1% fibers, are labeled simply as UW. Test Series 3, which is OU materials with 2% fibers, is labeled as OU.

A prior project from UW, Peruchini et al. [22], used UW materials and resulted in data for compression, direct tension, and flexural strength of UHPC. The UHPC mix was not the same as the current project, but the same mix procedure and equipment were used. Table 6-1 gives the mix design. All results from Peruchini are named P-UW in reference to the researcher's last name.

Additional data were collected from two theses at the University of Oklahoma, written by Richard Campos [28] and Yana Dyachkova [29]. Campos performed compression and direct tension tests on UHPC using the same mix design as the present UW project, but using OU materials and with fiber content ranging from 0 to 6 percent. These results are labeled as C-OU, in reference to the author's last name. Dyachkova performed compression and flexural beam tests on UHPC using the same mix design as C-OU and UW, but using both OU and FIU (Florida International University) materials with fiber content ranging from 0 to 6 percent. The OU results are referred to as D-OU and FIU results referred to as D-FIU, in reference to the author's last name.

Table 6-1: Mix Design Comparison

UHPC Mix Design Comparison (per yd^3)											
			Type 1 Cement	Slag	Silica Fume	Fine Sand	Steel Fibers	Fiber Content	HRWR	Retarder	Water
Name	Testing Location	Materials Location	lb	lb	lb	lb	mm	%	oz/cwt	oz/cwt	w/c
UW	UW	UW	1179.6	589.8	196.6	1966	13/0.2	1, 2	20.7	5.66	0.2
OU	UW	OU						2			
C-OU	OU	OU						0, 1, 2, 4, 6			
D-OU	OU	OU						0, 1, 2, 4, 6			
D-FIU	OU	FIU						0, 1, 2, 4, 6			
P-UW	UW	UW	1500	0	260	1574	13/0.2	1.8	41.5	0	0.185

A summary of the material test results including- compression, modulus of elasticity, direct tension, and flexural beam, is shown in Table 6-2.

Table 6-2: Summary of all UHPC Batch Material Test Results

Summary of all UHPC Batch Material Test Results						
Fibers (%)	Age of UHPC (days)	Batch	Compressive Strength (MPa)	Modulus of Elasticity (MPa)	Tensile Strength (MPa)	Flexural Strength (MPa)
0	28	C-OU	127	N/A	6.41	N/A
	28	D-OU	117	36414	N/A	8.73
	28	D-FIU	97.8	N/A	N/A	13.5
1	60	UW	132	36582	4.40	12.9
	28	C-OU	124	N/A	7.03	N/A
	28	D-OU	117	37379	N/A	12.2
	28	D-FIU	105	N/A	N/A	15
1.8	14	P-UW	90.3	34345	6.62	18.3
2	60	UW	134	39398	6.56	18.3
	60	OU	133	42106	6.44	18.2
	28	C-OU	139	N/A	8.21	N/A
	28	D-OU	125	38966	N/A	16.9
	28	D-FIU	111	N/A	N/A	19.3
4	28	C-OU	144	N/A	11	N/A
	28	D-OU	122	38897	N/A	29.5
	28	D-FIU	115	N/A	N/A	28
6	28	C-OU	165	N/A	10.17	N/A
	28	D-OU	126	41586	N/A	26.1
	28	D-FIU	134	N/A	N/A	31

6.1.1 Compression

Figure 6.1 shows compressive strength as a function of fiber content. The UW tests performed as part of this study are shown in solid black; all other sources are denoted in the legend.

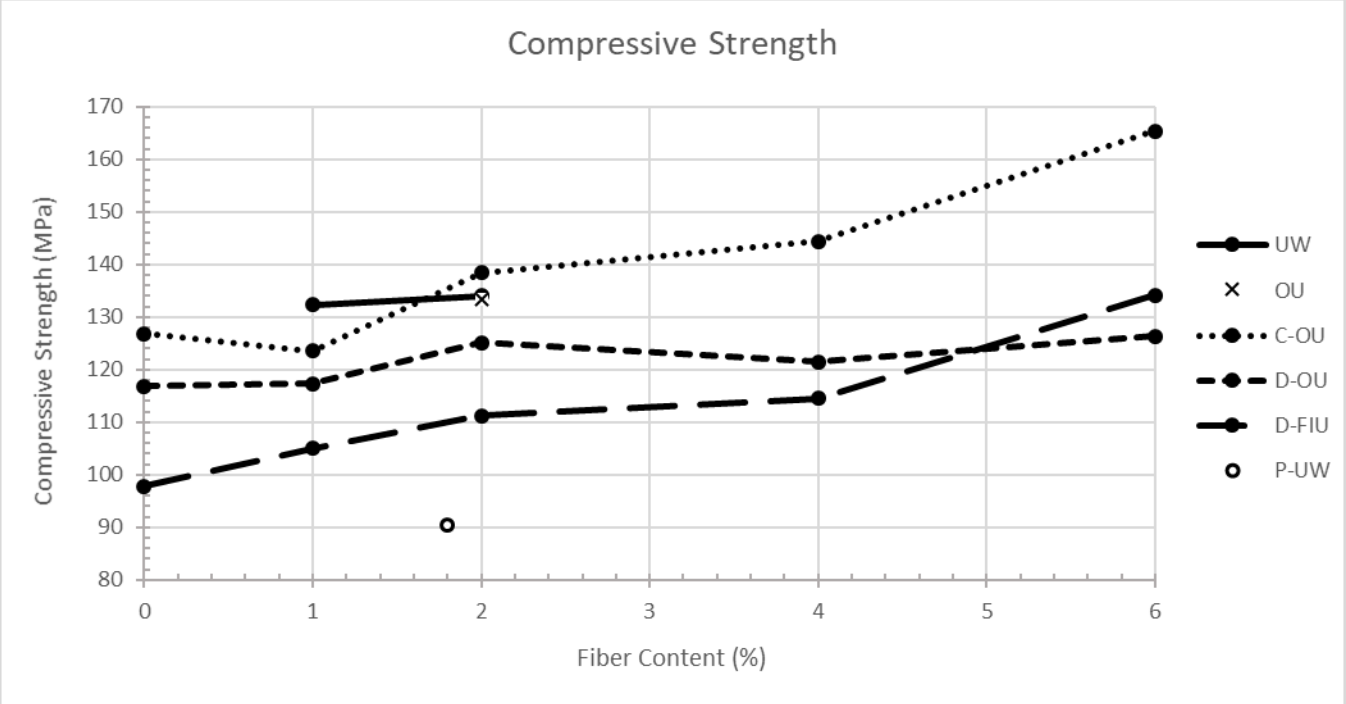

Figure 6.1: Compressive strength comparison

The Federal Highway Administration (FHWA) defines UHPC as having a compressive strength no less than 150 MPa, which is a requirement met only by one out of these nineteen batches. However, the Portland Cement Association (PCA) defines UHPC as having a minimum compressive strength of 120 MPa [3]. The FHWA and PCA definitions apply to a 28-day strength, so P-UW, tested at 14 days, should not be judged according to those criteria.

Material Source

Based on Figure 6.1, the strengths obtained in this research project, UW and OU, were typically higher than those tested at OU, using materials sourced from different locations, using the same mix design. The OU batch matches more closely with UW than it does with any of the other UHPC tested in Oklahoma using Oklahoma materials (C-OU and D-OU). This could be due to differences in mix procedure, mixing equipment, curing, or consolidation. D-OU and D-FIU used the same

mix design and were mixed at the same university, but they used different mixing equipment for each batch. Therefore, the difference in strength cannot be contributed only to material sourcing and it is likely that material sourcing does not typically have a big impact on UHPC strength.

Mixing Procedure

D-OU hardly saw any increase in strength as fibers were increased. The 2% strength was essentially equal to the strength of the 6% batch. Problems with the mixing procedure become more prominent as fibers increase, based on the experience at UW, which could explain why the D-OU batch saw little increase in strength with higher fiber content. In the C-OU and D-FIU batches, compression strength increased significantly with fiber content, implying fewer mixing problems, even though they were cast and tested at the same lab as D-OU. This suggests that human dependent processes have a large effect on the UHPC.

Fiber Content

Finally, the strength of each UHPC batch increased as fiber content increased, but the amount of the increase was not consistent for all batches. This shows that compressive strength depends on fiber content, but the degree of dependency may vary based on the other factors discussed. In order to judge the influence of fiber content, the results were averaged and fit with a linear trendline in Figure 6.2. The trendline was found to be:

$$f_c' = 115.4 + 4.2v_{sf}\ (MPa) \quad (6.1)$$

Where:

$v_{sf} = volumetric\ ratio\ of\ steel\ fibers$ (%)

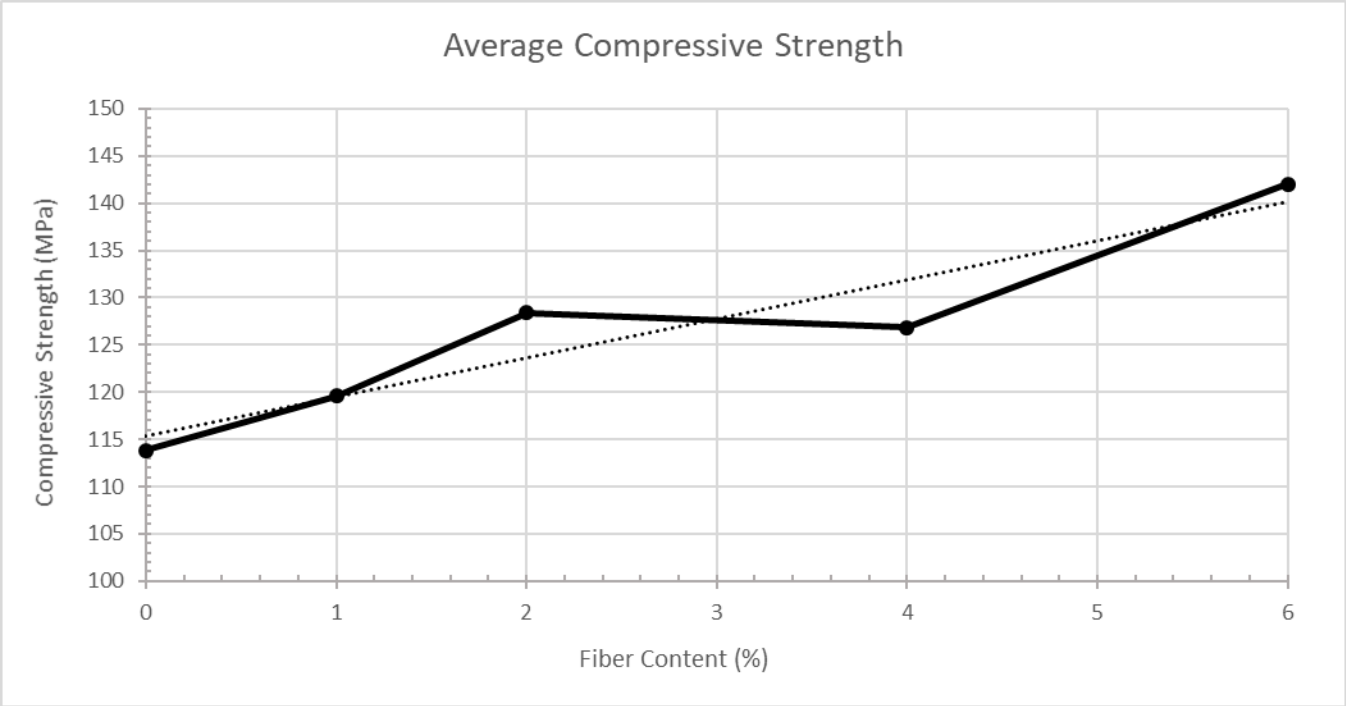

Figure 6.2: Average compressive strength

All of the compressive strength observations support the idea that the compressive strength of UHPC depends highly on mixing procedure and cementitious component and not as much on fiber content. Additionally, since not many samples met the minimum industry guidelines for UHPC, it may suggest that these guidelines are unreasonable for small batches without industrial quality equipment.

The foregoing comparisons address compressive strength. Ductility is also of interest. Information of ductility is available only for the specimens tested at UW, and even then it is observational rather than numerical. However, it was observed that compression tests on 1% fiber failed explosively, while those of 2% did not. This implies that the increase of fibers offers a marked improvement in ductility.

6.1.2 Modulus of Elasticity

The Graybeal equation used to estimate modulus of elasticity was developed using the general AASHTO modulus of elasticity equation [10]. It is based on the compressive strength of the UHPC and is estimated to be applicable for UHPC with compressive strengths between 28 and 193 MPa. The equation is as follows:

$$E_c = 46200\sqrt{f'_c}\ (psi) \quad (6.2)$$

$$E_c = 3836\sqrt{f'_c}\ (MPa) \quad (6.3)$$

Where:

$E_c = modulus\ of\ elasticity$

$f'_c = compressive\ strength$

To compare the modulus of elasticity experimental results with the Graybeal equation, the experimental results were divided by $\sqrt{f'_c}$ and plotted in Figure 6.3 against fiber content.

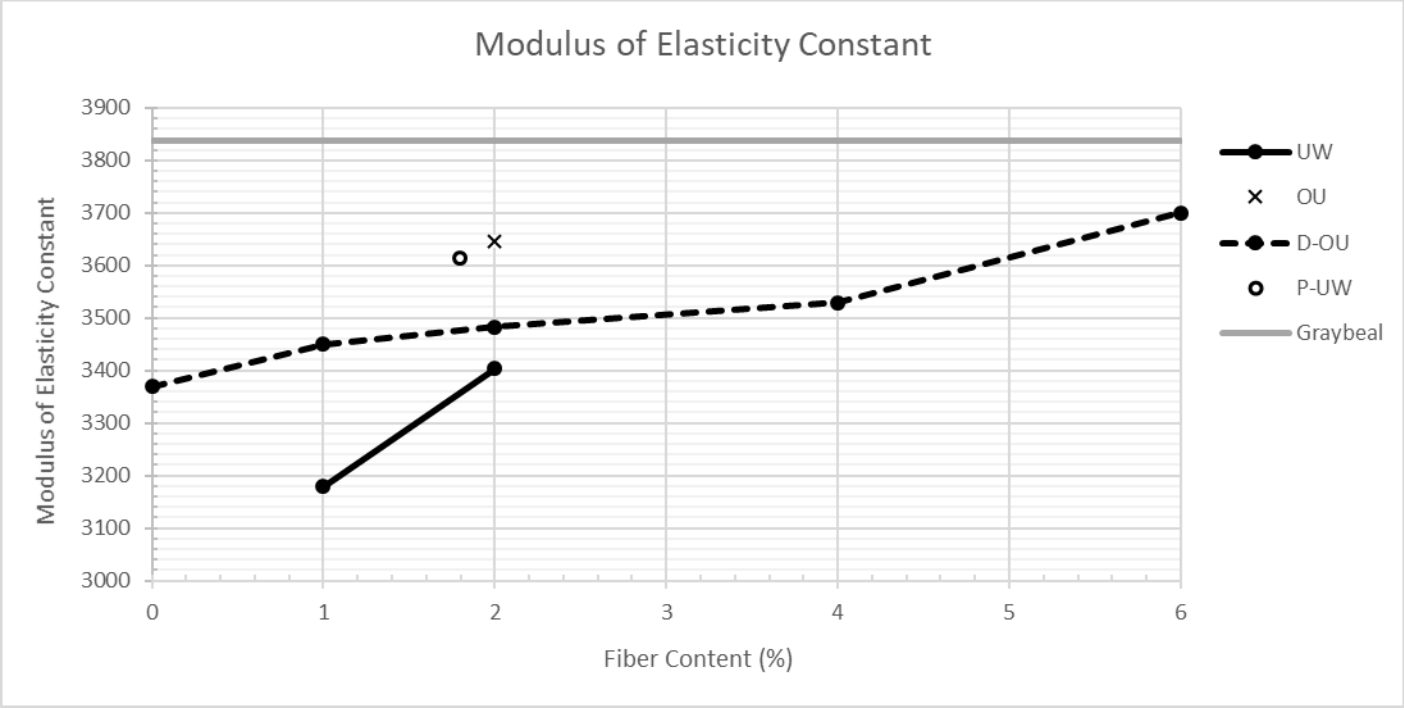

Figure 6.3: Modulus of elasticity comparison

As shown in Figure 6.3, Graybeal's equation overestimated the modulus of elasticity for every UHPC batch tested, no matter the material source or mix design. On average, the equation predicted a value 10% higher than the measured modulus of elasticity. The most accurate estimate was 4% higher (D-OU 6%) and the least accurate was 20% higher (UW 1%). The level of accuracy of Graybeal's equation appears to increase as fiber content increases.

When comparing the test results against each other, the observations are similar to those based on compressive strength. First of all, there is little change in the result with increasing fibers. The D-OU batch only sees an increase of 10% when going from zero fibers to 6% fibers. This is because, similar to compressive strength, it is likely that fibers do not affect the modulus of elasticity as much as compressive strength does. The P-UW modulus of elasticity is the lowest, like it was for compressive strength.

Since it has been shown that modulus of elasticity is more related to compressive strength than fiber content, the modulus of elasticity results are plotted against compressive strength in Figure 6.4. The trendline of the experimental results is shown with a dotted line and the Graybeal equation is shown in the gray line. The equation of the trendline was found to be:

$$E_c = 3482\sqrt{f_c'}\ (MPa) \tag{6.4}$$

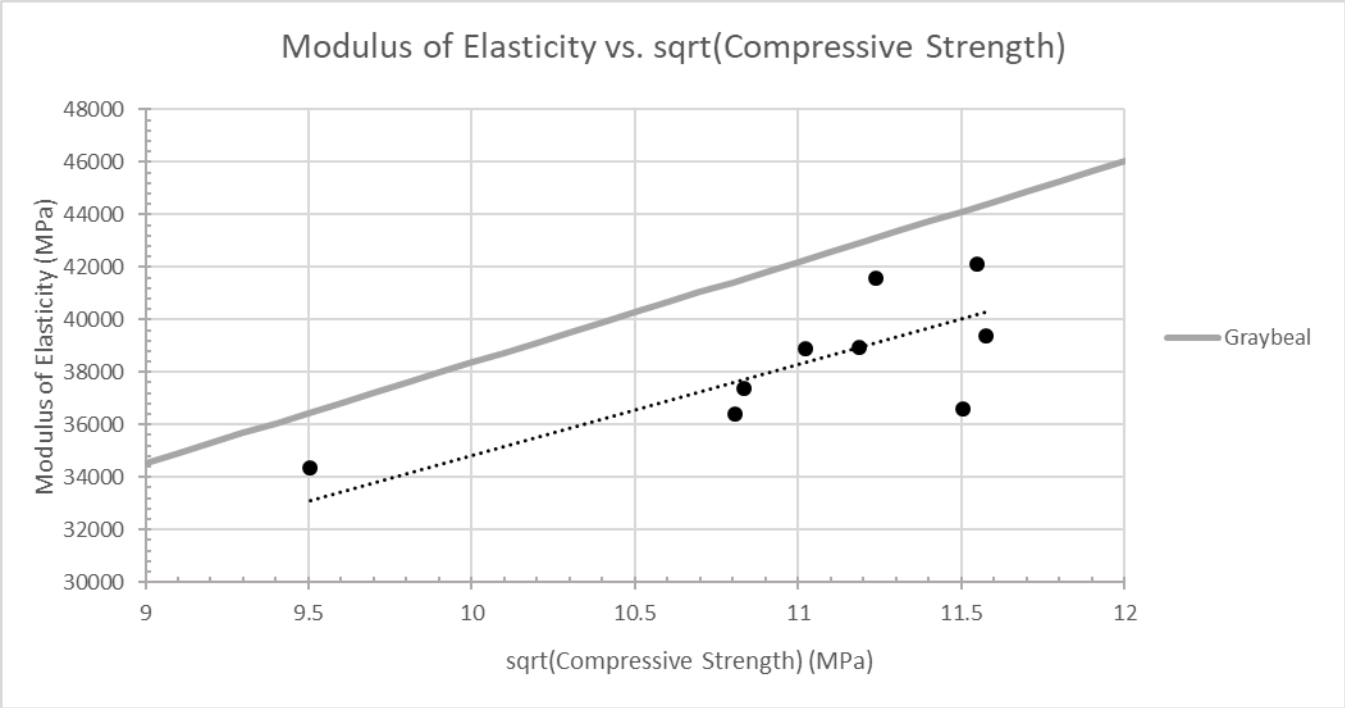

Figure 6.4: Modulus of elasticity vs. compressive strength

6.1.3 Direct Tension

Meaningful discussion of tension strength requires consideration of several parameters, because they have a significant effect on the outcome. For concretes without fiber reinforcement, the stress to cause first cracking is essentially the same as the peak strength; because failure is brittle and sudden, distinguishing between first cracking and peak load is difficult in a test. Additionally, the type of test (direct tension vs. split cylinder vs. flexural beam) influences the result, since the stress field is different in each case. In some cases, such as the direct tension test, considerable scatter is to be expected because even small eccentricities in the load path affect the results.

In fiber-reinforced concrete, including UHPC, these same characteristics affect the measured results, but an additional issue is important: what constitutes the tension strength? First cracking, peak strength, and strength at large strain (taken here to be 1%) all measure different features of the tension properties of the material. Furthermore, first cracking might be expected to be related

to the cementitious properties (and hence compressive strength) and to correlate poorly to the fiber content, because the stress in the fibers is so small when the cement matrix cracks. By contrast, the peak stress and stress at 1% strain might be expected to correlate better with the fiber content (and the bond of the paste to the fibers) because the cracks are then wide enough that little tension strength remains in the paste. Unless the UHPC contains coarse aggregate, which is uncommon, aggregate interlock will play no role.

Measurements of first cracking were not available for the C-OU or P-UW tests. In the UW tests, the value was based on visual observation which is not entirely reliable. Consequently, the values used here are mainly the peak stress in tension and the comparisons between samples are made using the fiber content as the independent variable.

The Graybeal equation used to estimate tensile strength was based on multiple experimental studies. It is based on the compressive strength of the UHPC and varies slightly based on curing method. The equation for no steam curing is given as Equation (6.5) and (6.6):

$$f_{ct} = 6.7\sqrt{f'_c}\ (psi) \tag{6.5}$$

$$f_{ct} = 0.556\sqrt{f'_c}\ (MPa) \tag{6.6}$$

The equation with steam curing is given as Equation (6.7) and (6.8):

$$f_{ct} = 8.3\sqrt{f'_c}\ (psi) \tag{6.7}$$

$$f_{ct} = 0.689\sqrt{f'_c}\ (MPa) \tag{6.8}$$

Where:

$f_t = tensile\ strength$

$f'_c = compressive\ strength$

To compare the direct tension experimental results with the Graybeal equation, the experimental results were divided by $\sqrt{f'_c}$ to find the constant. The constant was then plotted in Figure 6.5 for

each experimental result as well as the Graybeal equation constant for no steam curing and steam curing. The only UHPC batch that was steam cured was C-OU.

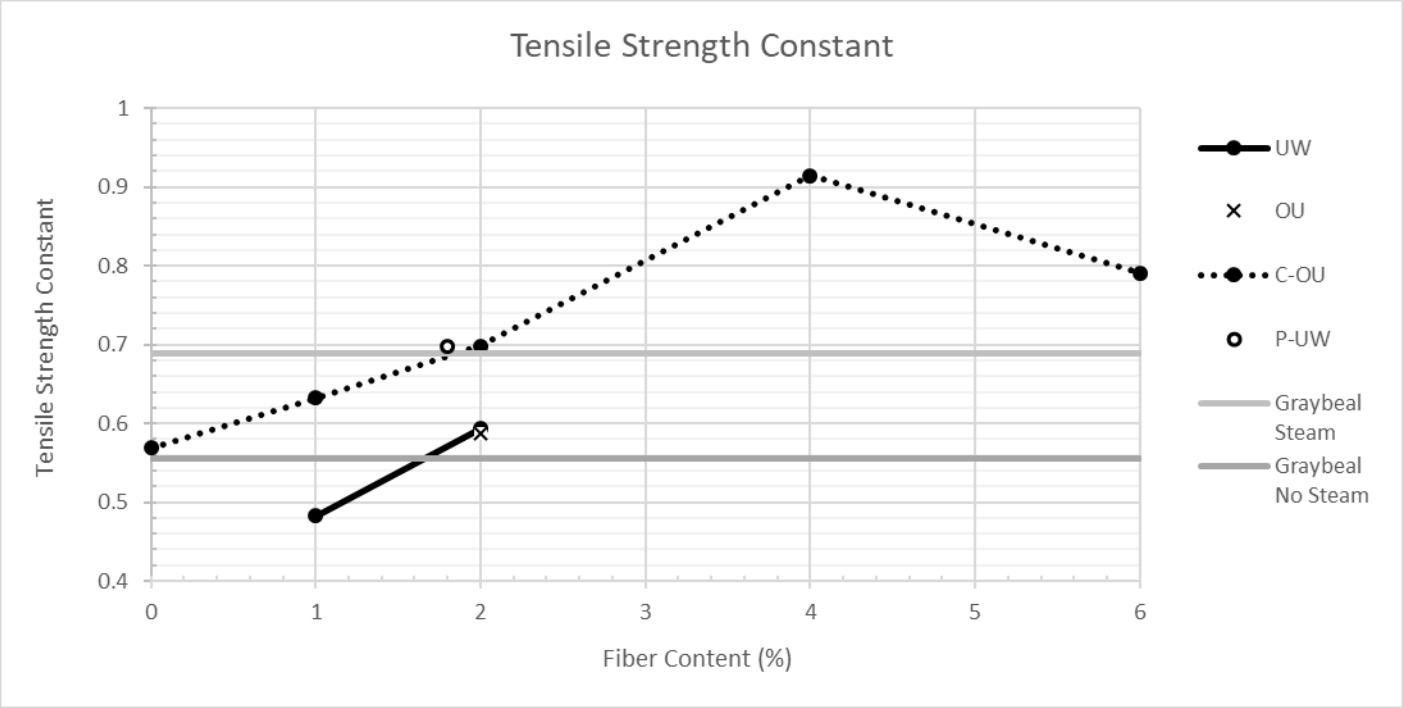

Figure 6.5: Tensile strength comparison

Based on Figure 6.5, the equation overestimates tensile strength for low fiber content and underestimates the strength for higher fiber content. This may be because while first cracking was dictated by the tensile strength of concrete, as the strain increased fibers became engaged resulting in an increase in strength. The more fibers crossing the crack, the more the tension strength increases.

The results from C-OU show a drop in tensile strength when the fiber content increases from 4% to 6%, which is the opposite trend that is seen for the range 0% to 4%. Three samples were tested with 6% fiber content, none of which showed higher tension strength than the 4% samples. It is unclear whether the result is anomalous or reflects a real trend. The C-OU results for 0% to 4%, and the work of previous researchers, show that the tension strength is directly related to the fiber

content, so, in the absence of other effects, more fiber should be expected to lead to higher tension strength. Thus, if the results are not anomalous, some other characteristic must be active. Possibilities include difficulties with complete mixing, or perhaps the need for adjustment to the cementitious component to allow full bonding of the fibers.

The direct tension test results indicate that while compressive strength and modulus of elasticity depend more on concrete than fibers, tensile strength depends on both materials. With that being said, the C-OU results prove that steam curing does result in higher strengths. For 2% fibers, steam curing led to an increase of almost 20% in strength. This is likely because the method of curing affects the bond between the cement matrix and steel fibers. In this case steam curing had a positive effect on the bond.

The theory that fiber content has a large impact on tensile strength is also supported by comparing the UHPC batches individually as fiber content increases. There is an increase of 60% between zero and 6 percent fibers for the C-OU, proving that fibers make a substantial difference. Additionally, while P-UW has shown the lowest results for compressive strength and modulus of elasticity, it is much closer to the results from UW and OU in tension. This may show that the difference in the cementitious component of the mix design that had a large effect on the compression and modulus of elasticity, has a lower impact on tensile strength. Especially since the P-UW samples were tested at 14 days after casting, instead of 28 days after casting like the rest of the samples.

In order to judge the influence of fiber content on tensile strength, the results were averaged and fit with a linear trendline in Figure 6.6. The trendline was found to be:

$$f_t = 5.89 + 0.84 v_{sf}\ (MPa) \quad (6.9)$$

Where:

$v_{sf} = volumetric\ ratio\ of\ steel\ fibers\ (\%)$

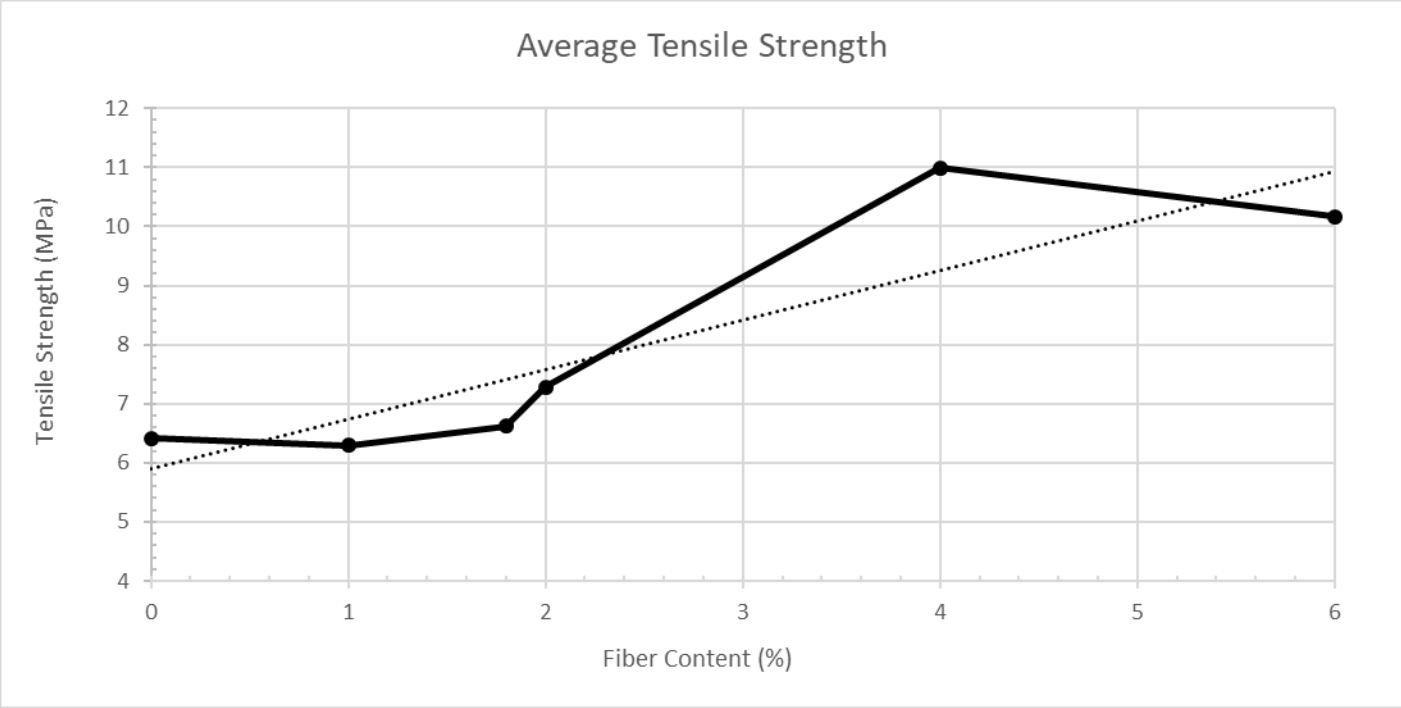

Figure 6.6: Average tensile strength

Graybeal's equation contains the effect of fiber content only to the degree that compressive strength depends on fiber content, which Figure 6.2 shows to be modest. The data shown in Figure 6.6 show that the tensile strength is strongly correlated with fiber content, and physical arguments about the mechanical behavior also support that view. Thus it is proposed here that the tension strength of UHPC be treated primarily as a function of fiber content. Other characteristics, such as curing method and fiber dimensions, might also be relevant, but they lay outside the scope of this study.

Graybeal Tensile Response Idealization

Graybeal identified three phases of the tensile response of UHPC. The first phase is the elastic phase. It is the portion of the test where the material experiences elastic straining before discrete cracks are formed. The elastic phase ends when first cracking occurs. Next, Phase Two refers to the multi-cracking phase. The UHPC forms multiple cracks in the reduced section of the test specimen due to the post-cracking strength of the fibers. Finally, Phase Three is the localized deformation phase. One crack within the region starts to dominate, and continues to widen as the

fibers debond and pull out, resulting in a gradual decrease in stress. Figure 6.7 is the idealized tensile response curve based on these phases.

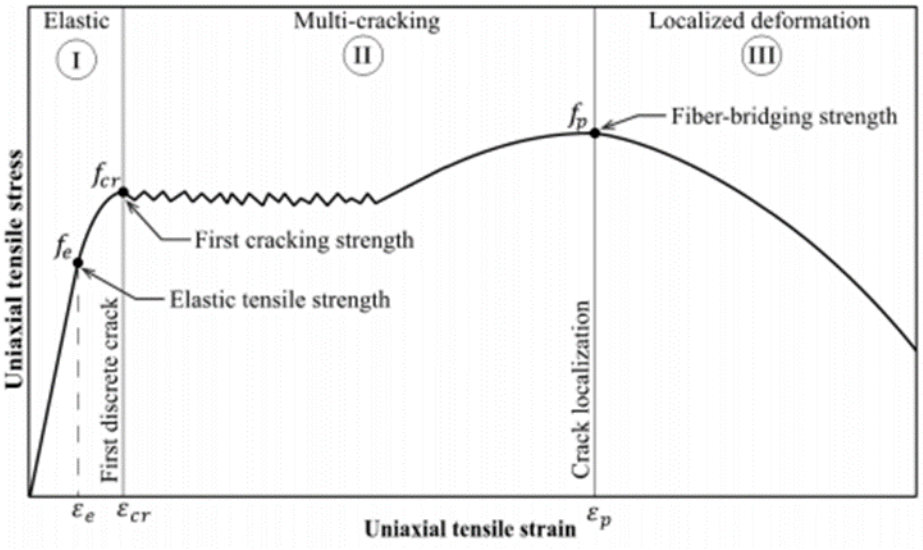

Figure 6.7: Idealized tensile response of UHPC

The tensile response observed by Graybeal experimentally was not quite as exaggerated as the idealized model suggests. Figure 6.8 shows the stress vs. strain curves for 2% fiber UHPC tested by Graybeal. The details of the study, including mix designs for each batch, are included in Chapter 2.

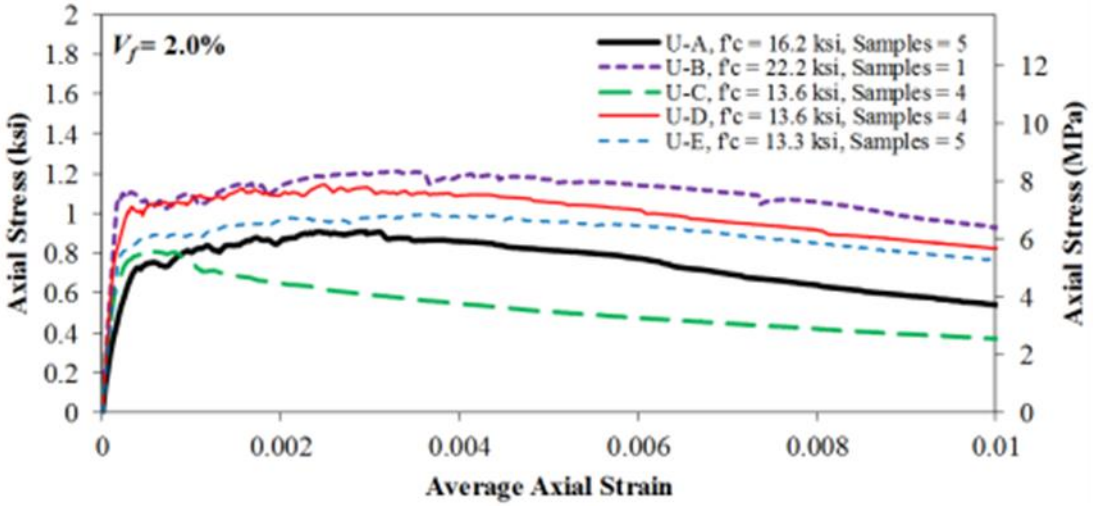

Figure 6.8: Tensile stress-strain responses for UHPC with 2% fiber

Table 6-3 shows the corresponding first cracking, ultimate stress, crack localization, and sustained strength data from the study. All units are MPa.

Table 6-3: Summary of Graybeal Direct Tension Results

Summary of Graybeal Direct Tension Results											
			First Cracking		Crack Localization		Ultimate Point		Sustained Strength		
Batch	Age of UHPC (days)	Compressive Strength (MPa)	Stress (MPa)	Strain	Stress (MPa)	Strain	Stress (MPa)	Strain	Stress (MPa)	% Ultimate	Strain
U-A	6	112	5.5	0.00052	6.42	0.00347	6.47	0.00287	3.8	59	0.01
U-B	28	153	7.32	0.00018	8.32	0.00356	8.36	0.00328	6.2	74	0.01
U-C	4	93.8	5.79	0.00048	5.73	0.00102	5.87	0.00051	2.5	43	0.01
U-D	1	93.8	7.03	0.00032	7.76	0.00392	8.09	0.00247	5.8	72	0.01
U-E	4	91.7	6.51	0.00030	6.96	0.00404	7.06	0.00321	5.5	78	0.01
									Mean	*65.2*	
									Standard Deviation	*12.8*	

The sustained strength is noticeably varied for the UHPC batches. While all of the mixes used 2% fiber content, the mix designs had different dry powders, admixtures, water-to-cement ratios, and fiber size/shape. The detailed mix designs are provided in Table 2-1 in Chapter 2. U-A used the largest fibers at 1.18 in long, while the remaining batches used fibers 0.5 in long. Since most of the fiber lengths were similar, that was likely not the main factor contributing to sustained strength. Therefore, the cementitious component of UHPC must play a role. It is likely that the different cement pastes resulted in different bond strength with the fibers, leading to varied sustained strength results. Additionally, the ages of the UHPC batches varied. Most of the batches were tested very soon after casting, which could lead to inconsistent results since the UHPC has not had sufficient time to cure.

Figure 6.9 shows the tensile stress-strain curve for the UHPC tests performed at UW and Table 6-4 shows the recorded stress and strain for each testing phase defined by Graybeal.

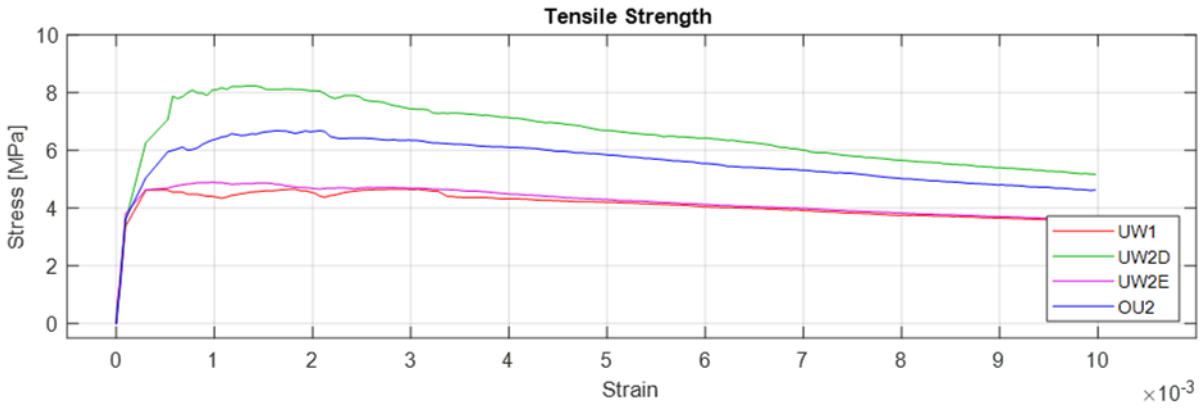

Figure 6.9: Tensile stress-strain responses for UHPC tested at UW

Table 6-4: Summary of UW Direct Tension Results

Summary of UW Direct Tension Results											
			First Cracking		Crack Localization		Ultimate Point		Sustained Strength		
Batch	Fiber %	Compressive Strength (MPa)	Stress (MPa)	Strain	Stress (MPa)	Strain	Stress (MPa)	Strain	Stress (MPa)	% Ultimate	Strain
UW2D	2	139	7.875	0.000525	7.295	0.003225	8.23	0.001375	5.171	63	0.01
UW2E	2	134	4.635	0.0003	4.666	0.002425	4.89	0.000975	3.58	73	0.01
UW1	1	133	4.62	0.0003	4.402	0.003375	4.66	0.002875	3.54	76	0.01
OU2	2	133	6.114	0.000675	6.442	0.002225	6.68	0.002075	4.623	69	0.01
									Mean	*70.25*	
									Standard Deviation	*4.9*	

The first cracking point was determined based on visual inspection during testing, which is operator dependent and therefore not reliable enough for meaningful comparison with Graybeal's data. Graybeal's multi-cracking, and the plateau shown in Figure 6.7, were not observed during the testing of UW specimens. Instead of seeing multiple initial cracks form into one, a single crack dominated immediately after the initiation of cracking. Even though the physical description of this phase of the UW tests did not match with Graybeal's idealization, the stress-strain curves in both look fairly similar. This could either mean that there were multiple cracks undetectable to the eye during the UW tests, or the description of multi-cracking overestimates the relative size of the cracks formed before localization.

The localized deformation phase also looked different experimentally than theoretically. Instead of seeing a concave curve with increasing strain, the curve almost linearly decreased. Additionally, the ultimate tensile stress occurred during the multi-cracking phase of the response for almost all of the specimens instead of during the localized deformation phase as suggested by Graybeal's idealized curve. Again, while both sets of experimental results did not match the idealized UHPC tensile response curve, they did match each other.

Finally, the sustained strengths of the UW specimens were more nearly constant among specimens than Graybeal's. This is likely due to the fact that the UW mix designs were consistent for each batch while Graybeal tested five different mix designs. With that being said, the percent stress maintained at 1% strain is not a perfect indicator of sustained strength of UHPC since it depends on multiple factors. The most impactful of these factors being fiber length and gage length of the displacement instrumentation. In order to combat the inaccuracies caused by these factors, fracture energy of the tensile response was calculated for the UW results, out to the point where the specimen completely fell apart. It was calculated by taking the area under the stress-strain curve. The fracture energy results are shown in Table 6-5. Unfortunately, this data was not available for the Graybeal model.

Table 6-5: UW Direct Tension Sustained Strength Results

UW Direct Tension Sustained Strength Results (MPa)								
			Ultimate Point		Sustained Strength			Fracture Energy
Batch	Fiber %	Compressive Strength (MPa)	Stress (MPa)	Strain (mm/mm)	Stress (MPa)	% Ultimate	Strain (mm/mm)	Energy (MPa)
UW2D	2	139	8.23	0.001375	5.171	63	0.01	0.1053
UW2E	2	134	4.89	0.000975	3.58	73	0.01	0.0668
UW1	1	133	4.66	0.002875	3.54	76	0.01	0.0692
OU2	2	133	6.68	0.002075	4.623	69	0.01	0.0853

The fracture energy may provide a better picture of the tensile response of UHCPC than sustained strength at 1% strain does since it takes into account the entire stress-strain curve rather than just

two data points. Table 6-5 shows that higher sustained strength does not correspond to higher fracture energy.

6.1.4 Flexural Beam

Flexural strength for the various UHPC experiments is shown in Figure 6.10 as a function of fiber content.

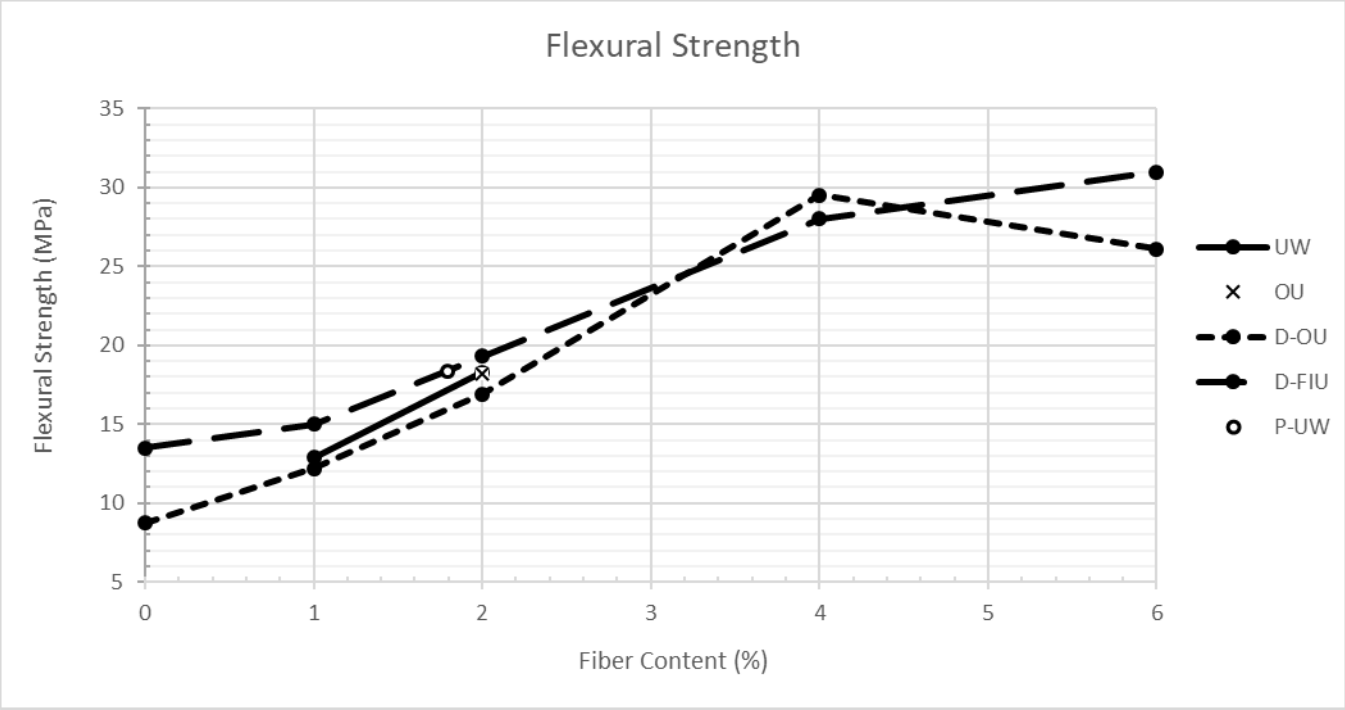

Figure 6.10: Flexural strength comparison

No standard equation exists for estimating flexural strength of UHPC. Therefore, the test results are only compared against each other. The flexural strength was found using Equation (3.6) by assuming an elastic response.

The flexural beam test results follow a similar pattern to the direct tension tests in that the flexural strength rises significantly with increasing fiber content. However, the results from different test series are also more closely grouped than was observed for the tension tests, implying less inherent scatter. With that being said, between 4% and 6% fiber, the D-OU strength drops and the D-FIU strength rises much less slowly than in the 0% to 4% fiber range. This is the same pattern as was

seen for the C-OU direct tension tests. Since the D-OU tests were conducted by different personnel than the C-OU tests, and because the direct tension and flexural beam tests both rely in some sense on the tension strength of the material, the probability of adverse effects at 6% fiber is real. Unfortunately, lab notes from the C-OU and D-OU tests were not available.

According to the results from D-OU and D-FIU, the flexural strength increased by a factor of 2.6 when switching from 0% fibers to 6% fibers. This indicates that the fibrous component of UHPC has a big impact on the flexural strength. This increase is consistent with the observations of tensile strength which makes sense since the two properties are related.

In order to judge the influence of fiber content, the results were averaged and fit with a linear trendline in Figure 6.11. The trendline was found to be:

$$f_r = 11.68 + 3.26v_{sf}\ (MPa) \quad (6.10)$$

Where:

$v_{sf} = volumetric\ ratio\ of\ steel\ fibers$ (%)

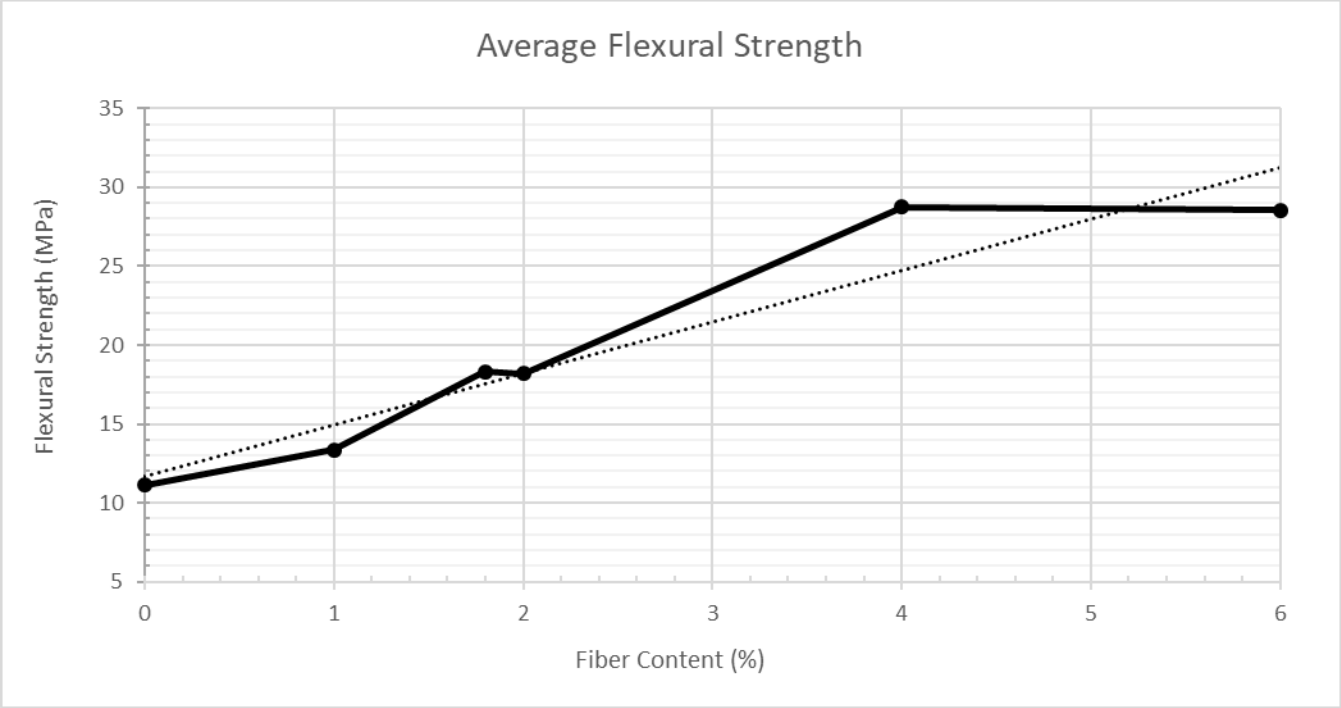

Figure 6.11: Average flexural strength

6.1.5 Tensile Strength

Tensile strength can be determined from both the direct tension tests and the flexural beam tests using Equations 3.3 and 3.8, respectively. Direct tension testing is particularly sensitive, due to issues such as eccentricity and rebar pull-out, and tensile strength derived from flexural loading can be inaccurate since it assumes a plastic material model. Since neither method is without flaws, using both results provides a range of estimated tension strength.

Unfortunately, the only research projects that included both direct tensile and flexural beam tests were this project, and Peruchini's project. Table 6-6 shows the available tensile strength results from both test types. Tension strength from direct tension testing is referred to as f_{td} and tension strength from flexural testing is referred to as f_{tf}.

Table 6-6: UHPC Tensile Strength from Direct Tension and Flexural Testing

UHPC Tensile Strength Results						
Batch	Fibers (%)	f_{td} (MPa)	f_{td}/v_{sf}	f_{tf} (MPa)	f_{tf}/v_{sf}	% Difference
UW2D	2	8.23	4.12	5.73	2.87	30.4
UW2E	2	4.89	2.45	6.07	3.04	24.1
OU2	2	6.68	3.34	5.59	2.80	16.3
2% Average		*6.60*	*3.30*	*5.79*	*2.90*	*23.6*
2% Standard Deviation		*1.36*	*0.68*	*0.20*	*0.10*	*5.76*
UW1	1	4.66	4.66	4.30	4.30	8.37
P-UW	1.8	6.62	3.68	6.09	3.38	8.01
					Overall Average	*19.6*
					Overall Standard Deviation	*8.5*

Table 6-6 shows that the tensile strength from flexural testing is, on average, within 24% of the measured direct tensile strength. It varied whether the difference was positive or negative. The standard deviation of the direct tensile strength was roughly 7 times higher than that of the flexural tensile strength. Therefore, the flexural tests provide a more consistent estimate of strength. This is likely due to the fact that direct tension tests are sensitive to induced error, as previously discussed.

The P-UW sample experienced the best matched tensile strengths. This could indicate that the direct tension testing method used by Peruchini was more reliable than the one used in this project, but with limited test results this cannot be confirmed.

Table 6-6 also shows the tensile strengths divided by fiber content. This metric demonstrates how much tensile strength comes from each percent of fibers in the UHPC. The results show that the UHPC with lower fiber content contributes more shear strength per percent fiber. This suggests that as fiber content increases, there may be a point of diminishing increase in tensile strength.

6.2 Shear Test Results

Most shear studies on UHPC have used reinforced beam specimens, in which the loading inevitably causes shear and bending. Therefore, the equations derived from them for estimating shear capacity are usually not applicable to the pure shear panel tests. However, panel tests have been conducted using fiber reinforced concrete (FRC). Fiber reinforced concrete contains steel fibers, but the concrete component is similar to conventional concrete and the compressive strength of FRC is generally about one third the strength of UHPC. In chapter 5, it was determined that shear strength of UHPC is dependent on both concrete strength and fiber content. Although the concrete component of FRC is different than UHPC, the nature of its shear behavior, even if not the strength values, might be expected to be similar to that of UHPC based on the fiber content. Consequently, this section includes a comparison between shear panel tests on UHPC and FRC, and a comparison of the UW shear results against such equations as are available. Shear models based on only the UW shear results are also proposed. Peak shear strength will be the main focus of the comparison.

6.2.1 Shear Panel Tests on FRC

Results from the study by Susetyo [20] at the University of Toronto will be used to compare the relationship between shear strength, compressive strength, and fiber content. The concrete specimens were tested in a panel testing machine similar to the UW machine and were approximately the same size. The specimens included full length longitudinal reinforcing bars and therefore did not include a designated test region, as did the UW specimens (see Figure 3.11), so the specimens were free to fail in either shear slip, bar pull-out, or bar yield. Only specimens that experienced shear slip failure will be used in comparisons with the UW UHPC specimens.

Results from an experimental study by Ishtewi at the University of Dayton [21] will also be used to compare. The details of Ishtewi's study can be found in Chapter 2. Information about the Susetyo and Ishtewi results are given in Table 6-7. Dimensions were not available for the fibers used in Ishtewi's research but the fiber shape was given.

Table 6-7: Summary of FRC Shear Panel Test Results

	Summary of FRC Shear Panel Test Results					
Researcher	Name	Fiber Content (%)	Compressive Strength (MPa)	Shear Strength (MPa)	Fiber Length (mm)	Fiber Diameter (mm)
Susetyo	C1F1V1	0.5	51.4	3.53	50	0.62
	C1F1V2	1	53.4	5.17	50	0.62
	C1F1V3	1.5	49.7	5.37	50	0.62
	C1F2V3	1.5	59.7	6.68	30	0.38
	C1F3V3	1.5	45.5	5.59	35	0.55
	C2F1V3	1.5	79	6.9	50	0.62
	C2F2V3	1.5	76.5	6.31	30	0.38
	C2F3V3	1.5	62	5.57	35	0.55
Ishtewi	N-0	0	35.5	1.9	N/A	N/A
	AC-0.5	0.5	44.8	2.93	Arched Crimped	
	AC-1	1	44.6	3.28		
	AC-1.5	1.5	43.6	3.93		
	C-0.5	0.5	44.4	3.04	Crimped	
	C-1	1	41.3	4.27		
	C-1.5	1.5	33.6	4.11		
	H-0.5	0.5	36.7	2.95	Hooked	
	H-1	1	35.5	4.2		
	H-1.5	1.5	42.3	5.75		

The Susetyo specimens varied based on designated compressive strength, fiber size, and fiber percentage. In total the design options were two different compressive strengths, three different sizes of fibers, and three different options for fiber percentage. The specimens are named based on designated compressive strength (C), fiber size (F), and fiber percentage (V).

The Ishtewi specimens varied based on fiber shape and fiber percentage. There were three different shapes of fibers: arched crimped (AC), crimped (C), and hooked). The fiber percentage varied from zero to 1.5. The specimens are named based on fiber shape and percentage.

Figure 6.12 shows the compressive strength versus the fiber content of the fiber-reinforced concrete samples.

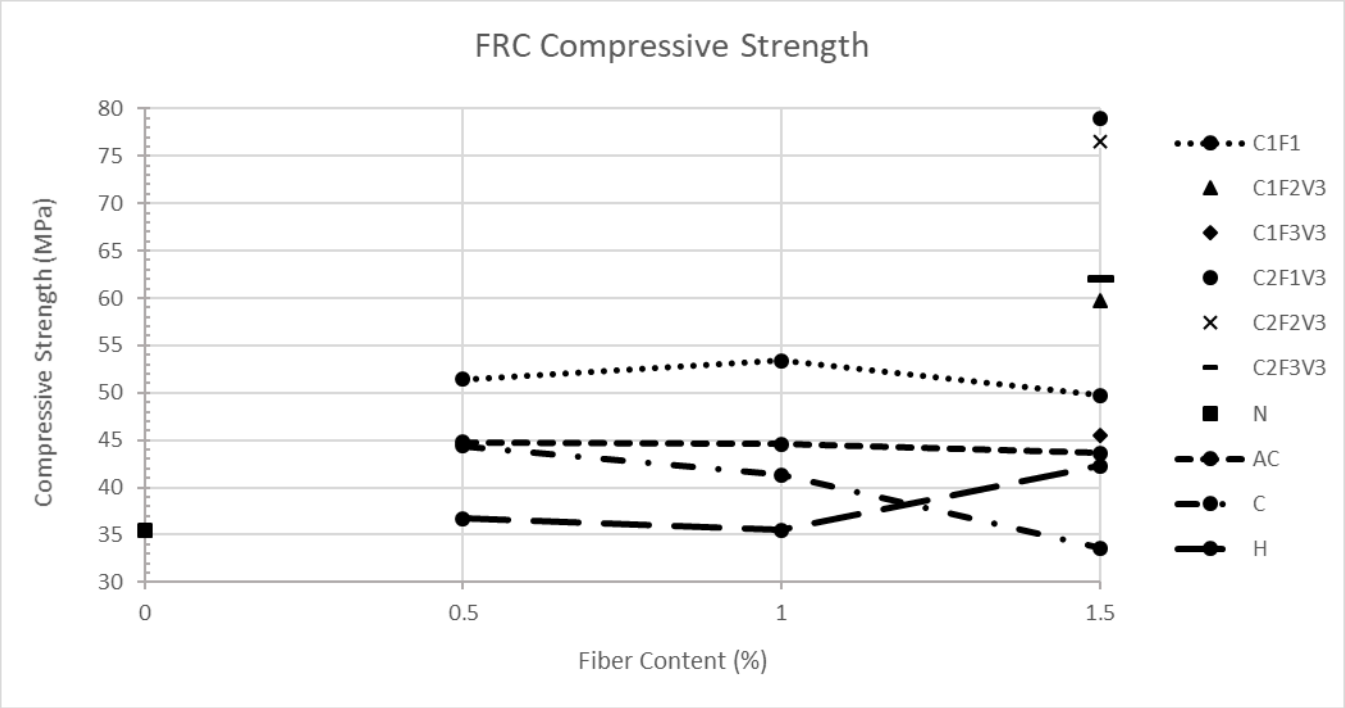

Figure 6.12: FRC compressive strength

According to the data collected by Susetyo and Ishtewi, there was little strength gain from increasing fiber content. The only FRC batch that experienced an increase in compressive strength was Series H (hooked fibers) tested by Ishtewi. The remaining FRC batches either stayed at a constant strength or decreased in strength as fibers increased. The FRC samples that had the highest compressive strength were from Series C2 (Susetyo), which used a different cementitious mix design than C1. The mix design was specified to have a higher strength than C1 during the design stages of the project. Series C1F1 included specimens with the same mix design and fiber type, but varied fiber percentage. As shown in Figure 6.12, the compressive strength did not consistently increase as fiber percentage did. This was also the case with each test series from Ishtewi. The fiber shape and mix design was consistent for all of the samples, therefore the only changing variable was fiber percentage. The compressive strength for arched crimped fibers (AC) was essentially constant no matter the fiber percentage. The crimped fibers (C) actually decreased in strength as fiber percentage increased. Hooked fibers (H) increased with fiber percentage, however, the compressive strength for 1% fiber was equal to that of the zero fiber specimen (N). All of these

observations from the FRC compressive strength results suggest that compressive strength depends more on the concrete component of fiber-reinforced concrete than the fiber component, which is consistent with what was found from the UHPC tests in this study.

Figure 6.13 shows the shear strength versus the fiber content of the fiber-reinforced concrete samples.

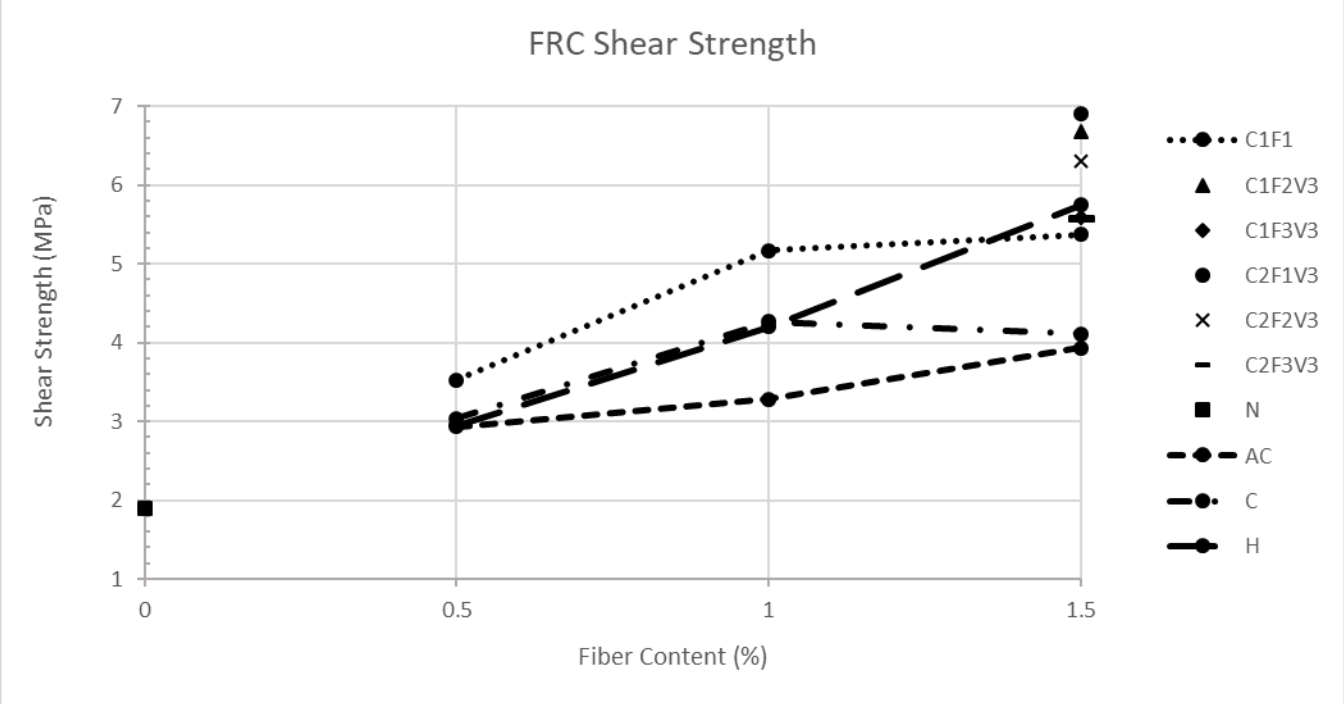

Figure 6.13: FRC shear strength

Almost every FRC batch experienced an increase in shear strength as fiber content increased. Additionally, there is much less difference between the series C1 and C2 batches than there was in compressive strength. For example, the compressive strength of C2F1V3 was 22% higher than that of C1F2V3, but the shear strength was 5% lower. The patterns exhibited in the FRC shear strength plot indicate that shear strength depends heavily on fiber content, and less so on the cementitious component. This is consistent with what was observed in the UHPC pure shear tests. In Figure 6.14, shear strength is plotted against fiber content. The best-fit trendline is shown with a dotted line.

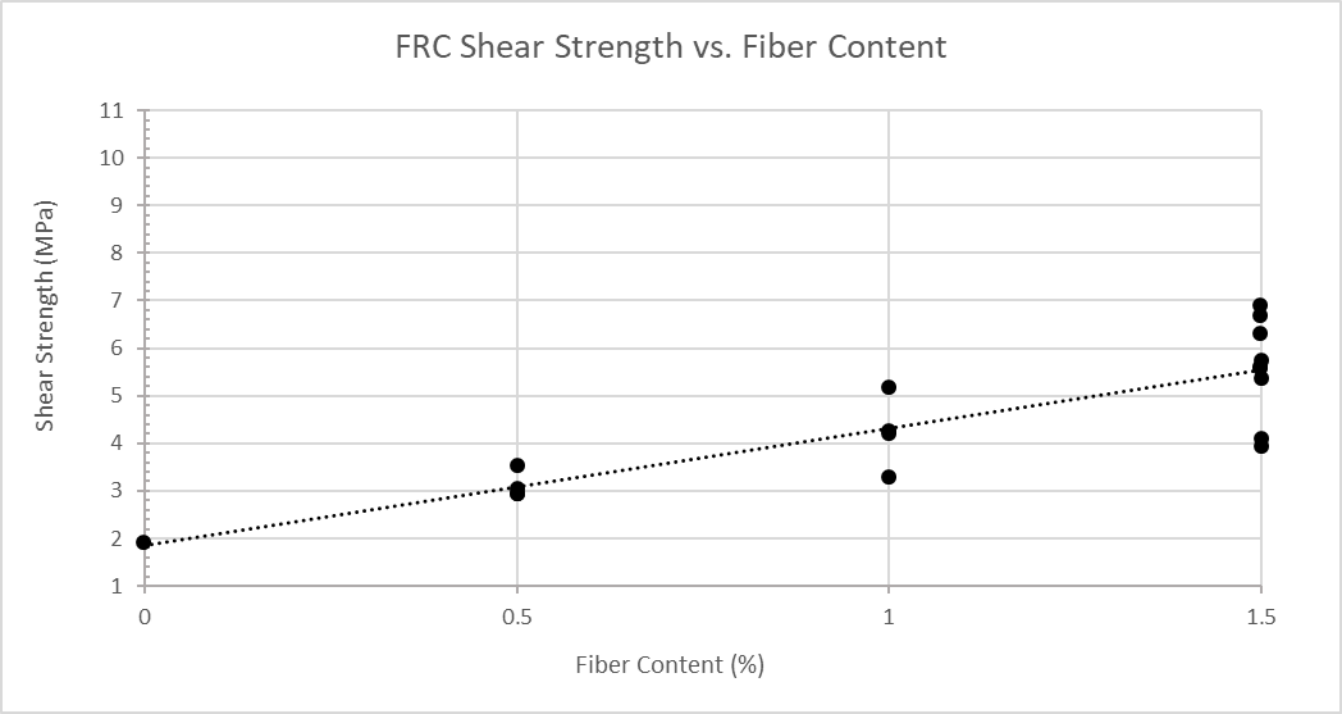

Figure 6.14: FRC shear strength vs. fiber content

The trendline that fit best to the data was an exponential model. The model was found to have an R^2 value of 0.77, indicating that trendline is well matched to the data. It is shown at Equation (6.11).

$$v = 1.85 + 2.47v_f\ (MPa) \qquad (6.11)$$

Where:

$v = shear\ stress$

$v_f = volumetric\ ratio\ of\ steel\ fibers$ (%)

The FRC shear strength was also plotted against $\sqrt{f_c'}$ in Figure 6.15. A linear model with the y-intercept set to (0,0) was used to fit the data. The trendline is shown as a dotted line.

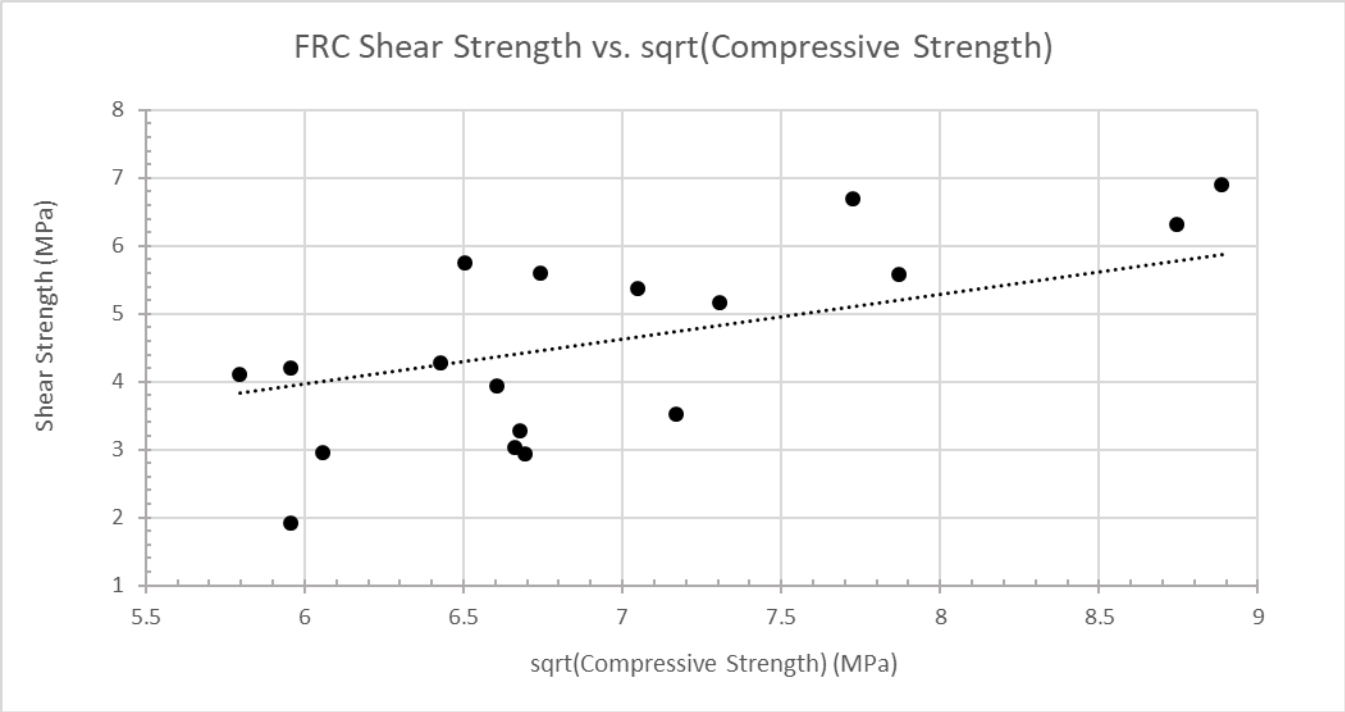

Figure 6.15: FRC shear strength vs. sqrt(compressive strength)

The equation of the trendline is:

$$v = 0.66\sqrt{f_c'}\ (MPa) \qquad (6.12)$$

While the model relating shear strength to fiber content had an R^2 value of 0.77, this model had a value of 0.4. Therefore, shear strength has a stronger correlation to fiber content than to compressive strength.

6.2.2 Available FRC Shear Models

The shear models discussed in Chapter 2 were applied to the UHPC shear test results. The shear models by Sharma [15], Narayanan/Darwish [17], and Ashour [18] were developed based on shear beam tests. Therefore, the models are not entirely applicable to the pure shear panel tests. Refer to

Chapter 3 for the equations used and details on how they were developed. In place of the beam depth and span dimensions in the equations, dimensions of the panel were used. Table 6-8 provides the experimental shear capacity found from testing panels at UW, as well as the calculated values based on the shear models.

Table 6-8: UW Experimental Results vs Proposed Shear Equations

UW Experimental Results vs Proposed Shear Equations							
Source	UW	Sharma		Narayanan/Darwish		Ashour	
Batch	v_u (MPa)	v_u (MPa)	EQ/EXP	v_u (MPa)	EQ/EXP	v_u (MPa)	EQ/EXP
UW2C	8.89	11.40	1.28	6.63	0.75	9.21	1.04
UW2D	9.75	11.84	1.21	6.98	0.72	9.54	0.98
UW2E	9.91	11.63	1.17	6.82	0.69	9.38	0.95
UW1	7.38	11.57	1.57	5.99	0.81	9.12	1.24
OU2	9.29	11.60	1.25	6.79	0.73	9.36	1.01
Average Ratio		*1.30*		*0.74*		*1.04*	
Standard Deviation		*0.14*		*0.04*		*0.10*	

Table 6-8 shows that the Ashour model matched the experimental data best, while the Sharma and Narayanan/Darwish models were equally inaccurate, in opposite directions. This is likely because the Sharma model does not depend on fiber content at all, only compressive strength. Since, in that model, there is no fiber contribution to the shear capacity, the model overestimates the contribution of compressive strength. This is especially apparent in the one percent batch, where the experimental data was only 64% of the estimated value. The Narayanan/Darwish model does depend on both compressive strength and fiber content, but the estimated values are all lower than the experimental results. This could be due to the fact that the model was created based on shear beam tests using heavy reinforcement and is therefore unable to make accurate predictions in this case. Finally, the Ashour model fit the UW data well and had a low standard deviation. The one percent UHPC batch yet again has the worst fit, which might be because the model was developed using mostly 2 percent UHPC since that is a more common fiber percentage.

Although the Ashour model fit well, it was not intended to be used in this context and should therefore not be accepted as a pure shear model for UHPC. The difficulty in finding appropriate equations to estimate shear strength shows that there is a need for more research on pure shear testing of UHPC.

6.2.3 Proposed UHPC Shear Model

Equations for a shear strength estimation of UHPC were developed by looking at the relationship between shear strength and fiber content, compressive strength, and tensile strength of the UW test results.

The figures used to model the FRC shear strength are first recreated using the UHPC results.

Figure 6.16 is the UHPC shear strength plotted against fiber content. The best-fit trendline was a linear model, with an R^2 value of 0.85. The equation is shown below the figure.

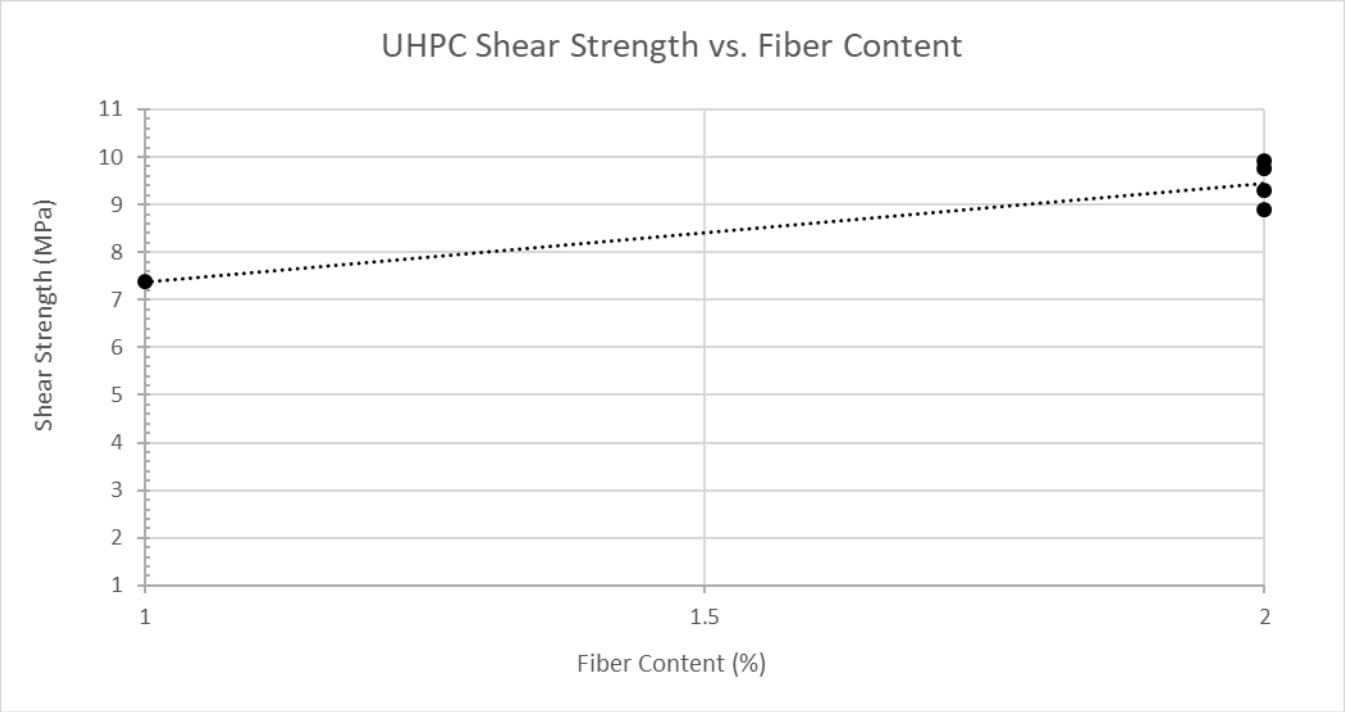

Figure 6.16: UHPC shear strength vs. fiber content

$$v_u = 5.3 + 2.08v_f\ (MPa) \quad (6.13)$$

The shear strength is strongly correlated to fiber content, as demonstrated by the high R^2 value. Compared to the FRC equation based on fiber content (Equation 6.11), the UHPC equation has a higher initial shear strength with zero fiber content. This is due to the fact that the cementitious

component of UHPC is much stronger than that of FRC, therefore it contributes more to the shear strength. However, the cement paste only accounts for so much shear strength. The rest of the shear response of UHPC is due to the steel fibers.

The shear strength is shown plotted against $\sqrt{f_c'}$ in Figure 6.17. It is noticeable that a clear trend is lacking from the figure. In fact, no possible trendline provided an R^2 value above 0.1. Therefore, no equation has been proposed to estimate shear strength from compressive strength for UHPC.

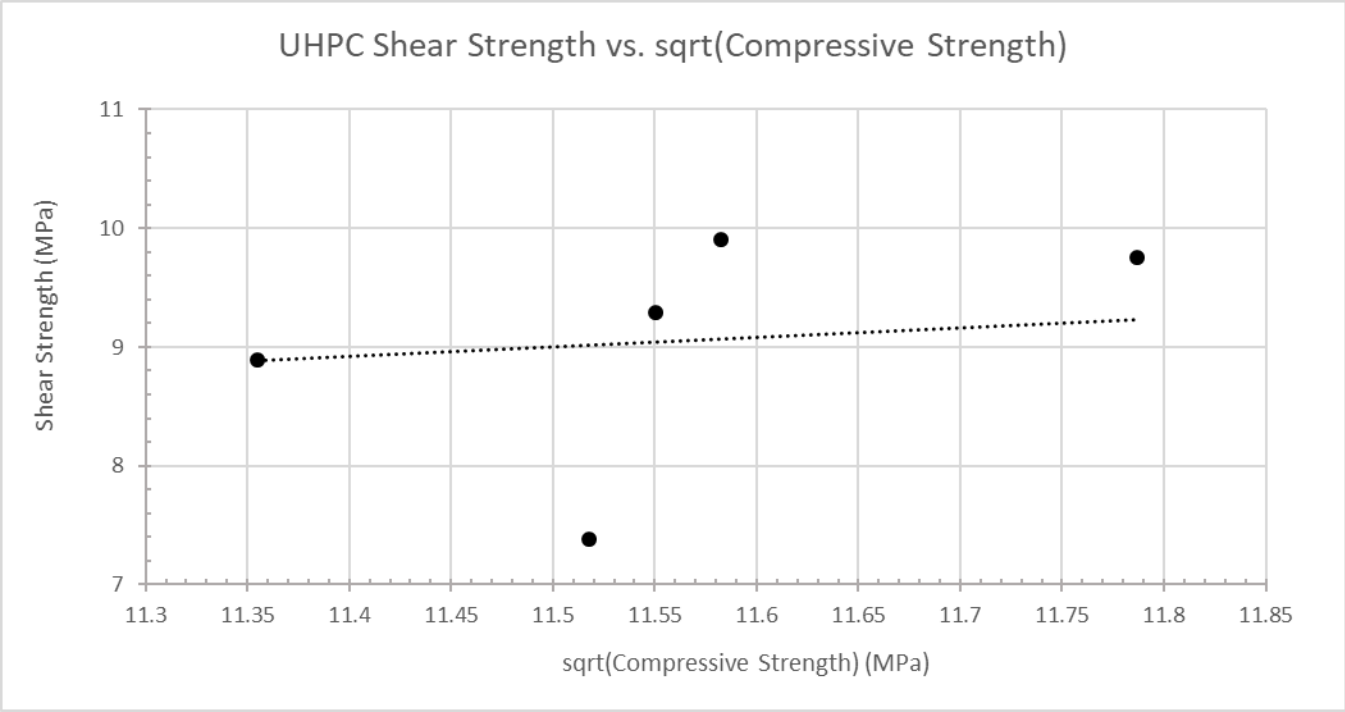

Figure 6.17: UHPC shear strength vs. sqrt(compressive strength)

Next, UHPC shear strength is shown versus tensile strength from direct tension testing in Figure 6.18.

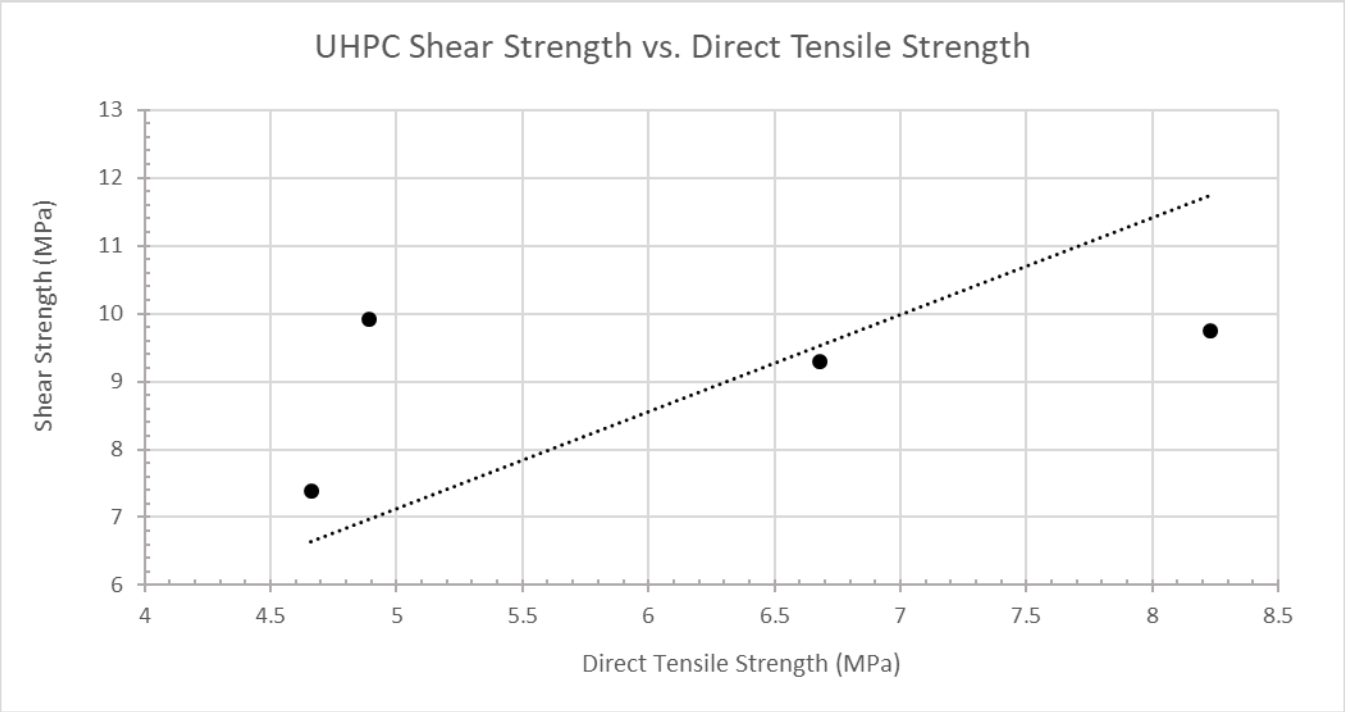

Figure 6.18: UHPC shear strength vs. direct tensile strength

The trendline that fit best to the data was a linear model. The equation is shown below.

$$v = 1.43 f_{td}\ (MPa) \tag{6.14}$$

Where:

$v = shear\ stress$

$f_{td} = tensile\ strength\ from\ direct\ tension\ testing$

Figure 6.18 shows no clear pattern and the best-fit equation only had an R^2 value of -2 indicating that the model does not fit the data well. Therefore, equation 6.14 is likely not a strong model to use to estimate shear strength of UHPC.

Finally, UHPC shear strength is shown versus tensile strength from flexural testing in Figure 6.19.

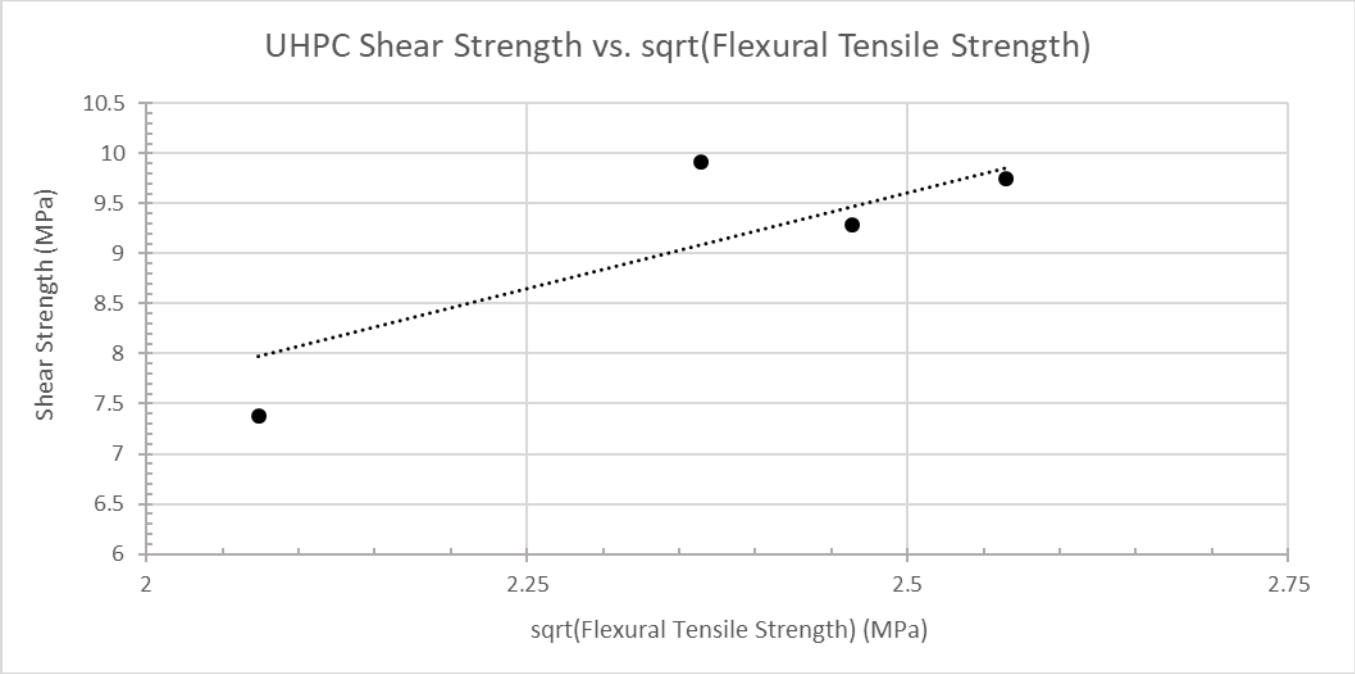

Figure 6.19: UHPC shear strength vs. flexural tensile strength

The trendline that fit best to the data was a linear model. The equation is shown below.

$$v = 3.84\sqrt{f_{tf}}\ (MPa) \qquad (6.15)$$

Where:

$v\ = shear\ stress$

$f_{tf} = tensile\ strength\ from\ flexural\ testing$

Figure 6.19 shows a clear linear relationship and the best-fit equation had an R^2 value of 7.4 indicating that the model fits the data well. Therefore, equation 6.15 is an option to estimate shear strength of UHPC.

According to the analysis of UW results, the most appropriate UHPC shear strength equations are 6.13, which is based on fiber content, and 6.15, which is based on the tensile strength from flexural testing. This discovery is consistent with the observations throughout the duration of the research project. Namely, fiber content has a larger impact on the shear strength of UHPC than compressive strength does. With that being said, the equations were developed based on only a few data points, all using the same non-proprietary mix design, with little variation in fiber content. Therefore, the proposed models are likely not entirely accurate for all UHPC mixes.

Chapter 7: Summary, Conclusions, and Recommendations

7.1 Summary

This research program investigated the impact of fiber content and material source on the strength of a non-proprietary UHPC, focusing on materials tests and pure shear panel tests. The materials test results were compared with similar studies conducted at a number of institutions. Next, models that estimate UHPC strength in various modes, such as compression, tension, and shear, were assessed to determine how well they fit the experimental data. For modulus of elasticity and tension, models provided by Graybeal [9] were used. For shear, models provided by Sharma [15], Narayanan and Darwish [17], and Ashour et al. [18] were used. The experimental test program and analysis is summarized below.

- The goals of the study were to run tests on non-proprietary UHPC to provide materials test data of UHPC using Seattle based materials for comparison with UHPC using materials sourced elsewhere, to determine the effect of fiber content on UHPC, and to evaluate the shear strength of UHPC.
- Seven batches of UHPC were cast in the form of shear test panels, and material test cylinders, tension dogbone specimens, and beam specimens. They were split into four test series:
    - Test Series 0: Trial Panels (UW2A, UW2B)
    - Test Series 1: 2% Fibers using UW Materials (UW2C, UW2D, UW2E)
    - Test Series 2: 1% Fibers using UW Materials (UW1)
    - Test Series 3: 2% Fibers using OU Materials (OU2)
- For each batch of UHPC, material tests and pure shear panel tests were performed. The tests produced the following data:
    - Compression (6): compressive strength at 3 days and 60 days post-cast
    - Modulus of Elasticity (3): modulus of elasticity at 28 days post-cast
    - Direct Tension (3): tensile stress and strain at 28 days post-cast
    - Flexural Beam (3): flexural strength at 28 days post-cast
    - Pure Shear Panel (1): shear stress, crack width, crack slip, and shear strain
- The data was analyzed by itself, focusing on the effect of fiber content and material source.

- The data was compared to experimental results from other sources to determine the effects of fiber content, material source, mix design, and mix procedure, on the properties of the non-proprietary UHPC.
- Selected equations proposed by others for predicting the material strength in different modes were compared with the measured results. The equations for modulus of elasticity and tension strength were derived for proprietary UHPC mixes.
- No predictive equations were available for pure shear tests of UHPC, so the measured results were compared with both pure shear test results of fiber-reinforced concrete, and equations derived for shear beam tests.
- An equation for shear strength of UHPC was developed based on the pure shear panel test results.

7.2 Conclusions

The following conclusions were drawn from the study on UHPC:

- Fiber content: The fiber content has little effect on compressive strength and modulus of elasticity. It has a large effect on tensile strength, flexural strength, and shear strength.
- Material source: The variations in results due to material source were smaller than the differences between nominally identical samples from the same source. Therefore, material sourcing has a negligible effect on UHPC performance.
- Mix design: Components of the mix design such as w/c ratio heavily impact concrete dependent properties such as compressive strength and modulus of elasticity.
- Mix procedure: The properties of the fresh concrete were found to be very sensitive to the mixing procedure and the quantity of superplasticizer used. Changes that would be considered small for conventional concrete made the difference between UHPC material that was too stiff to deposit and consolidate in the forms, or too fluid to prevent the fibers from sinking.
- Mixing UHPC requires significantly more energy than mixing the same quantity of conventional concrete. A high energy mixer would have facilitated the research conducted in this study.
- Predictive models: Available UHPC models focus on concrete contribution more than fiber contribution. This focus overlooks a characteristic that is important for tension strength and shear strength. No shear models have been developed specifically for pure shear response of UHPC with no transverse reinforcement.
- Proposed models: Equations were developed from the material test results for predicting the compressive strength, modulus of elasticity, tensile strength, and flexural strength of UHPC. They are provided in Chapter 6 of this report.
- Proposed models: Equations were developed from the shear test results for predicting the shear strength of UHPC. They are given as Equation (6.13) and Equation (6.15) in Chapter 6 of this report.

7.3 Recommendations

The following are suggestions for future work relating to UHPC:

- Fiber content was studied based only on varying percentages, and not types, of fibers. There are many types of fibers of different materials, sizes, shapes, and coating. In order to get a better idea of how fibers contribute to UHPC, studies should be conducted where fiber type is the only changing variable.
- Optimize UHPC mix design based on workability and cost. A cost-benefit analysis of the currently available UHPC data will help to meet this goal, but there may need to be more research focused on workability. Fibers and superplasticizer are the most expensive components of UHPC, so studying their impact further will also help to meet this goal.
- Develop methods for estimating tensile strength and flexural strength that take into account the contribution of fibers in UHPC. The available equations are currently based only on compressive strength which results in inaccurate estimations.
- Conduct more pure shear tests on UHPC with different fiber contents. The resulting database of test results should be used to verify or modify the proposed equation for predicting shear strength of UHPC.
- Model the shear response of UHPC with available software programs, such as Vectr, using the research results as means of validation.

Notation List

$a = shear\ span\ of\ beam$

$A = cross - sectional\ area$

$A_v = area\ of\ shear\ reinforcement$

$A_f = cross - sectional\ area\ of\ failure\ region$

$A_{act} = area\ of\ either\ advance\ (3.19\ in^2)\ or\ retract\ (6.49\ in^2)\ actuator$

$b = width\ of\ beam$

$D = fiber\ diameter$

$d = depth\ of\ beam$

$\frac{du}{dy} = rate\ of\ change\ in\ x - displacement\ with\ respect\ to\ y - axis$

$\frac{dv}{dx} = rate\ of\ change\ in\ y - displacement\ with\ respect\ to\ x - axis$

$E_c = modulus\ of\ elasticity$

$F = fiber\ factor$

$F = force$

$f'_c = compressive\ strength$

$f_r = flexural\ strength\ (modulus\ of\ rupture)$

$f_t = tensile\ strength$

$f_{td} = tensile\ strength\ from\ direct\ tension\ testing$

$f_{tf} = tensile\ strength\ from\ flexural\ testing$

$f_y = yield\ strength\ of\ shear\ reinforcement$

$L = span\ length$

$M = moment$

$P = load$

$p_{act} = pressure\ of\ either\ advance\ or\ retract\ line$

$s = spacing\ of\ shear\ reinforcement$

$S = elastic\ section\ modulus$

$V = shear\ force$

$v = shear\ stress$

$v_f = volumetric\ ratio\ of\ steel\ fibers\ (\%)$

$V_s = shear\ strength\ from\ shear\ reinforcement$

$v_u = ultimate\ shear\ strength$

$Z = plastic\ section\ modulus$

$\varepsilon = strain$

$\gamma = shear\ strain$

$\eta_f = fiber\ bond\ factor$

$\rho = ratio\ of\ longitudinal\ reinforcement$

$\rho_f = volumetric\ fiber\ content\ expressed\ as\ a\ decimal$

$\sigma = stress$

$\tau = ultimate\ bond\ stress\ of\ fiber\ matrix, taken\ as\ 4.15\ MPa$

References

[1] ACI Committee 239. ACI 239R-18 Ultra-High Performance Concrete. American Concrete Institute, 2018.

[2] Haber, Zachary B., et al. Properties and Behavior of UHPC-Class Materials. FHWA, 2018.

[3] "Ultra-High Performance Concrete." PCA - The Portland Cement Association - America's Cement Manufacturer, https://www.cement.org. 2001.

[4] "What Is UHPC? | UHPC | Ready-Mix UHPC | Proven Results | Steelike®." UHPC | Ready-Mix UHPC | Proven Results | Steelike®, https://steelike.com. 2021.

[5] UHPC Solutions. "Quick Guide to the History of UHPC." UHPC Solutions | Infrastructure Rehabilitation Contractors, https://www.uhpcsolutions.com. 2018.

[6] "Ductal® Engineering Applications." Ductal®, 29 June 2016, https://www.ductal.com.

[7] Leonard, Mark. "Public Roads-Building Connections That Last." Federal Highway Administration, FHWA-HRT-18-002, 2018, https://www.fhwa.dot.gov.

[8] "How Ultra-High-Performance Concrete (UHPC) Has Accelerated Infrastructure Development in Malaysia - Construction Plus Asia." Construction Plus Asia, 6 Sept. 2020, https://www.constructionplusasia.com.

[9] Graybeal, Benjamin A., et al. "Properties and Behavior of UHPC-Class Materials." FHWA, 2018.

[10] Graybeal, Benjamin A., et al. "Durability of an Ultra-High Performance Concrete." FHWA, 2007.

[11] Graybeal, Benjamin A., et al. "Development of Direct Tension Test Method for Ultra-High-Performance Fiber-Reinforced Concrete." ACI Materials Journal, no. 2, American Concrete Institute, 2013.

[12] Russell, Henry G., and Benjamin A. Graybeal. Ultra-High Performance Concrete: A State-of-the-Art Report for the Bridge Community. FHWA, 2013.

[13] Azizinamini, Atorod, et al. “A Comparison of Existing Analytical Methods to Predict the Flexural Capacity of Ultra High Performance Concrete (UHPC) Beams.” Construction and Building Materials. May 2018.

[14] Looney, Trevor, et al. “Evaluation of UHltra-High Performance Concrete for Use in Bridge Connections and Repair”, 2019, https://www.slagcement.org.

[15] Sharma, A. K. Shear Strength of Steel Fiber Reinforced Concrete Beams. ACI Journal, 83, 624-628. 1986.

[16] Aci 318-19

[17] Narayanan, R., & Darwish, I. Use of Steel Fibers as Shear Reinforcement. ACI. Structural Journal, 84(2), 1987.

[18] Ashour, S. A., Hassanain, G. S., & Wafa, F. F.. Shear Behavior of High-Strength Fiber Reinforced Concrete Beams. ACI Structural Journal, 89(2), 176-184. 1992.

[19] Kwak, Y.-K., Eberhard, M. O., Kim, W.-S., & Kim, J.. Shear Strength of Steel Fiber-Reinforced Concrete Beams without Stirrups. ACI Structural Journal, 99(4), 530-538. 2002.

[20] Susetyo, Jimmy, and Frank J. Vecchio. “Effectiveness of Steel Fiber as Minimum Shear Reinforcement: Panel Tests.” Fib Bulletin 57. Shear and Punching Shear in RC and FRC Elements Technical Report, fib. The International Federation for Structural Concrete, 2010.

[21] Ishtewi, Ahmad. “Shear Capacity of Fiber Reinforced Concrete under Pure Shear.” University of Dayton. 2012.

[22] Peruchini, Timothy. “Investigation of Ultra-High Performance Concrete for Longitudinal Joints in Deck Bulb TeeBridge Girders.” University of Washington. 2017.

[23] ASTM International. C1116/C1116M-10a(2015) Standard Specification for Fiber-Reinforced Concrete. West Conshohocken, PA, 2015.

[24] ASTM International. C39/C39M-21 Standard Test Method for Compressive Strength of Cylindrical Concrete Specimens. West Conshohocken, PA, 2021.

[25] ASTM International. C469/C469M-14e1 Standard Test Method for Static Modulus of Elasticity and Poisson's Ratio of Concrete in Compression. West Conshohocken, PA, 2014.

[26] ASTM International. C78/C78M-21 Standard Test Method for Flexural Strength of Concrete (Using Simple Beam with Third-Point Loading). West Conshohocken, PA, 2021.

[27] Optotrak Certus NDI, https://www.ndigital.com. 2015.

[28] Campos, Richard. Effect of Fiber Content on Tensile Strength of Non-Proprietary Ultra-High Performance Concrete. University of Oklahoma. 2020.

[29] Dyachkova, Yana. Effect of Fiber Content on Mechanical Properties of Non-Proprietary Ultra-High Performance Concrete. University of Oklahoma. 2020.

Appendix

Mixing Procedure

Equipment

A pan mixer with capacity of 2 cubic feet, shown below, was used to mix each batch of UHPC.

Figure A.1: Pan mixer

Mixing Prep

1. Sand moisture content test (weigh given sand, soak it, get it to SSD, weigh SSD sand, oven dry it, weigh OD sand)
2. Measure out materials in buckets
3. Orange mixer and block for under
4. Drill with hand mixer
5. Wheelbarrow
6. Plastic on floor surrounding panel and material test forms
7. Shake table next to mat test forms
8. Scoops, trowels, small shovel, rods
9. Masks, gloves, glasses

Materials Prep

1. Calculate what weight of each material you will need based on mix design and batch size
2. Separate total cement weight equally into buckets
3. Separate total slag weight equally into buckets
4. Weigh total amount of silica fume into one bucket

5. Weigh out amount of sand equal to silica fume weight and put in separate bucket
6. Weigh out remaining amount of sand and separate equally into buckets
7. Separate total fiber weight equally into buckets
8. Separate total water weight into two buckets, one with 1/3 the other with 2/3
9. Separate total Glenium weight into two cups, one with 1/3 the other with 2/3
10. Weigh total amount of Daratard in one cup

Mixing UHPC

1. DO NOT MIX MORE THAN 2 CUBIC FEET IN ORANGE MIXER
2. READ PROCEDURE THE WHOLE WAY THROUGH BEFORE STARTING
3. Lift up mixer lid
4. Turn on mixer
5. Add sand (except for bucket equal to silica fume weight) into mixer followed by all cement then all slag
6. Lower mixer lid
7. Let mix until evenly distributed
8. Empty all dry mix into buckets that were previously holding sand, slag, cement
9. Turn off mixer
10. Place block under mixer opening
11. Add remaining sand to silica fume bucket
12. Add 2/3 water to silica fume bucket
13. Add 2/3 Glenium to silica fume bucket
14. Add Daratard to silica fume bucket
15. Mix with hand drill until well mixed to create a slurry, should be about two minutes
16. Place 2/3 water bucket (that is now empty) under the mixer opening on top of the block
17. Lift up mixer lid
18. Turn on mixer
19. Pour the slurry into mixer (the mixer leaks when holding wet materials which is why the empty bucket is under the opening to catch any lost materials)
20. Lower mixer lid
21. STEPS 22-24 AND 25 SHOULD BE DONE SIMULTANEOUSLY

22. Rinse hand drill paddle in small bucket of water
23. Use 1/3 bucket of water to clean out empty slurry bucket
24. Dump all water into mixer
25. Immediately begin adding the first bucket of dry mix
26. DO NOT ADD ALL DRY MIX QUICKLY AT ONCE
27. Gently set the bucket down on its side on top of the mixer cover, use one hand to hold the bucket steady and the other to guide dry mix into the bucket one handful at a time
28. Move quicker for the first bucket of dry mix so that the slurry thickens and the mixer stops leaking
29. Slow down the rate of dumping as you continue- you should go at a slow steady rate, but any time you notice the concrete balling up stop until all balls smooth out then continue adding
30. Fill syringe with Glenium from the 1/3 cup
31. As you continue adding dry mix, shoot Glenium from syringe into mixer as needed (aka if the concrete looks very dry and is balling up a lot)
32. Once you are about halfway through the dry mix, add any slurry that leaked from the mixer into the bucket under the mixer opening back into the mixer
33. The mixer will be less effective towards the center, so concentrate syringe Glenium there
34. Time to add dry mix will depend on your batch size, it will take about 40 mins for 2 cubic feet
35. All Glenium from the syringe should be in concrete by the time the dry mix has all been added
36. ONLY ADD AS MUCH GLENIUM AS IS REQUIRED- IF YOU ADD TOO MUCH TO MAKE THE MIX MORE “WORKABLE” THE FIBERS WILL NOT STAY SUSPENDED IN CONCRETE
37. Once all dry mix is added and no big clumps are present, stop mixer
38. Lift up mixer lid
39. Quickly go into concrete using your hand or trowel and make sure any dry mix that is stuck on the blades is added to the concrete (concrete might clump up between the inside blade and the center of the mixer, so make sure it gets broken up)
40. Lower mixer lid
41. Turn on mixer and run for a minute to make sure all dry mix is incorporated into concrete

42. Add steel fibers to concrete using the same method as the dry mix but at a quicker speed
43. Make sure fibers are not added in big balls- pick up a handful of fibers and sprinkle them into mixer to break up any clumps
44. Concentrate the fibers towards the outside of the mixer because this will avoid getting them stuck on blades and will mix them better
45. Once all fibers have been added stop the mixer and lift the mixer lid
46. Using your hand or a trowel, break up any chunks of fibers in the center of the mixer and dust off any fibers that are stuck on the blades
47. Lower the mixer lid and turn on the mixer
48. The fibers are magnetic so they will stick to the mixer lid, once you are done adding them make sure to get the ones on the lid into the mixer
49. Once all fibers are well dispersed remove the empty bucket and block from under the mixer
50. Place the wheelbarrow under the mixer opening (should be rinsed out but not have excess water at the bottom)
51. With the mixer still on, open the door and let the concrete flow into the wheelbarrow
52. One person should stay back and rinse out the mixer while the other takes the wheelbarrow, scoops, rod, and trowels to the specimen molds and begins casting

Casting

1. Mat test molds- fill halfway, shake table for 10 seconds, fill rest of way, rod, shake table for 10 seconds
2. Panel- fill halfway, rod, fill rest of way, rod
3. Move as quickly as possible because UHPC will set quicker than normal concrete
4. Finish all molds with trowel- may not need it because UHPC will be smooth since no large aggregate

Post-Cast

1. Keep wet burlap on panel
2. Remove all molds 24 hours after cast- do not break any wooden molds that can be reused
3. Label with name/date
4. Place in bath

Testing Procedure

Panel Placement

1. Lift panel with forklift
2. Place two I-holes in corner blocks of panel- blocks 5&6
3. Connect I-holes to crane
4. Lift panel and lower on piece of plywood, lean on table- should be resting on corners
5. Remove I-holes from panel and crane
6. Attach two L-rods to crane
7. Place ends of L-rods into corner blocks of panel
8. Lift panel to machine & place inside of actuators
9. Attach front bottom vertical blocks with bolts
10. Wiggle panel in place to line up block hole with the pinned actuators
11. Put metal rod though hole on side of moment frame to hold pinned actuators in place
12. Put bolt through the pinned actuators and panel block
13. Individually move horizontal actuator that goes with third pinned actuator until it is in place
14. Put bolt through the pinned and free actuators and the panel block
15. Should not have bolts in middle blocks on both bottom sides
16. Remove the L-rods from the panel and move the crane
17. Individually move each of the actuators until all blocks are aligned with a horizontal and vertical actuator (pump hose, tank hose, pump, advance two T-hoses, retract two T-hoses) (big ladder back small ladder front)
18. Screw washers & nuts on each bolt

Test Preparation

1. Paint panel white
2. Draw 25 points on front of panel (insert pic w dimensions here)
3. Draw 16 points on back of panel (insert pic w dimensions here)
4. Pots

a. Need six 0.5 inch Pots, calibration table, DAQ with LabView, voltage reader

b. LabView open Panel file

c. Set excitation to 10.006 V

d. Calibrate all Pots using calibration table, LabView, and Cal Solver Excel sheet (0.3 and 12 in excel)

e. Label Pot with factor and enter factor into LabView (set as default, save)

f. Number Pots corresponding to their channel

g. Match Pots with the appropriate rod/bracket

h. Glue Pot onto end of rod towards bracket with hot glue

i. Use hot glue to adhere brackets on back of panel in correct orientation (insert pic w numbering here)

j. Plug Pots into DAQ matching each of the numbers with their channels

5. Optotrak

a. Get double sided tape, 13 sensor bags, two blocks, computer with system, Optotrak

b. Cut pieces of double sided tape and stick to 25 points on front of panel

c. Unwrap 25 sensors (come in pairs) and label corresponding to the numbers on the blocks

d. Stick sensors to tape on front of panel, matching the numbers

e. Try to keep untangled

f. Plug all sensors back into blocks

g. Plug blocks into each other and into Optotrak

h. Plug Optotrak into computer

i. Start program, tell it how many sensors (24, 1)

j. Set frequency to 4 Hz

k. Set run time to 99999 seconds

l. Place Optotrak in front of panel with clear view of sensors

6. Pressure sensors (option 1)

a. Get three load transducers, three wires, one T valve, one T hose, computer with LabView, voltage reader, hydraulic pump (red on wheels in locker room), DAQ, pressure gauge, pump thing

b. Connect each sensor to a wire, connect wire to port in DAQ, connect channel wire from computer to port in DAQ

c. Label each set up as sensor 1, 2, 3

d. Set excitation in DAQ as 5 V

e. Set factor on DAQ to 0.5

f. Hook up hose to pump thing

g. Load pump thing in little Baldwin

h. Hook up hydraulic pump to T hose

i. Hook other open part of T hose to free T

j. Hook up pressure gauge to one open end of T

k. Hook up sensor to other open end of T

l. Open hydraulic pump

m. Zero pressure gauge

n. Use cal solver excel sheet (10000, 12)

o. Calibrate sensor

p. Enter factor in LabView

q. Repeat for all sensors

7. Pressure Sensors (option 2)

a. Get three load transducers, three wires, computer with LabView, hydraulic pump, pressure gauge, T valve, X valve

b. Connect T valve to pump

c. Hook up pressure gauge to T

d. Connect X valve to T valve

e. Hook up all three pressure sensors to X valve

f. Plug everything into DAQ

g. Turn on pump

h. Open and close pump until LabView matches pressure gauge for all sensors

8. Load maintainer

a. Turn on pump without anything attached to pump hose

b. Adjust pressure to 7000 psi

c. Connect pump to load maintainer, tank and pump to corresponding spots

d. Use two pressure sensors- one in valve 1 other in valve 5

e. Open valves 1 and 5 and move little metal things

f. Turn on DAQ and load maintainer

g. Send pressure to pump

h. Turn wheel on load maintainer stopping in increments of 1000

i. Compare readings in LabView- the sensor in valve 5 should be 0.492 times the reading for the sensor in valve 1

j. Add little balls to make ratio match up

k. Decrease back to zero in increments of 1000

l. Turn off pump

m. Turn off load maintainer

n. Close valves, put little metal things back in place

Panel Test

1. Set up hoses; HP-3R 4R, LP-1A 2A, all else return
2. Plug pots, pressure sensors into DAQ
3. Plug in all Optotrak
4. Turn on DAQ and Optotrak
5. Set up camera
6. Run Labview, Optotrak
7. Turn on pump & load maintainer
8. Increase load in increments of 1000 psi, stopping each time to check for cracks
9. Take one photo with board in front that says stop number and load
10. Once cracks start, mark cracks on front and back
11. Change increments to 500 psi
12. Before marking cracks on panel at higher pressures, unload a little first
13. After panel fails, press emergency off button on load maintainer and quickly turn off pump, then manually unload load maintainer

Panel Removal

1. Remove optotrak, pots, and in-plane
2. Remove all washers and nuts from bolts
3. Remove bolts from top two corner blocks
4. Retract all four actuators that correspond to blocks
5. Hook L-rods to crane
6. Insert L-rods into top blocks

7. Remove all bolts except for bottom left corner
8. Retract all actuators (using big hoses) except bottom vertical and bottom left horizontal
9. Lift top half out using crane
10. Remove L-rods from crane
11. Insert I-hooks into top blocks on each side of bottom half of panel
12. Hook up crane in I-hooks
13. Remove all remaining bolts
14. Left bottom half out using crane
15. Remove front bottom vertical blocks- do not retract after

Test Photos

Compression Test

Figure A.2: Compression test (a) typical 2% failure, (b) typical 1% failure, (c) sinking fibers, (d) poor consolidation

Direct Tension Test

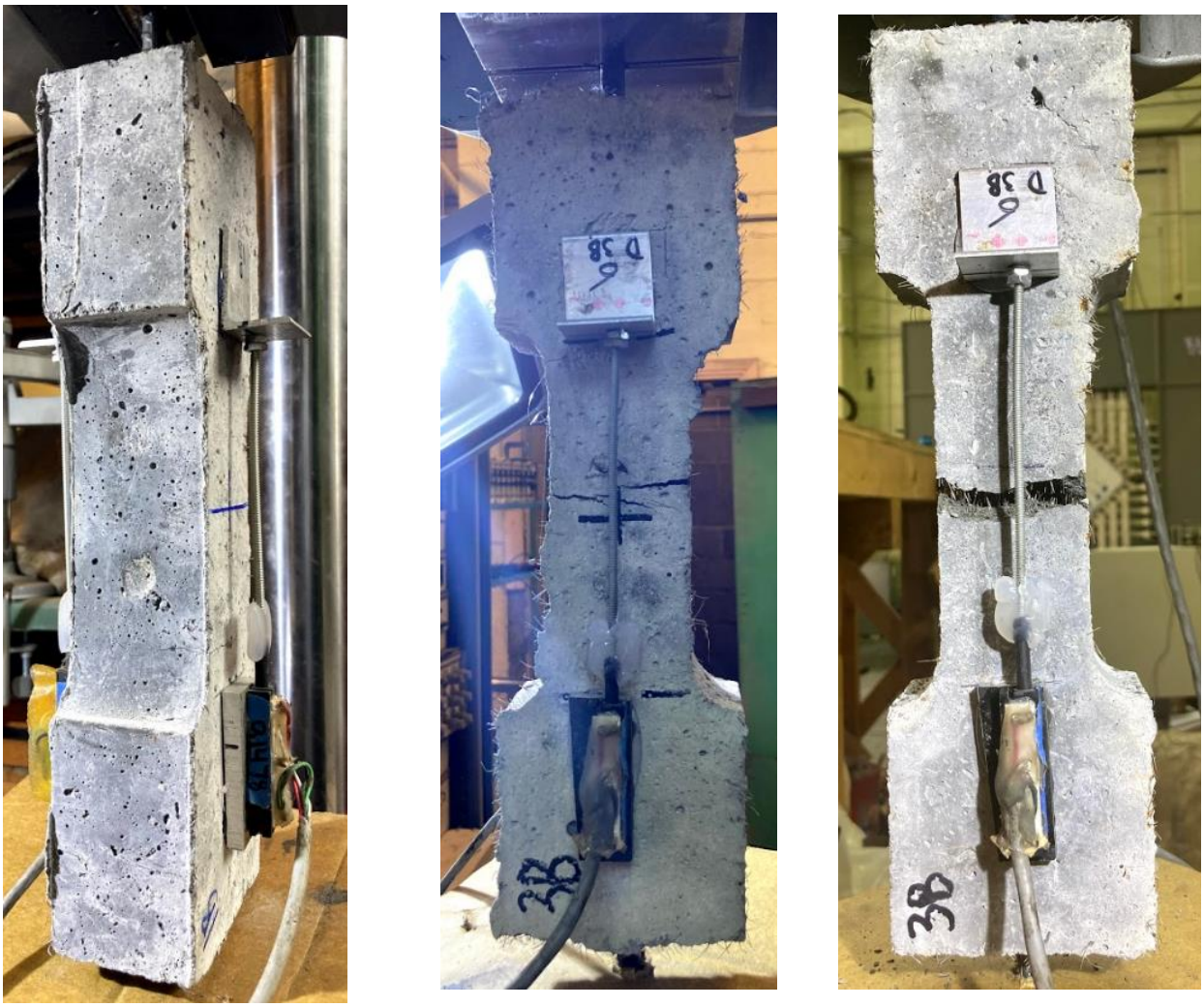

Figure A.3: Direct tension test (a) setup, (b) typical cracking, (c) typical failure

Flexural Beam Test

Figure A.4: Flexural beam test (a) setup, (b) typical failure

Shear Panel Test

Figure A.5: Panel test equipment (a) pressure sensors, (b) load maintainer, and (c) hydraulic pump

Figure A.6: Panel with poor consolidation